COMMITTEE III.1
ULTIMATE STRENGTH

COMMITTEE MANDATE

Concern for the ductile behaviour of ships and offshore structures and their structural components under ultimate conditions. Attention shall be given to the influence of fabrication imperfections and in-service damage and degradation on reserve strength. Uncertainties in strength models for design shall be highlighted. Consideration shall be given to the practical application of methods.

COMMITTEE MEMBERS

Chairman: T. Yoshikawa, *Japan* (*Chair*)
              A. Bayatfar, *Belgium*
              B. J. Kim, *Korea*
              C. P. Chen, *Taiwan*
              D. Wang, *China*
              J. Boulares, *USA*
              J. M. Gordo, *Portugal*
              L. Josefson, *Sweden*
              M. Smith, *Canada*
              P. Kaeding, *Germany*
              P. Jensen, *Norway*
              R. Ojeda, *Australia*
              S. Benson, *UK*
              S. Vhanmane, *India*
              S. Zhang, *UK*
              X. Jiang, *Netherlands*
              X. Qian, *Singapore*

KEYWORDS

Ultimate strength, buckling strength, yielding strength, nonlinear analysis, steel structures, aluminium structures, composite structures, ship structures, offshore structures, initial imperfections, in-service degradation, uncertainties, reliability, static/quasi-static loads.

CONTENTS

1.   INTRODUCTION

Ultimate strength is a critical and fundamental assessment in the design of a ship or offshore structure. The global ultimate strength of a structure is usually first assessed in the early phases of design. Evaluation of the local ultimate strength of scantlings is also an important part of structural design and analysis. Buckling and elasto-plastic collapse dominate the ultimate strength of slender members in compression while yielding dominates the ultimate strength of members in tension.

This report concerns ductile behaviour of structural and components. Due to the improvements of toughness of the material used in ships and offshore structures, brittle fracture is now a rare occurrence. For plates greater than 50 mm in thickness, such as may be used in the upper deck plating of a container ship, brittle fracture can developed as the result of fatigue crack propagation from an initial defect. As this can be avoided through adequate inspection of defects, the limit state of brittle fracture is excluded from discussion in this report.

It is now common to design ship and offshore structures to withstand buckling or yielding under the design load. However, until the middle of the 19th century, the design criterion was the breaking strength of the material. This is partly because brittle iron of low tensile strength was used for ship structures at that time, and partly because buckling was not then well understood. It was after (Bryan, 1891) that panel buckling was theoretically understood and calculated.

From the beginning of the 20th century, it had become common to consider the buckling strength as a design criterion. Moving into the 21st century, this has evolved into the ultimate strength criteria.

The first attempt to evaluate the ultimate strength of ship structure was performed by Caldwell (1965). He applied "Rigid Plastic Mechanism Analysis" to evaluate the ultimate hull girder strength. The influence of buckling was considered by reducing the yield stress of the material in the buckled part.

The finite element method (FEM) was introduced in 1956 by Turner et al. (1956). At first FEM was used only for the analysis of elastic behaviour of structures. To evaluate the ultimate strength of structural members and systems, it is necessary to consider the influence of both buckling of structural members and yielding of materials. Since the early 1970's, such analysis, so called elasto-plastic large deflection analysis, has become possible to perform using FEM. However, computations were time consuming and it was two decades before commercial codes were commonly used for such analysis.

As with previous ISSC reports, a literature survey is performed related to assessment procedures for ultimate strength (see Chapter 3) and ultimate strength of various structures, such as tubular members, plates and stiffened plates, shells, ship structures, offshore structures, composite structures, and aluminum structures (see Chapter 4). It was from the 10th ISSC that benchmark calculation using different nonlinear codes were completed by this committee (Oliveira, 1988), and benchmark calculations have been performed in each committee since 1988.

For this report two benchmark calculations are performed (see Chapter 5). Both benchmarks show the application of nonlinear finite element analysis to the ultimate strength problem. The first investigates a box girder ultimate strength under four point bending loads and compares results with the experimental results by Gordo et al. (2009). The second benchmark investigates the hull girder ultimate strength of a bulk carrier considering the effect of initial imperfections and lateral loadings.

To complete a rational based design, it is usual to consider the ultimate strength as the strength standard instead of yielding and buckling strength. Recent developments in design standards for the marine industry have led to the Goal-Based New Ship Construction Standards (GBS) by International Maritime Organization (IMO), and Common Structural Rules (CSR) by International Association of Classification Societies (IACS). The GBS consists of five tiers as indicated in Figure 1. In Tier I, goals are specified for design and construction of new ships. In Tier II, functional requirements are specified to achieve the goals. Tier III, is verification of Tier IV, which is an existing framework of regulations, IMO conventions and rules of recognized organization such as classification societies. CSR are closely related to GBS though Tier IV. An important aspect of CSR is the requirement to evaluate ultimate hull girder strength as well as the ultimate strength of plates and stiffened plates.

In the Common Structure Rules (CSR), which came into force in April 2006, the multi-step procedure (Smith's method) is applied for calculating hull girder ultimate strength of bulk carriers (CSR-BC). In the Harmonized Common Structure Rules (CSR-H), which combines CSR-BC(for bulk carriers) and CSR-T (for double hull tankers) and comes into force in 2016, a double bottom factor, γ_{db} will be introduced to take account of the effect of lateral loading on the hull girder ultimate strength. Structural redundancy is also taken into account in CSR-H according to SOLAS regulations.

With these developments ultimate strength assessment is now becoming a more important issue to ensure the safety of ship structures. From this point of view the role of this committee continues to be very important.
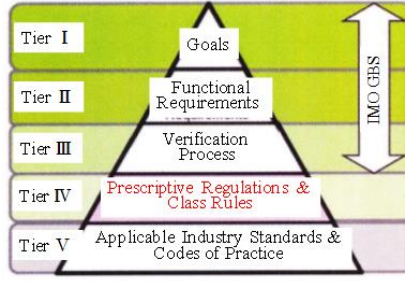
Figure 1. Framework of IMO GBS (Goal Based Standard)

2.   FUNDAMENTALS

2.1   Design for Ultimate Strength

A limit state is defined as a condition that a structural member or an entire structure fails to perform its designed function. There are four types of limit states: Ultimate limit states (ULS); serviceability limit states (SLS); fatigue limit states (FLS) and accidental limit states (ALS). This report is concerned with ULS, with a focus on the global hull girder strength of a ship. An equivalent treatment could be applied to an offshore structure.

A ship hull girder, which is composed of stiffened plates, is subjected to a variety of forces including self-weight, cargo weight, buoyancy force and wave load. Under these loads, bending moment, torsional moment, and shear force are exerted on the hull girder cross section. The strength of the hull girder to resist these forces and moments is called longitudinal strength. This is the most fundamental and important strength of ship structure. Ships must be designed to withstand the maximum expected loading, especially bending moment, throughout its lifetime.

The following criterion is usually applied for hull girder ultimate strength assessment, using a partial safety factor approach:

$$\gamma_S M_S + \gamma_W M_W \leq M_U / \gamma_M \tag{1}$$

where, M_S and M_W are the maximum still water vertical bending moment and wave vertical bending moment respectively, M_U is ultimate moment capacity of the hull girder, and γ_S, γ_W and γ_R are the partial safety factors reflecting uncertainties and ensuring the overall required target safety margin

Recently, a probabilistic approach using the reliability index β and AFORM method (advanced first order second moment method) was attempted to apply for the assessment of ultimate strength:

$$\beta = \frac{\mu_D - \mu_C}{\sqrt{\sigma_D{}^2 - \sigma_C{}^2}} \tag{2}$$

where, μ_D and μ_C are the mean value of demand (load) and capacity (strength) respectively, σ_D and σ_C are the standard deviations of demand (load) and capacity (strength) respectively.

2.2   General Characteristics of Ultimate Strength

The ultimate strength is affected by many factors including:

1)   Component scantlings (plate thickness, scantling of stiffener, supported span and space of plate and stiffeners, etc.)
2)   Material properties (elastic modulus, yield strength, stress- strain curve after yielding, etc)
3)   Initial imperfections (initial distortion, residual stress)
4)   Load type (static or dynamic (ratio between duration and natural period of structures), etc.)
5)   Additional loads (thermal load, lateral load in hull girder strength, etc.)
6)   Age-related deteriorations (corrosion, fatigue crack)
7)   Accidental issues (collision, grounding, and fire)
8)   Human factors (mal- operation)

It can be said that among the above-mentioned factors, imperfection is one of the most influential parameters on ultimate strength. The effect of imperfection, especially initial deflection, on the ultimate strength is briefly explained as follows.

In the case of stiffened panel under compressive loading, greater deflection is produced when initial deflection is present as an additional destabilizing moment is generated, and it reduces the ultimate strength.

As shown in the numerical results by Ueda et al. (1985), after buckling under the compressive loading, especially in the case of elastic buckling, the deflection of buckling mode increases more while deflection of the other mode decreases. Therefore, in discussing the effect of initial deflection on ultimate strength, it is necessary to discuss not only the magnitude but also the mode shape of initial deflection, as both can significantly influence ultimate strength.

The effect of initial deflection on buckling and ultimate strength is larger in shell structures that in column and plate structures because of the difference in the post buckling behaviour. The load carrying capacity of shell structure reduces greatly after buckling, and therefore the buckling strength can be usually treated as the ultimate strength in shell structure. A constrained plate structure under in-plane compression gradually increases after elastic buckling and reaches ultimate strength when it yields due to the bending moment caused by lateral deflection. In this case, the ultimate strength is different from the buckling strength.

The ultimate stage of hull girder bending under hogging moment occurs when the bottom reaches ultimate strength in compression after the strength deck reaches the yield stress in tension. In this case, the deck structure can maintain the yield stress after yielding.

Under the sagging moment, the hull girder can endure excessive bending moment after the strength deck reaches ultimate strength by redistributing the stress and sharing the load with other members. It then reaches ultimate strength when the stress of bottom structure achieves yield stress in tension. But in this case, the deck structure cannot maintain its resistance after reaching ultimate strength in compression. Accordingly, the hull girder reaches ultimate strength just after the time when the deck reaches ultimate strength. Therefore it is important to take into account the post buckling strength of stiffened structure for estimating accurately the hull girder ultimate strength under sagging condition.

The ultimate hull girder strength is reduced by the residual deformation from accidental loads such as grounding and collision, and it is also affected by corrosion and fatigue cracks due to repeated loads. The assessment of these effects on ultimate strength is essential.

In the case of composite structures, especially produced by fiber reinforced plastic, such as GFRP (Grass Fiber Reinforced Plastic), CFRP (Carbon Fiber Reinforced Plastic), and AFRP (Aramid Fiber Reinforced Plastic), the collapse behaviours differ from those of metallic structure, such as welded steel and aluminum alloy. In tension, FRPs only show small plastic deformation after yielding. An exception is when the composite material is composed of short length metal fiber and resin, in which sliding between fiber and resin can take place. In compression, buckling of fibers can occur in addition to buckling of structural member. Fiber buckling may greatly reduce the ultimate strength of the structural member in compression. When the structure is damaged by lateral impact loading, delamination between fiber and resin takes place, thus reducing the buckling strength of the fiber. Considerable research in this area in the aerospace field can be applied to the design of ship structure using composite materials.

3.   ASSESSMENT PROCEDURE FOR ULTIMATE STRENGTH

3.1   *Empirical and analytical methods*

3.1.1   *Introduction*

Analytical methods for predicting hull girder ultimate strength began with Caldwell (1965), who developed a direct assessment method for a simple rectangular stiffened hull section, taking into account material yield and buckling. Direct assessment methods were further developed by Paik and Mansour (1995) and others, but as these methods normally assume a stress distribution through the ship section, they tend to be limited to simple structural geometries, and cannot account for reduced post-collapse strength in compression. An alternative incremental iterative approach developed by Smith (1977) takes account of the longitudinal elasto-plastic response of individual structural components, including their post-buckling behaviour. In the years since these pioneering efforts, progressive improvements to both direct assessment and incremental iterative methods have led to versions of both approaches being adopted in the IACS rules.

Current research is focused on extension of these methods to biaxial bending and damaged structures; and the development of empirical formula for the strength of damaged structure.

3.1.2   Hull structures

Paik et al. (2013) further extended the Paik-Mansour direct assessment method by improving the assumed distribution of bending stresses at failure. Whereas the earlier Paik-Mansour formula assumed that only the tension flange (i.e., the deck or hull bottom) achieves yield stress in tension, the Modified Paik-Mansour formula allows for a more extensive region of tensile yielding (see Figure 2). On the compression side, the approach is the same as in the Paik-Mansour method, with the entire compression flange and a portion of the side shells at the compressive ultimate strength, and the remaining parts of the side shells in a state of elastic stress. The heights of the yielded area (h_Y) and the collapsed area (h_C) in the side shells are unknowns to be determined by satisfying force equilibrium in the section. An iterative procedure is described for determining these two unknowns.
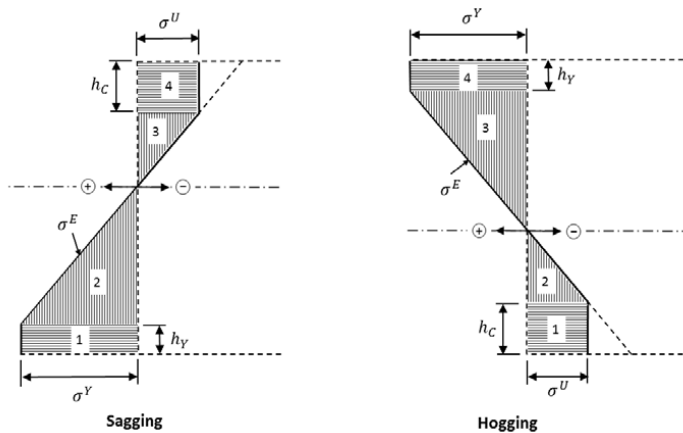

Figure 2. Assumed stress distributions used in the Modified Paik-Mansour method (Paik et al., 2013).

As with previous approaches based on aassumed stress distributions, the post-collapse behaviour of structure is not accounted for, potentially leading to un-conservative ultimate strength predictions. However, the results presented show that the method gives comparable ultimate strength predictions to other calculation methods (Smith's method, ISFEM, and FEA) for a wide range of hull types. The improvements to the original Paik-Mansour approach are shown to be most significant for double hull structures in hogging, where large regions of yielding can develop in the upper side shell. In other cases, the height of yield area (h_Y) remains small. Paik et al. (2012a) applied the modified method to the assessment of double hull oil tankers with grounding damage and compared the results with those obtained with FEA, ISFEM, and Smith's method.

Another important development has been the extension of Smith's method for progressive collapse to compartment level failure modes. Benson (2011) and Benson et al. (2013d) describe an approach in which load-shortening curves for compartment-length grillage panels are incorporated within the framework of a Smith's method approach. The load-shortening behaviour of grillage panels is determined using a semi-analytic method based on large deflection orthotropic plate theory. Benson (2011) describes the semi-analytical method in detail, which involves computing the collapse load for all overall collapse modes and comparing these with interframe collapse loads for plate, stiffener and beam-column modes to determine the mode of failure. The method can be used to determine the load-shortening behaviour of a grillage panel as well as the ultimate strength. The method is more efficient than nonlinear FEA of large grillage panels, and can be used when sufficient regularity exists in the structure. Example applications of box girders and aluminium hulls show that the compartment level collapse scheme can take into account interframe as well as overall grillage collapse modes.

Figure 3 gives the moment-curvature relationships for a box girder designs predicted using the compartment-level collapse analysis (ProColl), nonlinear FEM, and a semi-analytical interframe analysis method similar to the standard Smith's method. The results are given for both a lightly framed (T1) and a heavily framed (T2) design variants. The results indicate that the moment curvature responses and ultimate strengths for lightly framed designs deviate widely from the interframe solution; while ProColl predictions agree well with FEM results obtained using ABAQUS.

Reliability studies of hull girder ultimate strength often use Smith's method within the context of a Monte Carlo simulation scheme (e.g. (Gaspar and Guedes Soares, 2013)). This work is covered more fully in the Reliability section.

(a) Moment-curvature response under vertical bending   (b) Deformed mesh plot
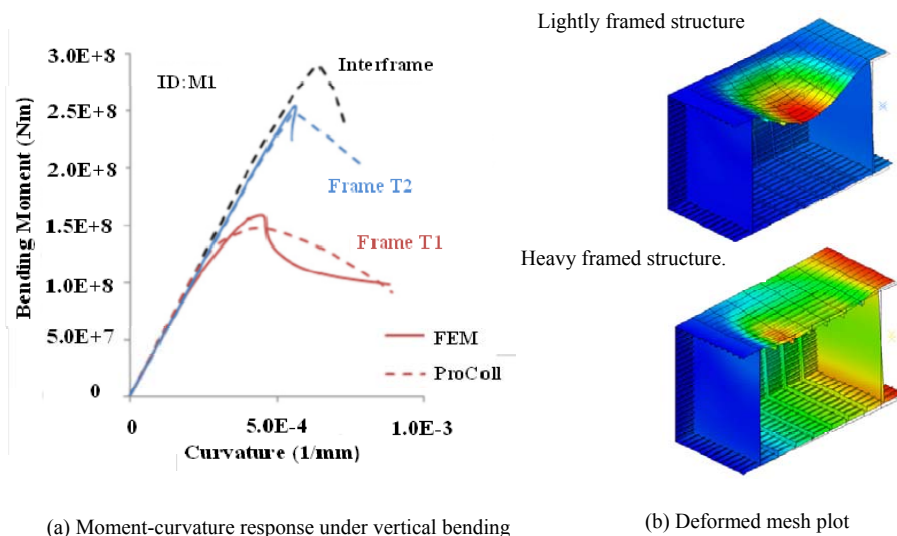
Figure 3. Calculation results of ultimate strength for box girder models (from (Benson et al., 2013d))

3.1.3   Residual Strength of Damage Hull Structures

An important step forward has been the development of Residual Strength vs Damage Index (R-D) diagrams and their associated empirical formula for representing the residual bending strength of hull girders with grounding damage. Paik et al. (2012a) developed empirical formulas for residual strength of double hull oil tankers of the form,

$$\frac{M_u}{M_{u0}} = A_2 GDI^2 + A_1 GDI + 1.0 \tag{3}$$

where, M_u is the residual strength of the damage hull girder, M_{u0} is the ultimate strength of the undamaged hull girder, and the grounding damage index (GDI) is given by

$$GDI = \frac{A_{ro}}{A_{oo}} + \alpha \frac{A_{ri}}{A_{oi}} \tag{4}$$

where the first term is the ratio of the area lost by grounding damage (A_{ro}) and the original area of the outer bottom (A_{oo}), and the second term involves a similar area ratio for the inner bottom. The parameter α is a correction factor that weights the contribution of the inner bottom to the hull girder ultimate strength.

The coefficients A_1 and A_2 are determined by fitting curves to ultimate strength calculations plotted on an R-D diagram. By these empirical relations, the upper limits of GDI satisfying the IMO requirement for residual strength of $M_u/M_{u0} \geq 0.9$ are determined for the four tanker designs. The results, given in Table 1, show that that the Panamax design is more damage tolerant to grounding than Suezmax, Aframax and VLCC designs. The main factor influencing sensitivity to damage appears to be ship length, and the upper limit of GDI is found to be linearly related to the overall length.

Table 1. Upper limits for the grounding damage index (GDI) for four sizes of double hull tanker (from (Paik et al., 2012a)).

	VLCC	Suezmax	Aframax	Panamax
Hog	0.2882	0.2992	0.3376	0.3965
Sag	0.4225	0.4344	0.4366	0.4363

Kim et al. (2013a) used a similar approach to develop R-D diagrams and empirical relations for four container ship designs with grounding damage. The upper limits of GDI satisfying the IMO residual strength requirement are given in Table 2 for four sizes of container ship. Kim et al. (2014) also developed time-dependent R-D diagrams and associated empirical formula to describe the combined effect of grounding damage and time-based corrosion wastage.

Table 2. Upper limits for the grounding damage index (GDI) for four sizes of container ship (Kim et al., 2013a) .

	3500 TEU	5000 TEU	7500 TEU	13,000 TEU
Hog	0.2882	0.2992	0.3376	0.3965
Sag	0.4225	0.4344	0.4366	0.4363

In general, asymmetric damage to a hull results in structural asymmetry as well as a biaxial loading condition if flooding results in a non-zero heel angle. Some researchers have attempted to improve the accuracy of Smith's method in this situation. Choung et al. (2012a) developed version of Smith's method in which the position and rotation angle of the neutral axis plane is calculated and updated as bending moment loads are applied. Their work differs from previous biaxial formulations of Smith's method in that the moment plane (plane normal to the moment-producing shear forces acting on the hull) is defined as an entity distinct from the neutral axis plane. In the general case of an asymmetric hull with a nonzero heel angle, the neutral axis plane may be both displaced and rotated from the moment plane. By this method, the vertical bending strength of a double hull tanker is evaluated using a Smith's method scheme for grounding and collision damage scenarios, in which damage is modelled as loss of structure. It is shown that the standard Smith's method approach (as recommended in the IACS CSR) can result in overestimation of the ultimate strength, particularly when asymmetric damage to the hull girder and a large heel angle are present.

Muis Alie et al. (2012) and Muis Alie (2013) derive a generalized expression for the incremental moment-curvature relation of an asymmetric cross section under-biaxial bending. Their expression is similar to those that have been previously developed, but use a derivation that is closer to the original Smith's method approach developed by Smith C.S. They apply their formulation to two bulk carrier and one oil tanker designs with different amounts of damage to the side shell, where damage is again modelled as loss of structure. The moment-curvature relations are computed both with and without rotation of the neutral axis for the case of an applied vertical bending moment. In their formulation, neutral axis rotation arises from the growth of a horizontal component of curvature of the asymmetrically damaged hull. Their results show that in some cases, a significant overestimation of the vertical strength can arise by not considering the neutral axis rotation (horizontal curvature component). Fujikubo et al. (2012a) extended this work by deriving simplified formulae for the residual strength in terms of elastic properties of the section and the strength of a critical member. The simplified expression is shown to compare well with direct calculation of the residual strength using the HULLST program.

Two studies have treated residual hull girder strength for more specific damage cases than simple loss of structure. Liu et al. (2012) proposed a combined elastic and rigid-plastic approach to determine simplified load-shortening curves of double bottom structure subject to indentation damage. The ultimate strength of damaged longitudinal stiffener-plate combination was determined to be the intersection point of the load-deflection response for elastic compression and bending, and that of the rigid plastic mechanism. The indentation damage for a longitudinal stiffener-plate combination was parameterized as a vertical denting distance (Δh) and a tripping angle γ (see Figure 4).

The method is applied to determine the ultimate strength and resistance-strain relationship for a double bottom structure with different amounts of indentation damage. Good comparisons between analytical with purely numerical assessments were obtained, as shown in Figure 5 for the case of 150 mm indentation damage of five stiffeners in an outer bottom structure.

Shi et al. (2012b) proposed a simplified formula for the strength under combined torsion and bending of an open box girder with crack damage. The proposed formula employs a cross-sectional area reduction factor to account for the loss in strength due to the presence of a vertically oriented crack in the side shell, as well as a reduction factor to account for loss of stiffness from the large opening in the girder. The proposed formula is applied to cases of pure bending, pure torsion, and combined bending and torsion. In general, ultimate strengths predicted by this method are very conservative in comparison to FEM calculations.
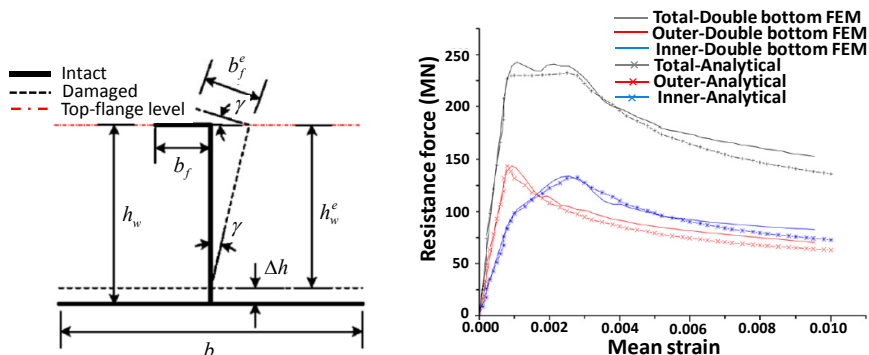
Figure 4. Simplified representation of indentation damage (left) and comparison of load-shortening curves (right) (from (Liu and Amdahl, 2012)).

3.1.4   Plates and stiffened plates

Researchers frequently use the results of a large number of FEA simulations to derive formulas describing the strength as a function of one or more parameters. For example, Silva et al. (2013) used this approach to describe the ultimate strength of rectangular plates with exponential functions of time, plate slenderness, and the degree of degradation (DOD) from randomized patterns of corrosion pits. By this approach, the expected (mean) value and standard deviation of ultimate strength is characterized. Jiang et al. (2012b)used the results of numerical analysis of plates with partial depth pitting to derive empirical formulas for the strength under uniaxial loading in terms of the plate slenderness ratio and the volume loss due to corrosion. Jiang et al. (2012a) followed a similar approach to derive empirical limit state relations for the strength of pitted mild steel plates under biaxial loading, also as a function of the plate slenderness ratio and the volume loss due to corrosion.

Brubak et al. (2013) developed limit state criteria for rectangular stiffened plates under compressive loading, where plate edges are either simply supported on four sides, or are simply supported on three sides and with one free or partially restrained edge. The ultimate strength of the stiffened plates is calculated using these criteria using a Rayleigh-Ritz method in conjunction with large-deflection theory and an arc-length solution method. Examples of stiffened plates with different support and stiffener arrangements are compared with FEM results. Yang et al. (2013) used a similar semi-analytical approach in the context of small deflection theory to analyse the compressive ultimate strength of simply-supported rectangular composite plates under uniaxial loading.

A different approach was taken by Cho et al. (2013), who adopted the generalized Merchant-Rankine formula as the basis of an empirical representation for the ultimate strength of stiffened plates subject to axial and transverse compression, shear loads and lateral pressure. Euler-column buckling, overall grillage buckling, stiffener tripping, and plate buckling in compression and shear, are all accounted for using elastic buckling stresses, each with an applied knockdown factor. The knockdown factors are determined by regression, using numerical results in which each load type (axial compression, transverse compression, and shear force) is applied separately. Predictions for combined axial and transverse loading show good comparison with numerical results, except for thickest plates where the proposed formula tends to underestimate ultimate strength. The stiffened plates used in the study were similar to those described in the ISSC 2000 committee V1.2 report. These included flat bar, angle-bar and tee-bar stiffened plates, with plate, column and stiffener tilt imperfections.

3.2   Numerical methods

3.2.1   Introduction

Since Caldwell (1965) firstly proposed a rational method considering both buckling and yielding effects, there has been continuous effort worldwide with regard to the study of ultimate hull structure strength and many researches have been carried out. The existing methods for calculating ultimate strength of hull structures can be classified into three categories: direct methods (linear method, empirical formulas), progressive collapse analysis (Smith method), and numerical methods such as idealized structural unit method (ISUM) and nonlinear finite element method (nonlinear FEM). Currently, numerical research on ultimate strength of hull structures focuses on the idealized structural unit method and nonlinear FE approaches.

3.2.2   Nonlinear FE method

An early application of nonlinear FEM for the analysis of hull girders is presented by Kutt et al. (1985), who uses the ABS nonlinear FEM program USAS to calculate the longitudinal strength of four ship hulls including a passenger ship and a tanker. In recent years, with the development of computer technology, many FE programs have been applied to ultimate strength analyses of hull structures, such as ABAQUS, ANSYS, MARC, ADINA.

Typically, nonlinear FEM analyses of the progressive collapse utilize a static solver together with an equilibrium convergence iterator using either the Riks arc length method or modified Newton-Raphson method, (Cook et al., 2002). The static solver assumes that the time dependent mass and inertia effects are small and thus can be neglected, (Hibbitt et al., 2010), which implies a quasi-static structural response. This is usually valid if the loading frequency is less than a quarter of the lowest natural frequency of the structure.

S4R quad elements (4 node finite strain elements with reduced integration) are widely applied when dealing with nonlinear problems using ABAQUS, (Shi and Wang, 2012a) (Shi and Wang, 2012b), (AbuBakar and Dow, 2013), (Benson et al., 2013a), but other shell elements in ABAQUS are also used, such as S8R5, (Shanmugam et al., 2014), S4, (Amlashi and Moan, 2008), and S9R5, (Kim and Yoo, 2008). In analyses using ANSYS, the "Shell 181" element is commonly used as it is well suited for large rotation and large strain nonlinear applications.

Other FEM software such as ADINA and MARC are sometimes used for assessing the ultimate strength of hull structures. Hu et al. (Hu and Jiang, 1998) carried out the collapse analysis of 12 full-scale stiffened plates under axial and out-of-plane loads using the nonlinear FE program ADINA. Ferreira and used ADINA to perform nonlinear FE simulations for the ultimate strength prediction of isotropic and orthotropic plates under uniaxial compression and a four-node shell element MITC4 was applied. A series of collapse analyses were performed by Tanaka et al. (2014) applying the program MSC.MARC to stiffened panels subjected to longitudinal thrust by varying numbers, types and sizes of stiffeners.

Although the quasi-static response is commonly of interest for ultimate strength assessment, explicit dynamic solvers, such as LS Dyna, are now also used to overcome convergence difficulties in large models. Extending the model size for ultimate strength analyses to one hold or three hold models (to consider the effect of lateral loading on the ultimate strength) increases the complexity of the numerical model so that implicit static solvers often fail in convergence before reaching the post ultimate range of the structure, leaving the analyst without a result. Explicit dynamic solvers do not face this convergence challenges, but their results rely on controlling inertia and damping effects properly. Only if the inertia effect is reduced as far as possible, e.g. by increasing the time step size or reducing the displacement increment, i.e. reducing the loading velocity, a quasi-static solution can be expected. Otherwise the ultimate strength will be overestimated by a dynamic response. The box-girder benchmark of this committee, as presented in section 5.1, shows that a well-controlled explicit dynamic solution gives comparable results to implicit static solutions. The benchmark on a hull girder by this committee, given in section 5.2, clearly demonstrates the advantage of the explicit solver: Only the explicit dynamic solver obtains results for all cases to be analyzed. The implicit static solvers often do not convergence up to the final collapse. In cases where both implicit and explicit solvers have given results, it is again shown that the results agree well.

AbuBakar et al. (2013) provide a general approach for calculating the ultimate strength of box girders using a dynamic solver which was carried out in the ABAQUS explicit code. Benson et al. (2013a) compare static with dynamic FEM solvers for the intact box girder which indicates that either approach is valid for the purpose of progressive collapse analysis. LS Dyna is used for ultimate strength assessment considering lateral loads by Toh et al. (2014). Yamada (2014) demonstrates the feasibility of using explicit dynamic solvers to combine collision and collapse analyses.

Ships and marine components are examples of complex thin-walled structures that are composed of various plate elements including stiffened and unstiffened plates characterized by different combinations of geometry and loading conditions which are widely studied.

Hu et al. (Hu et al., 2004) analyzed the tensile and compressive residual ultimate strength of stiffened panels and unstiffened plates considering the effects of fatigue cracks using the FE method. Paik (2007) undertook series of ANSYS nonlinear FE analyses with varying the cutout size as well as plate dimensions to investigate the ultimate strength characteristics of perforated steel plates under edge shear loading. Alinia et al. (2007) (2008) investigate the influence of central cracks and edge cracks on the residual strength and stiffness degradation of shear panels considering various geometrical and mechanical characteristics of cracked panels using the FE program ANSYS. Paik (2008) investigated the ultimate strength characteristics of perforated steel plates under combined biaxial compression and edge shear loads with various plate dimensions. Paik (2009) examined the residual ultimate strength

characteristics of steel plates with longitudinal cracks under axial compressive actions by varying the crack location, the crack size, the plate thickness and the plate aspect ratio. Kumar et al. (2009) investigated ultimate load carrying capacity of stiffened plates with openings under axial load, and with axial and out-of-plane loads using ANSYS. Considering the effects of a random corrosion thickness distribution, Silva et al. (2013) investigated the ultimate strength of unstiffened rectangular steel plates subjected to uniaxial compressive load. Shanmugam et al. (2014) investigated the ultimate load capacity of stiffened plates subjected to combined action of in-plane load and lateral pressure using the computer code ABAQUS.

To simplify the numerical models and structure strength problems, hull box girders are commonly used by many authors to simulate large surface ships and double hull tankers.

Series of comparisons between results from nonlinear FEM analyses and tests of box girders are presented by Qi et al. (2005) providing an integrated framework of finite element analysis which can be used as benchmark of comparative study of ultimate hull girder strength. Amlashi et al. (2008) carried out ultimate strength assessments of the hull girder of a bulk carrier under alternate hold loading conditions based on the nonlinear FEA program ABAQUS. Kim et al. (2008) investigated the ultimate strengths of steel rectangular box beams subjected to combined action of bending and torsion incorporating the effects of residual stresses and initial imperfections using ABAQUS which proved in good agreement with those from other researchers' experimental investigations. The residual ultimate strength of cracked box girders was studied as a function of crack sizes and crack locations subjected to torsional loading using same FEA program by Shi et al. (2012a) and residual ultimate strength of open box girders with cracked damage under combined loads was investigated by Shi et al. (2012b).

3.2.3   Idealized structural unit method

The idealized structural unit method (ISUM) can allow rapid assessment of large structural arrangements by simplification into smaller constituent parts. The method has been widely recognized by researchers due to large advantage in reducing modelling effort and computing time compared with nonlinear FEM.

Ueda et al. (1974) proposed the concept of idealized structural unit in which a large structure member is regarded as one unit and this method was then applied to an analysis of offshore structures by Ueda et al. (1983). Paik et al. (1996) developed a program of non-linear analysis of large plated structure using ISUM which employed five types of the ISUM units (beam-column unit, unstiffened plate unit, stiffened plate unit, hard unit and virtual unit). Paik et al. (2001) used the ALPS/HULL software to investigate the ultimate strength characteristics of ship hulls with large hatch openings under torsion based on the ISUM units. Fujikubo et al. (2002) proposed a new simplified model for collapse analysis of stiffened plates in the framework of ISUM combining plate and beam-column elements. Paik et al. (2003a) presented a summary of pertinent ISUM theory and its application to nonlinear analysis of steel plated structures which illustrated the possible accuracy and versatility of the ISUM method. ALPA/SCOL (ALPS/SCOL, 2006) applied the ISUM as a computer program for the progressive structural crashworthiness analysis under collisions and grounding using three types of ISUM elements. Paik et al. (Paik et al., 2008b) compared ANSYS FEA with ALPS/HULL to analyze the ultimate vertical bending moment capacity of a double hull oil tanker structure which proved the validation of ALPS/HULL method solutions. Paik et al. (Paik and Kim, 2008) modeled the rectangular plate elements as ISUM plate elements to investigate the progressive collapse of box columns which was verified by a comparison with ANSYS nonlinear FEM solutions. Underwood et al. (2012b) used ISUM to investigate the collapse of stiffened steel panels and proposed a new ISUM for strength assessment of damaged structural arrangements.

3.2.4   Conclusion

In maritime industry, the ultimate limit state is now applied as a basis of structural design and strength assessment, (IACS, 2006b) (IACS, 2006a), (IMO, 2006) and (ISO, 2006), and it is now a mandatory task for structural design of ships and offshore structures. The nonlinear finite element method (FEM) has become a dominant computational approach for complex structural engineering problems with all modelling herein considers both geometrical and material nonlinearities. However, taking into account modelling effort and computing time when using FEM, ISUM can provide a preview of the ultimate collapse of ship structures before considering the conduct of nonlinear FEM, and more valid ISUM elements need to be developed. It seems that most of the collapse analyses neglect the time dependent mass and inertia effects and imply quasi-static structural responses while ultimate dynamic responses of hull structures due to the damage of grounding, collision and wave loads are still rarely studied.

3.3 *Experimental methods*

Experimental studies to assess the ultimate strength of whole ship structures are few. However, to understand the trend and direction, some experimental studies which can be helpful are discussed in this section. Generally, static ultimate strength experiments are controlled by applied displacement with very slow velocity, such as 0.05mm/s applied on compressive stiffened plate which can be considered as static or quasi-static loading regardless inertia effect, and static ultimate strength of stiffened plate can be obtained once reacting load reaches maximum value, followed by a decline process of the reacting load. Two series of longitudinally stiffened steel plates with and without transversal stiffeners subjected to uniform axial in-plane load carried out to study the buckling and post-buckling up to final failure (Ghavami and Khedmati, 2006).

Compressive tests on short, long and intermediate stiffened panels are conducted by Gordo et al. (2008a) (2011) (2012) by changing distance between transverse frames. Every kind of stiffened plate with different length has eight stiffened panels subjected to axial compression until collapse and beyond. The specimens are three-bay stiffened panels with associated plate made of very high tensile steel S690. The use of this very high strength steel led to the unconventional solution of using U stiffeners. Comparisons of this new stiffener type and conventional bar stiffeners or 'L' stiffeners are applied.
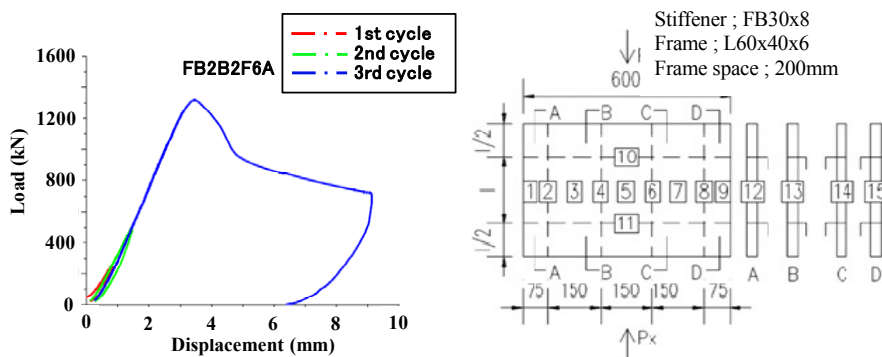

Figure 5. Load-displacement curve for a sample panel (Xu and Soares, 2013a).

Tests of narrow and wide Stiffened Panels under axial compression until collapse and beyond are presented to investigate the collapse behaviour and strength by Xu et al. (2013a) (2013b) which allows analyzing the effect of the width on the strength of stiffened panels. The tests were made on panels with two half bays plus one full bay in the longitudinal direction.

There are several ultimate strength experiments on plate or stiffened plate with cutout. Experimental investigations are carried out up to collapse on eighteen stiffened steel plates having square cutout, rectangular cutout and reinforcement around rectangular cutout (Alagusundaramoorthy et al., 1999). Rectangular plates made by 1200A aluminum alloy with central inclined crack subjected to axial compression are carried out (Paik, 2009). Residual ultimate strength of steel plates with longitudinal cracks under axial compressive actions is examined (Seifi and Khoda-yari, 2011) . Tests of buckling and post-buckling behaviours of steel plates having groove-shaped cutouts of various dimensions and angles subjected to axial compression are investigated (Shariati, 2012).

An experimental study on stiffened plates subjected to combined action of in-plane load and lateral pressure is investigated (Shanmugam et al., 2014). Lateral load carrying capacity of stiffened plate drops with increase in axial load and vice-versa. It is found that plate slenderness ratio has significant influence on the ultimate load capacity of stiffened plates subjected to both in-plane load and lateral pressure.

There are several ultimate strength experiments on aluminum plate or stiffened plates. Axial compression tests on longitudinally stiffened aluminum panels with open section (L-shaped) stiffeners and closed section stiffeners were carried out. And two deformation modes were observed in the tests; regular flexural buckling of the entire panel towards either the stiffener side or the plating side, and, for the case of the panels with L-shaped stiffeners, collapse initiated by stiffener tripping (Aalberg et al., 2001) . An experimental investigation of the torsional buckling strength of longitudinal stiffeners in aluminum panels subjected to axial compression is conducted by Zha et al. (2003). Torsion buckling strength of the stiffened panels is affected by the heat-affected zones and the reduction of ultimate strength is up to 34%. Mechanical collapse testing on aluminum stiffened plate about fabrication related

initial imperfections is investigated by Paik et al. (2008a). And corresponding statistical database of fabrication related initial imperfections on welded aluminum stiffened plate structures is also developed. An experimental investigation was carried out to determine the ultimate strength of welded stiffened aluminum panels subjected to in-plane compressive loads normal to the directions of the stiffeners by Rønning et al. (2010). A total of 21 panel specimens with various aspect ratios and both open and closed stiffener sections were tested. The panels failed by two different deformation modes; global flexural buckling and local buckling of the plate elements between the stiffeners.

A series of experimental studies by Gordo and Guedes Soares feature a box girder structure under vertical bending load. Pure bending test of a box girder with one span is conducted by Gordo et al. (2004). Then pure bending test of box girder made by mild steel and high tensile steel are conducted (Gordo & Guedes Soares, 2008b) (Gordo & Guedes Soares, 2009). Box girders with different spacing between frames are also investigated (Gordo and Guedes Soares, 2014).

Experimental assessment of the ultimate strength of a box girder with different levels of corrosion is conducted by Saad-Eldeen et al. (2011), (2013b). Corroded plate thicknesses have been measured in 212 points and a statistical analysis has been performed. The resulting corrosion wastage has been fitted by a non-linear time variant degradation model. Pure bending test of a hull model with three longitudinal box girder set on the deck is conducted by Wang et al. (2011).

Pure bending test of a container ship hull model under hogging is investigated to find possible failure modes and ultimate strength, based on similar conversion relationship (Gui-Jie & De-Yu, 2012) . Pure torque test of a ship-type hull girder with a large deck opening was investigated to find possible failure mode and torsional ultimate strength by Sun et al. (2003).

Dynamic ultimate strength of ship or offshore structures, due to the time-dependence of the load, is more complicated than static ultimate strength. In this condition, some additional issues have to be considered, such as inertia effect, dynamic constitutive equation of the material. A fluid-solid impact experiment was carried out by Li et al. (1993) for a plate falling on water from an over-water slamming tower. Results showed that fluid-solid impact load has the millisecond order duration and a half sine wave shape. According to the equivalent strain of a measuring point near the impacting end of the plate, three critical criteria were used to define the critical loads of dynamic buckling, dynamic plasticity and dynamic collapse. However, the position of the measuring point is somewhat arbitrary, which will results in uncertainty. Fluid-solid impact on stiffened plate was not investigated in Li's research. The elastic–plastic dynamic post-buckling characteristics of simply supported columns under axial solid–fluid slamming are experimentally investigated by Cui et al. (2000). According to observation of plastic collapse of the columns, a dynamic collapse criterion is defined. Experimental investigations on the dynamic plastic impact buckling of slender beams were conducted by Kenny et al. (2002). A 10 kg free-fall impact hammer applied an axial impulsive load to aluminum and cold rolled steel beams with a fixed-slide bearing boundary condition. Cui did similar experiments and numerical simulations, and presented similar conclusions Cu et al. (1999), Kiat et al. (2000) and compared to Li's research. A series of dynamic collapse tests were carried out on steel plates under axial compressive loads by Paik et al. (Paik and Thayamballi, 2003b), with loading speeds varying from 0.05mm/s to 400mm/s. Experiments showed that the dynamic ultimate strength of steel plates gets larger with the increase of the loading velocity. Experimental study was made for the dynamic crushing of thin plates stiffened by stamping with 1-3 parallel V-grooves in a clamped-end condition (So and Chen, 2007).

Currently structural reliability and uncertainty factors are seeing increased use in ship structures. Experimental data that can be used as target values for calibration of structural models is therefore necessary. Further experimental results on effect of ageing and imperfections in the analysis can be helpful.

3.4   *Reliability assessment*

Despite significant recent advancements in ultimate strength evaluation procedures, use of reliability methods to determine the level of uncertainty due to various parameters in the analysis is still ongoing, as is evident from the harmonization of the classification society rules. However, more and more studies are required in all the key design analysis of the ship structures so that uncertainty factors can be used in the rule calibration and reliability analysis can be used in daily design practice.

Deco et al. (2012) proposed a reliability assessment frame work of ships under different operational conditions. The reliability assessment was based on the flexural capacities associated with the ultimate hull failure and the failure of the first stiffened panel within the selected ship section. This study was extended to the development of a risk-informed decision tool for the optimal mission-oriented routing of ships by Deco et al. (2013).

Saydam et al. (2013) analyzed an oil tanker hull girder by varying speeds, headings and sea states and determined the reliability index for the intact and six damaged hull cases. The limit state function was based on ultimate strength of hull girder section at midship. Also, the robustness index associated with damage scenarios are presented using an optimization-based version of incremental curvature method. In addition, aging effects on ship reliability are investigated.

An advanced reliability assessment of ship hull is performed by Zhu et al. (2013) using a Bayesian updating method. They proposed an approach for reducing the uncertainty in the performance assessment of ship structures by updating the wave-induced load effects with the data acquired from structural heath monitoring (SHM). The proposed approach is illustrated with the Joint High Speed Sealift.

Zayed et al. (2013) considered the ultimate vertical bending moment capacity of the ship hull as a limit state to assess the structural reliability of ship hulls incorporating the effects of corrosion degradation and inspection and repair actions. The uncertainties in an inspection are accounted for by a probability of detection model that introduces additional probabilistic events at the different inspection times. Ship loading uncertainties are modelled based on the time ratio spent under each loading condition during the ship's service life.

An advanced study on the uncertainty analysis, Teixeira et al. (2013a) presented an approach to assess the ultimate strength response of plates considering the random initial distortions, random material and geometrical properties and random corrosion degradation. One important feature of this approach is that it provides both the information on the contribution of each variable to the uncertainty of the response as well as accurate predictions of the percentiles of the response in using general First-Order Reliability Method (FORM) considerations.

On the reliability assessment of damaged ship hull girder structure, Prestileo et al. (2013) investigated the scenario corresponding to bottom damage in the hull girder of an oil tanker. The accidental scenarios were modeled considering the mutual relationships that arise in this case between the load and strength stochastic variables involved. A wide range of specific bottom damage scenarios has been considered and different Bayesian Network models (as shown in the Figure 6) have been developed to investigate each one of them. The various damage cases are compared to each other and unconditioned to derive the probability of failure extended to the ship's life due to generic bottom damage. The vertical ultimate bending moment has been computed for many damage cases, using a simplified progressive collapse method.

Kim et al. (2013a) developed the residual ultimate longitudinal strength versus grounding damage index diagram (R–D diagram) for container ships. Each parameter (grounding damage location (transverse) in the direction of the ship's breadth, grounding damage height (vertical penetration extent), grounding damage breadth (transverse extent) and rock's angle) affecting the structural damage are dealt with as a random variable and are characterized probabilistically. In the present paper, the probability density distributions for the grounding damage parameters defined by IMO are applied. Also, due to computational cost limitations, only 50 damage scenarios have been selected. The grounding damage index is defined to represent the damage severity for each of the selected scenarios. The proposed R–D diagram should be useful for defining acceptance damage criteria and making rapid salvage plans or rescue schemes for containerships that have sustained a grounding accident.

Ibekwe et al. (2014) adopted Smith's progressive collapse approach to determine hull girder ultimate capacity. They combined the ultimate strength with user-defined iterative-numerical framework to determine the structural reliability of a frigate. Collision damage condition of the frigate is assessed under pure vertical bending and combined vertical-horizontal bending. Randomness in the geometrical, material and loading moment is considered and reliability analyses are performed by means of the curvature based Adaptive Importance Sampling (AIS). The user-defined framework is based on the application of an external numerical solver for the assessment of deterministic hull girder capacity and implicitly linked within a probabilistic model for structural reliability analysis.

Nam et al. (2012) predicted the ultimate longitudinal strengths of hull girder of a VLCC (designed according to the CSR-T) considering probabilistic damage extents due to collision and grounding accidents based on IMO Guideline. The probability density functions of damage extents are expressed as a function of non-dimensional damage variables. The accumulated probability levels of 10%, 30%, 50%, and 70% are taken into account for the damage extent estimation. The ultimate strengths have been calculated based on the progressive collapse method. Damage indices are provided for all heeling angles due to any possible flooding of compartments from 0 degree to 180 degree with 15deg increment which represent from sagging to hogging conditions, respectively. The analysis results reveal that minimum damage indices show different values according to heeling angles and damage levels. A concept of damage index is introduced in order to assess reduction of hull girder strength. In case of the collision, the damage index is lowest at the moment plane MP=0 deg. and highest at MP = 120 deg. In case of the grounding, the damage index is lowest at MP=180 deg. and highest at MP = 90 deg.
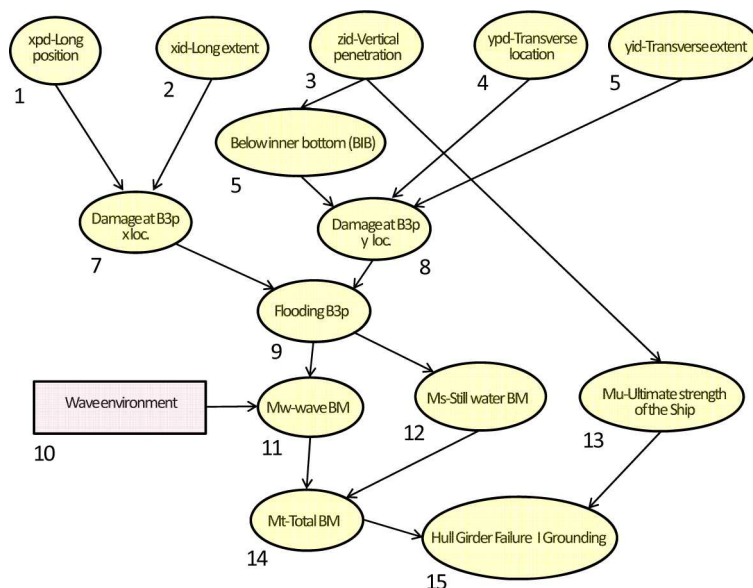
Figure 6. Example of Bayesian Network model (Prestileo et al., 2013)

In the continued study, Nam et al. (2014) investigated the effect of average compressive strength of stiffened panel on the hull girder strength and to assess the residual ultimate strength according to the damage extents of a very large crude oil carrier considering damage extents due to collision and grounding accidents. In order to determine extents of damage, two types of probabilistic approaches are employed: deterministic approach based on regulations (ABS, DNV and MARPOL) and probabilistic approach based on IMO probability density functions. Hull girder ultimate strength is calculated using Smith method which is dependent on how much average compressive strength of stiffened panel is accurate. A probability level of 80% in IMO; PDFs (Probability Density Function) is decided after comparison of reduced section area among other damage extent models. They concluded that the level of 80% in IMO PDF show similar or slightly larger area reduction than DNV ship rule.

Dyanati et al. (2014) estimated the seismic reliability of a fixed offshore platform against collapse in Persian Gulf area. With the base shear capacity and demand, seismic reliability analysis is performed using first order reliability method (FORM) and seismic fragility curves are developed. The analysis considers uncertainties in mechanical and hydrodynamic properties of members and foundation properties and loading from topside with different lateral load patterns (linear, quad and first mode) for pushover analysis. The capacity is evaluated through pushover analysis of the FEM at each iteration of FORM. Importance analysis of the design parameters is also assessed. The results of reliability analysis indicate that the seismic loading is not critical for the prototype structure as the lateral loads of wave and storm dominate the design of the structural members when PGA (seismic intensity measures) is less than 0.5g (that corresponds to much stronger earthquakes than rare intense earthquake in Persian Gulf, PGA=0.1g, where the platform is located). Moreover, different load patterns of seismic pushover do not affect the seismic fragilities in low probability of failures but do so noticeably when the probability of failure becomes higher. Also, the first mode load pattern leads to more conservative reliability results and is recommended to be used for the seismic pushover analysis of offshore platforms. Finally, importance analysis of the design parameters in the reliability analysis indicate that steel yield stress is the most important parameter that dominates the variability contribution to the limit state.

3.5   Rules and regulations

3.5.1   Harmonized common structural rules

(1) *Introduction and history*

The Harmonized Common Structural Rules (CSR-H) (IACS, 2014a) came to replace and combine the Common Structural Rules (CSR) for Double Hull Oil Tankers (IACS, 2006b) and Bulk Carriers (IACS, 2006a) that were adopted by IACS Council in December 2005 and came into force in April 2006 in one set of rules. The two sets of Rules were developed independently, and in an effort to remove variations and

achieve consistency, IACS made a commitment to Industry to harmonize the CSR. The harmonization project for the two sets of Rules began in 2008.

Table 3. Damage index for collision condition (Nam et al., 2014).

MP	Intact	ABS		DNV		MARPOL		IMO(80%)	
		CSR	FEA	CSR	FEA	CSR	FEA	CSR	FEA
0°	1.000	0.868	0.851	0.773	0.766	0.702	0.708	0.773	0.766
15°	1.000	0.874	0.863	0.778	0.763	0.693	0.681	0.778	0.763
30°	1.000	0.873	0.872	0.780	0.768	0.683	0.673	0.780	0.768
45°	1.000	0.873	0.876	0.779	0.772	0.671	0.663	0.779	0.773
60°	1.000	0.871	0.876	0.772	0.773	0.649	0.646	0.772	0.773
75°	1.000	0.856	0.861	0.749	0.751	0.599	0.597	0.749	0.751
90°	1.000	0.860	0.861	0.727	0.725	0.523	0.514	0.727	0.724
105°	1.000	0.991	0.986	0.904	0.893	0.661	0.654	0.904	0.892
120°	1.000	1.005	1.006	0.947	0.937	0.742	0.739	0.947	0.936
135°	1.000	0.989	0.996	0.950	0.945	0.762	0.760	0.950	0.945
150°	1.000	0.946	0.962	0.954	0.966	0.778	0.779	0.954	0.966
165°	1.000	0.924	0.932	0.886	0.898	0.794	0.804	0.886	0.898
180°	1.000	0.910	0.911	0.847	0.846	0.763	0.763	0.847	0.846

Table 4. Damage index for grounding condition (Nam et al., 2014).

MP	Intact	ABS		DNV		MARPOL		IMO(80%)	
		CSR	FEA	CSR	FEA	CSR	FEA	CSR	FEA
0°	1.000	0.983	0.981	0.848	0.863	0.988	0.991	0.773	0.779
15°	1.000	0.982	0.980	0.845	0.859	0.988	0.992	0.771	0.789
30°	1.000	0.978	0.979	0.829	0.840	0.986	0.991	0.758	0.771
45°	1.000	0.972	0.976	0.802	0.818	0.982	0.990	0.732	0.745
60°	1.000	0.967	0.975	0.776	0.799	0.981	0.990	0.703	0.721
75°	1.000	0.974	0.979	0.809	0.836	0.989	0.993	0.721	0.745
90°	1.000	0.999	0.999	0.861	0.884	0.996	0.995	0.798	0.828
105°	1.000	0.959	0.967	0.661	0.649	0.946	0.955	0.588	0.574
120°	1.000	0.949	0.951	0.669	0.657	0.945	0.946	0.588	0.581
135°	1.000	0.951	0.951	0.659	0.649	0.947	0.946	0.580	0.569
150°	1.000	0.950	0.951	0.653	0.635	0.946	0.946	0.576	0.555
165°	1.000	0.948	0.949	0.653	0.627	0.944	0.946	0.575	0.546
180°	1.000	0.947	0.948	0.654	0.620	0.944	0.946	0.578	0.543

The first CSR-H made available on 1st July 2012, they were issued in draft form for public review and comment during the first industry period from 1st July to 31st December 2012. This initial industry review period was followed by a second industry review period in the spring of 2013 and a review by IACS Societies' Technical Committees in the autumn of 2013. The rules were then adopted on 18 December 2013 and issued on 1 January 2014.

These Rules enter into force on 1st July 2015 and supersede the Common Structural Rules for double hull oil tankers, July 2012 and the Common Structural Rules for bulk carriers, July 2012.

CSR-H consists of two parts. Part one provides requirements common to both double hull oil tankers and bulk carriers and Part Two provides additional requirements applied to either double hull oil tankers or bulk carriers. CSR-H apply to the hull structures of single side skin bulk carriers having length L of 90 m or above and to hull structures of double hull oil tankers having length of 150m or above.

CSR-H covers the buckling and ultimate strength of structural members such as stiffened and unstiffened panels, corrugated bulkheads, struts, pillars, and brackets under part 1 Chapter 8. And also the CSR-H covers hull girder ultimate strength and hull girder residual strength in a damaged condition for ships with length greater than 150 m in under part 1 Chapter 5.

(2) *CSR-H vs GBS*

The IMO Global Based Standards (GBS) comes into force in 2016. Since the CSR was developed before the release of the GBS, it was expected that some of the requirements would not be covered while the CSR-H should be set out to achieve full compliance.

The original CSR complied with some of the GBS requirements when it came to considering the use of the wave scatter diagram of the North Atlantic and the design life of 25 years. This has consequences on several ship parameters; the long term period to be considered for the wave loads; the corrosion model to be considered for this design life; and finally, the influence on the fatigue damage calculations. The areas of

noncompliance were defined by IACS through a gap analysis and were addressed in the CSR-H. These areas included residual strength, structural redundancy and the wave induced hull girder vibration due to whipping and springing for oil tankers.

For residual strength, IACS introduced in CSR-H the evaluation of the residual strength of the hull girder of ships with length higher than 150m after collision or grounding as an effort to comply with the GBS requirement of providing a reasonable residual strength after damage. Also the ultimate strength of the hull girder is checked within the cargo area and in the machinery space for both collision and grounding scenarios. This is done by separately considering that the assumed damage zone is removed from the hull properties.

Structural redundancy was already applied to the side frames of single side skin bulk carriers. This approach was implemented to avoid the single failure of a side frame leading to an overloading of its side frame neighbours which could cause collapse and lead to the progressive collapse of adjacent frames. The result of the IACS approach was the scantling reinforcement of the side frames for yielding and for buckling. Subsequently IMO requested the same approach be extended to the areas of the cargo hold structure subject to impact by grabs. Based on in-service experience of IACS members, a stiffened panel typically does not collapse under a localized damage such as that which is defined. It is no longer a question of grab impact on the structure generating deformation or cracks. The considered damage is relative to normal sea-going operating conditions. Therefore in the IACS GBS submission IACS elected to demonstrate that stiffened panels of different sizes made of elements with different scantlings but which are of standard design in the shipping industry, have inherent structural redundancy to withstand localized damages.

(3) *Buckling and Ultimate strength Changes from CSR*

CSR-H presented some modification to the CSR hull girder ultimate strength and buckling requirements.
Hull girder ultimate strength
For hull girder ultimate strength, two major modifications were introduced. The first one was about the methods used for the appraisal of the ultimate bending moment and the second was to introduce a coefficient to take into account the local bending of the double bottom.
In the CSR-OT the hull girder ultimate bending capacity is calculated by the single step method or by the incremental-iterative method. The CSR-BC uses only the incremental-iterative method. As the single step method was used only for oil tankers, IACS decided in the harmonization process to remove the single step method and to keep only the incremental method.

For double bottom structure, where there is a large difference between external pressure acting on the bottom plating and internal cargo pressure loading the inner bottom plating, e.g. alternate loading condition, significant deformations and biaxial compressive stresses appear in the bottom plating in way of the mid-tank area and shear stresses load the ends of longitudinal girders in addition to hull girder stresses. These additional biaxial and shear stresses reduce the overall hull girder ultimate capacity. To account for this effect, a double bottom factor, γ_{db}, was introduced to consider the decrease of hull girder ultimate capacity by the above mentioned stresses corresponding to double bottom deformations. This effect obviously appears when the tanker is in the hogging condition. Consequently, the γ_{db} coefficient was fixed at 1.0 in the sagging and at 1.1 in the hogging condition except for empty cargo holds in alternate loading condition of BC-A bulk carrier. For this case, the γ_{db} coefficient was fixed at 1.25.

Direct Strength Analysis
In CSR, the direct strength analysis through finite element analysis is required only for amidships structure. After some concerns expressed about the validity of the approach and the strength of areas outside amidships, IACS decided to increase the scope of the direct analysis in the CSR-H to include the entire cargo hold region as well as the transition area forward and aft of the cargo region. As a result, loading conditions outside amidships and for the foremost and aft most cargo holds were developed and the boundary conditions, especially for the ends of the cargo area, were reconsidered and adjusted for this purpose.

Also, the details to be checked by the screening method in the midship area for CSR-OT are now to be checked in the full cargo area in CSR-H.

Buckling
The buckling control in CSR-H consists of three modules. The first module covers the slenderness requirements of plates, longitudinal and transverse stiffeners, primary supporting members and end brackets. The second module covers the prescriptive buckling requirements for members subjected to hull

girder stresses as plates and longitudinal stiffeners. The third module covers the buckling requirements for FE analysis of plates, stiffened panels and other structures such as cross ties.

The slenderness criteria are based on CSR-OT and consist of maximum permissible slenderness expressed as minimum thickness requirements, e.g. minimum thickness of plates, stiffener web or stiffener flange. For plates which will be assessed for buckling based on actual stress level, this requirement is a high slenderness requirement to avoid very thin plates resulting in very flexible structures with low stiffness. This is visualized as Area C in Figure 7. For flanges of stiffeners and primary supporting members a low slenderness requirement is applied so the flange is stocky and able to carry a stress very close to full yield stress to avoid local buckling of the free edge of flange/face plate. This is visualized as Area A in Figure 7.
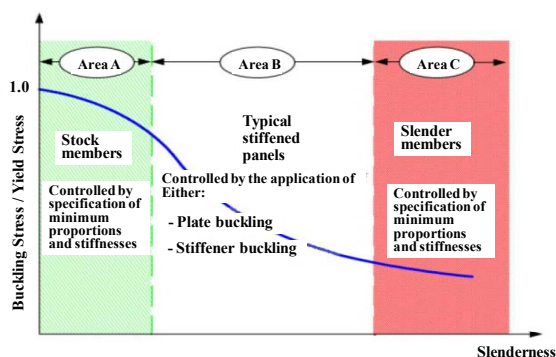

Figure 7 Concept of determination of scantling of stiffened panel in CSR-H.

The buckling capacity of plates and stiffeners is unified in a single toolbox applicable both for the prescriptive buckling check and the FE buckling assessment. This toolbox, referred to as the Closed Form Method (CFM), is a further development of the ultimate strength/buckling capacity method in CSR-BC and the prescriptive method in CSR-OT. The ultimate capacity of plate and stiffeners are defined as the ultimate limit state when the membrane Von Mises stress reaches specified minimum yield stress either in the plate or at the top of the stiffener. The main updates of the Closed Form Method are:

− Elastic buckling limit for stiffeners is included, as in the FE buckling method of the CSR-OT.
− Torsional buckling of stiffeners has been replaced with a warping stress component in the lateral buckling formulations for stiffeners.
− For short wave plate buckling pattern (longitudinal plate buckling), the rotational support along the long plate edge from the stiffener is taken into account.

Prescriptive Buckling Requirements

Buckling requirement for plates and stiffeners subjected to hull girder stresses are extended from the uni-axial buckling assessment in CSR-OT, where hull girder bending and hull girder shear are checked separately. In CSR-H, the prescriptive buckling assessment is based on a combination of hull girder bending, hull girder shear and local pressure similar to CSR-BC. Prescriptive buckling assessment shall be carried out both for acceptance criteria AC-S (frequent loads, static loads) and AC-SD (extreme loads in seagoing conditions, static + dynamic loads). This is also an increase in scope compared with CSR-OT which has only prescriptive buckling requirement for acceptance criteria AC-SD.

FE buckling

For FE buckling the scope is the same as in CSR-OT, however the method has been changed from the semi-analytical advanced buckling assessment method (PULS) to the Closed Form Method (CFM). The elastic buckling limit for the webs of primary supporting structures in CSR-OT has been replaced with the ultimate capacity based on plate panel without pull-in constraint at the plate edges, to avoid some of the conservatism in the elastic buckling

(4) *Consequence assessment*

A consequence assessment (CA) was carried out by IACS in order to determine the effect of applying CSR-H and presented in separate IACS individual Technical Background reports.

In the CA evaluation IACS Societies have used current and representative designs from major builders in Asia. The designs assessed in this CA are compliant with the July 2010 Common Structural Rules. For the consequence assessment the design has not been altered in any way. Strake size, seam locations, material properties, stiffener spacing etc. have not been altered. The consequence assessment is carried out using available software from each Classification Society and results were cross checked.

The consequence assessment was conducted on VLCC, Suezmax, Aframax, Panamax and Handymax oil tankers and also on Capsize, Babycape, Panamax and Handymax bulk carriers.

For most of the assessed tankers, the consequence assessment showed that CSR-H requirement for buckling and ultimate strength generates a scantling increase for most of the ship structure.

For mid cargo tanks, the keel, sheer strake plating and non-watertight girders in double bottom and non-watertight stringers in the double hull will see scantling increase due to minimum thickness increase. The main deck, longitudinal bulkhead and inner hull longitudinal stiffeners will see increase in section modulus due to more conservative buckling requirement. The FE buckling assessment also generated a scantling increase in areas located at the hopper structure, inner hull upper part, longitudinal bulkhead upper part, horizontal stringers in double hull and double bottom floors.

The keel in the fore-most and aft-most cargo tanks, sheer strake plating, non-watertight girders in double bottoms, and non-watertight stringers in double hulls will see scantling increases for most of the tankers assessed due to minimum thickness increase.

The fore part, aft part and machinery space will see scantling increase due to more conservative requirements for plating and stiffeners.

FE buckling assessment in CSR-H shows that the offered scantlings for transverse bulkheads and transverse web frames are not sufficient in some locations and will require reinforcement.

Also for most of the assessed bulk carriers, the consequence assessment showed that the CSR-H requirement for buckling and ultimate strength generates a scantling increase for most of the ship structure.

For the mid cargo holds, the Rule requirements for longitudinal stiffeners are more conservative in CSR-H (covering local pressure, prescriptive buckling) in comparison to CSR. Also some singe side shell plating does not meet the prescriptive or FE buckling requirements of CSR-H. This leads to scantling increase of various degrees.

The fore most and the aft most cargo hold will see increase in stiffener section modules due to more conservative stiffener requirements.

The aft part and the machinery space will see increase in side shell thickness due to minimum thickness requirement.

(5) *Technical and critical opinions for further work*

In the assessment of hull girder strength, the γ_{db} coefficient was introduced in CSR-H. Based on the CSR-H technical background (IACS, 2014b), the value of γ_{db} was determined from the nonlinear FE results. But the details of FEA, such as description of the solver used, model range, boundary conditions, mesh size, and imperfection amplitude etc …, were not shown. There are several papers that addressed the effect of lateral loading for hull girder ultimate strength. The calculated results are different each other, but the majority of these results show good agreement with CSR-H. But, further study is needed.

The scantlings according to CSR-H are somewhat more conservative than CSR. This is mainly due to using the conservative side of both CSR rules when a theoretical back ground is not clear. Further study is recommended in order to clarify the theoretical background, and if necessary, the rules should be modified accordingly.

Some of technical background documents are not sufficient. It is recommended that the unknown and unapparent items are clearly stated.

3.5.2   *Updates to offshore rules and guides*

No major changes have been made to the rules for buckling and ultimate strength for offshore structure. Below are the few minor changes that have been implemented to the ABS (2014), LR (Lloyd's, 2014) and DNV (DNV-OS-J101, 2014) documents.

The ABS guide for Buckling and Ultimate Strength Assessment for Offshore Structures introduced an additional check to its buckling control concept. In addition to checking the plate panels and the stiffened panels for bucking and ultimate strength, it was introduced a check to the overall strength of the entire stiffened panel to satisfy the required biaxial compression as satisfied in section 3-5.7 of the guide. The proposed change addressed the buckling state limit check for large panels. The original requirement is from ABS Rules for Building and Classing Steel Vessels.

The Lloyd's Register Rules and Regulations for the Classification of Offshore Units, July 2014 have been updated to implement similar buckling methods as in the CSR-H. For DNV, few updates related to buckling have been implemented to DNV document DNV-OS-J101 "Design of Offshore Wind Turbine Structures, May 2014".

In Section 7 "Design of Steel Structures" [7.3.1.4], the requirement for using a material factor of minimum of 1.2 for global buckling checks refers to IEC 61400-1 and is therefore changed to apply to towers. An extension to also cover monopiles is natural and has been included. An exception is made that a material factor of 1.1 can be used when formulas given in EN1993-1-6 are used for design.

In Sec.10 "Foundation design", a new item [10.3.2.7] regarding permanent buckling and plastic hinges in monopile foundations has been added.

4.   ULTIMATE STRENGTH OF VARIOUS STRUCTURES

4.1   Tubular members and joints

4.1.1   Tubular Members

Recent developments on the strength of tubular members focus on the various strengthening and reinforcing schemes for tubular members subjected to different loading conditions. Many researchers have examined two broad types of reinforcement on the strength of tubular members, i.e., the reinforcement using the fiber reinforced polymers and the steel-concrete composite structures. In addition, elliptical hollow sections, the design guides of which are still being developed, have emerged as an increasingly popular structural solution due to its aesthetic properties. As the accidental loading poses critical threats to the safety of such tubular members, recent research efforts have examined the resistance of tubular members subjected to lateral impacts.

Reinforced Tubular Members

Concrete-filled steel tubes (CFST) have emerged recently as a popular structural member owing to their significantly enhanced structural resistance with reasonably low cost. Goode et al. (2010) have examined the buckling of slender composite concrete-filled steel columns through an experimental program. The theoretical approach outlined in the Eurocode 4 presents a close estimation on the load bearing capacity of the concrete-filled, circular and rectangular hollow section stubs and long columns. Preloading on the concrete-filled hollow sections does not influence the load bearing capacities of the columns.

Lu et al. (2010) reported an experimental investigation on six full scale double skin tubular columns filled with self-consolidating concrete under fire tests. The double skin concrete-filled steel tubular columns exhibit superior fire performance compared to the hollow tubular columns and concrete-filled tubular columns. Kim et al. (2010) presented an experimental and numerical study on the load characteristics for steel and concrete tubular members under jet fire in floating production storage and offloading (FPSO) topsides, which can be used for the design of the passive fire protection. Uenaka et al. (2011) presented an experimental study on the mechanical behaviour of concrete-filled double skin tubular circular deep beams under three-point bending. Their study showed that the diameter ratio of the inner steel tube over the outer steel tube imposes a strong effect on the observed failure modes of the specimens. Han et al. (2011) (2012) reported some experimental investigations on the curved concrete filled steel tubular members under axial compression, with the focus on the following parameters: the tube shapes, the initial deflection and the slenderness ratio. The curved concrete filled steel tubes demonstrated a higher axial capacity than the straight concrete-filled steel tubes. Both types of members are designed with the same amount of eccentricity at the mid-height of the member. The eccentricity for the curved member, therefore, increases from zero at the support to the maximum value at the mid-height, while the straight members have a constant eccentricity along the length of the member. Dai et al. (2012) have proved the superior fire resistance of concrete-filled circular hollow sections in comparison to elliptical, rectangular and square hollow sections filled with concrete. Hou et al. (2013) developed the design equations to estimate the local bearing resistance of the CFST members based on a comprehensive experimental study.

Sundarraja and Prabhu (2012) have shown, through an experimental study of thirty specimens, that the external bonding of the carbon-fiber reinforced polymer (CFRP) on the CFST provides effective confinement pressure and delays the local buckling of the steel tuber under axial compression. The same authors have also demonstrated the significant enhancement on the flexural resistance of CFST members strengthened by CFRP composites through experimental studies. Li et al. (2013b) presented a calibrated numerical investigation on the high strength concrete filled square steel tubular columns with internal CFRP circular tube under bi-axial eccentric loading. Their study covers the effect of the material parameters for steel, concrete, CFRP, and the geometric slenderness ratios.

Elliptical Hollow Section

Elliptical hollow section (EHS) members have recently become a relatively new form of structural elements. Chan et al. (2010) presented a state-of-the-art review on recent researches on the elliptical hollow section members, including the elastic local-buckling and post-buckling, cross-section classification, response in shear, member instabilities, connections and behaviour of concrete-filled EHSs. Lam et al. (2010) have investigated experimentally the behaviour of axially loaded concrete-filled stainless steel elliptical hollow sections, with the objective to develop a set of new equations to predict axial capacity of the composite concrete-filled stainless steel elliptical hollow sections. Espinos et al. (2011) have reported a numerical investigation on the fire behaviour of concrete-filled elliptical steel columns. The fire resistance of the concrete-filled EHS depends on the slenderness of the column and the load level. For a certain column length and load bearing capacity, the circular columns attain higher fire resistance than the elliptical columns. Sheehan et al. (2012) examined the structural response of concrete-filled elliptical steel hollow sections under eccentric compression. Uenaka (2014) reported an experimental study on the capacity of concrete filled elliptical columns under compression and developed a method to predict the axial loading capacity to account for the confinement effects on the in-filled concrete. Dai et al. (2014) have subsequently confirmed from an extensive numerical investigation that the design rules in Eurocode 4 for circular and rectangular CFST columns can be used to calculate the axial buckling load of the elliptical CFST columns.

Impact Resistance

Accidental impact loads create a critical threat for the safety of the tubular members. Khedmati et al. (2012) have demonstrated, through a numerical investigation, that the impact resistance of tubular members decreases with increasing amounts of preloading. Their numerical study also confirms the significant effect imposed by different boundary conditions on the ends of the tubular members on the impact resistance. Wang et al. (2013) have investigated the impact response of concrete filled steel tubular members with various levels of confinement effect. The confinement ratio imposes a strong effect on the impact resistance of the CFST members. Han et al. (2014) developed a simplified model to estimate flexural capacity of CFST members under impact loads, based on an experimental program and a comprehensive numerical study. Wang et al. (2014) presented a comprehensive experimental and numerical investigation on the impact of circular hollow members and double-skin circular specimens (see Figure 8) filled with ultra-lightweight cement composite. They have demonstrated that the impact process for hollow pipes and double-skin pipes consists of three phases, namely the vibration phase, the stable phase and the unloading phase. The presence of the cement composite material in the annulus between the inner and outer steel pipes restricts the local indentation of the outer steel pipe and enhances significantly the impact resistance of the pipe structures.
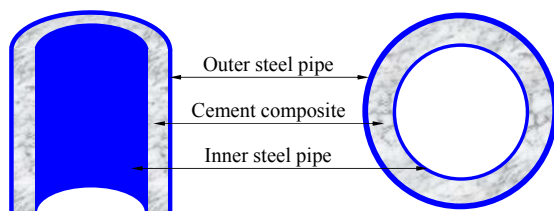

Figure 8. Configuration of the double-skin circular sections (Wang et al., 2014).

4.1.2   Tubular Joints

Similar to the latest development in tubular members, various reinforcement schemes have emerged recently for tubular joint due to the increasing demand by the industry to extend the operating life for existing offshore platforms. Due to the increasing number of aging facilities in both onshore and offshore infrastructure, the integrity assessment and residual strength examinations become increasingly important to ensure the safe operation of these structures in their remaining life. Recent research efforts have also covered the strength of complex tubular joints, e.g., the elliptical joints, multi-planar joints, for which the existing design codes do not provide explicit strength equations. In addition, many researchers have examined the strength of tubular joints under accidental loading, e.g., under fire and impact, to develop the basis for engineering guidelines in such limit states.

Reinforced Tubular Joints

Lohning et al. (2013) presented a finite-element based design of grouted joints with shear keys for offshore wind turbine. Their finite element analysis considers the complex interface between the grout

and steel materials, nonlinear material properties and geometric responses. Lesani et al. (2013b) have reported a numerical investigation on the fiber-reinforced polymer (FRP) strengthened T-joints under axial compression. The presence of the FRP delays the common failure modes, e.g., local bending of the chord member, punching shear, plastic failure of the chord, in otherwise un-stiffened joints.

Residual Strength and Assessment

In addition, residual strength of the fatigue cracked tubular joints has become an increasingly important concern for practicing engineers in assessing the aging structures. Qian (2013) have reported ductile tearing assessment procedure for high-strength tubular X-joints subjected to in-plane bending. Their study shows that the generic failure assessment curves do not provide a conservative assessment on the circular hollow section X-joints, compared to the geometric and material dependent failure assessment curve based on the option 3 failure assessment curve in BS7910 (2013). Qian et al. (2013a) has subsequently proposed a set of specific failure assessment curves for circular hollow section X and K-joints under brace axial loads. Meanwhile, Lie et al. (2014) have also presented a failure assessment diagram based approach to predict the plastic collapse load for cracked circular hollow section T and Y joints. Qian et al. (2013c) have further integrated the fracture representation in the load-deformation responses of tubular joints in the global frame analysis. Qian et al. (2013b) (2014) reported a new lamellar splitting failure for fatigue cracked tubular X-joints subjected to brace in-plane bending. The brittle splitting occurs at the mid-thickness of the chord wall and creates a fracture surface almost perpendicular to the fatigue crack surface.

Complex Tubular Joints

Zhao et al. (2011) have highlighted the recent developments in hollow section tubular joints, including the elliptical hollow section joints, the thick-walled joints, etc. He et al. (2013) compared the static strength of tubular Y-joints with and without partially thickened chord walls. They have proposed an equation to estimate the strength of the Y-joints based on a numerical parametric study. Chiew et al. (2012) presented an experimental and numerical study to examine the static strength of a complex tubular DKYY-joint. Internal reinforced circular plates in the chord member become necessary to avoid excessive plastic deformations in the chord. Lesani et al. (2013a) reported a detailed investigation on the un-stiffened T/Y tubular joints under axial compression. They have examined the critical stress fields near the brace-to-chord intersection of the T/Y joints and proposed subsequently a critical zone in the chord member near the crown point.

Strength under Accidental Loading

Recent research has examined tubular joints under accidental loads, e.g., the impact loads, the blast and fire conditions. Yu et al. (2011) reported an experimental study on the mechanical behaviour of tubular T-joint under fire loads. The T-joint specimen experienced an impact load before fire loadings were applied. Local buckling appeared to be the primary failure mechanism for T-joints under elevated temperatures. Jin et al. (2012) have presented an experimental and numerical study on the post-fire behaviour of tubular T-joints. The axial load level and the heating and cooling history impose significant effects on the compressive stiffness of the T-joints. Xu et al. (2012) have subsequently developed an artificial neural network approach to predict the ultimate bearing capacity of tubular T-joints under fire. The input parameter required in their neural network approach includes the diameter ratio between the brace and the chord, the chord radius to thickness ratio, the wall thickness ratio between the brace and the chord, and the temperature. The neural network prediction shows reasonable agreement with the finite element results. Tan et al. (2013) have also reported an experimental and numerical study on tubular T-joints subjected to axial compression in fire conditions. The increase in temperature leads to the deterioration of the material strength and therefore causes a more severe plastic deformation near the brace-to-chord intersection under elevated temperatures. He et al. (2013) reported the experimental investigation on circular hollow section K-joints subjected to brace axial loading under elevated temperatures. Local plastic yielding near the brace-to-chord intersection appears to be the primary failure mechanism for the K-joints studied. Qu et al. (2014) presented an experimental study on circular hollow section T-joints subjected to a drop hammer impact loading with the initial velocity between 7 to 10 m/s. They have proposed an approach to estimate the impact force based on the yield line theory.

4.2 Steel plate and stiffened plates

4.2.1 Introduction

Research efforts to further improve our understanding of the ultimate strength behaviour of stiffened panels is essential for the further development of methods for local and global strength assessment of ships and offshore structures. This is especially important when considering the continued adoption of

limit state practices for structural design. Stiffened plate panels form the fundamental building blocks of ships and offshore structures. A stiffened panel usually fulfils multiple functions within a structural arrangement, which may include:

- forming an external or internal barrier to water or other liquid cargo;
- supporting cargo or equipment loads;
- resisting local loads such as hydrostatic pressure, sloshing or slamming;
- contributing to the global strength of the platform under different loading conditions. A typical example in a ship is a longitudinally stiffened panel which forms part of the continuous longitudinal structure and resists longitudinal bending loads on the hull girder.

Proper treatment of all these functions, either in isolation or combination, is vital to a successful structural design of a stiffened panel.

Stiffened plating is usually arranged to form fully continuous or semi continuous structure running through the span of a thin plated structure. For a ship or ship shaped offshore platform, the continuous structure contributes to the resistance of global wave-induced bending loads of the main hull girder. Global bending of a hull girder imparts in plane axial loads on what are often relatively slender stiffened panels. They must therefore be designed with regard to buckling and elasto-plastic collapse when the dominant axial load acts in compression. This area of study continues to be important for improving code based design formulas and direct strength analysis procedures.

4.2.2 Analytical Formulations for Ultimate Strength of Stiffened Panels

Analytical methods continue to be developed for predicting the critical buckling load or ultimate capacity of a stiffened panel under in-plane compression. Whilst simple formulas may only predict an ultimate strength value, more advanced methods attempt to describe the nonlinear load-shortening behaviour of the panel. This may be useful for the direct strength assessment of the panel itself and is also essential information for application in ultimate strength analyses of the hull girder using the Smith progressive collapse method (known as the incremental-iterative method in IACS CSR) or Idealized Structural Unit Method (ISUM). Further development of methods for predicting plate and panel load-shortening behaviour under different loading conditions contribute to the enhancement of progressive collapse methods.

ISUM is an extendable approach where formulations for new types of elements (units) further improve its capability for different structural configurations. An extension to ISUM formulations for modelling the ultimate strength behaviour of very slender square plates and long plates under longitudinal axial load is proposed by Lindemann et al. (2013) using higher-order components to describe the collapse mode of such plates. Furthermore, a condensation procedure to eliminate the amplitudes of the panel deflection from the degrees of freedom for the plate is introduced so that ISUM elements can be more easily implemented in conventional finite element analysis frameworks, which handle only nodal degrees of freedom. The procedure is validated by comparison with the original ISUM plate formulation and with nonlinear FEA. Lindemann et al. (2013) investigate the influence of different components of the tangential stiffness matrix of a combined ISUM plate / beam-column element model as originally proposed by Fujikubo et al. (2002). It is highlighted that for the ISUM plate element the components derived by elastic large deflection analysis are dominant while for the beam-column element considering the rotational stiffness of the plating is essential.

The Smith method is well-established for predicting the interframe collapse of a hull girder under longitudinal bending, and is codified in IACS CSR for assessing the hull girder ultimate strength. An extension to the method, requiring an adapted large deflection orthotropic plate method with the capability to predict gross buckling of stiffened panels over multiple frame spaces, is proposed by Benson et al. (2013d). The adapted orthotropic plate method is able to produce the complete load shortening curve for a stiffened panel under uniaxial compression and accounts for the possibility of interframe and overall buckling modes. The method is used in an extended Smith-type progressive collapse method which can predict compartment level collapse modes of a lightweight hull girder.

4.2.3 Uniaxial Compression

IACS Common Structural Rules for Bulk Carriers (IACS, 2010a) and Tankers (IACS, 2010b), which are soon to be superseded by the recently adopted harmonized rules (IACS, 2014a), provide design formulations to determine the uniaxial buckling of the plating between stiffeners, column buckling of stiffeners with attached plating and lateral-torsional buckling or tripping of stiffeners. CSR formulae are also provided to determine the load-shortening curve for a stiffened panel for use in the incremental-iterative progressive collapse method. These code formulations form the basis of several recent validation studies, with differing levels of success in correlating between results.

Tanaka et al. (2014) examined the accuracy of the ultimate strength formulas in CSR for bulk carriers as well as PULS, which is a nonlinear orthotropic plate method by DNV. Nonlinear FE analyses of stiffened panels under uniaxial load are completed and show that both CSR and PULS give a good estimation of ultimate strength. The CSR formulae are also compared to equivalent nonlinear finite element analyses by Nam et al. (2013). This study showed some differences between methods and suggest some limitations in the CSR formulae, particularly for flat bar and angle bar stiffened panels. However, only three panels are investigated in total and so these findings cannot be taken as the general case.

Gaspar et al. (2011) applies structural reliability methods to assess the implicit safety levels of the buckling strength requirements for longitudinal stiffened panels implemented in the IACS Common Structural Rules (CSR) for double hull oil tankers. The study then uses this information to apply FORM optimization of the scantlings for both plates and longitudinal stiffeners in order to reflect the minimum strength required by the IACS formulations. The effect of corrosion is also considered for a sample of five typical oil tankers.

The ultimate strength of an arbitrary dimensioned stiffened panel can be related directly to the plate and column slenderness ratios. For example, the column collapse design curves published by Chalmers (1993) present a simple and direct way to determine the ultimate strength of panels stiffened by UK Admiralty long stalk tee bars. The curves are a function of plate slenderness, column slenderness and the ratio of stiffener cross section area to the total panel cross section area. However, as shown by Yasuoka et al. (2012), the ultimate strength can differ depending on the absolute size and number of stiffeners attached to the panel. When stiffeners are small, and attached to thin panels, overall buckling dominates and the ultimate strength differs depending on the number of stiffeners. When stiffeners are large and collapse is localized the ultimate strength does not vary so much regardless of the number of stiffeners.

Choung et al. (2012b) evaluated the distribution of slenderness ratios for plates and stiffened panels using data from 163 vessels including tankers, bulk carriers and container ships. The load shortening capacities of the stiffened panels derived from the CSR formulae are compared to equivalent nonlinear finite element analyses. Whilst ultimate strengths show reasonable correlation, the post ultimate behaviour shows considerable differences. A new relative average strain energy parameter is introduced to better account for post ultimate strength when using CSR formulations.

Several other papers present comparative studies of plates and stiffened panels with various geometries in uniaxial compression. Linear eigenvalue and nonlinear buckling analyses of 27 stiffened panels are presented by Ozdemir et al. (2013). El-Hanafi et al. (2013) present in-plane ultimate strength calculations for Y stiffened panels designed for a double hull tanker. The ultimate strength of cylindrical curved panels is investigated analytically, following the methodology outlined in Eurocode 3, and with nonlinear finite element analysis by Tran et al. (2012). The behaviour of cylindrical curved panels is shown to depend on curvature, slenderness and imperfections.

4.2.4   Multiple Load Effects

Secondary load components such as lateral pressure, biaxial load and shear may have a significant influence on the longitudinal capacity of a stiffened panel. Several papers use nonlinear FE analysis (NLFEA) to account for different combined loads.

Ergin et al. (2013) evaluate the effect of lateral pressure on the load shortening behaviour of 49 stiffened panels. Example results for four panels are given together with non-dimensional ultimate strength values for all 49 panels tested. The influence of lateral pressure on the average compressive strength of 189 panels including flat bar, angle bar and tee bar stiffener geometries are compared to CSR formulations by Choung et al. (2014). A new concept of the relative average compressive strain energy, instead of the ultimate strength, is introduced in order to rationally compare the average compressive strength through a complete compressive straining history. Similar to the authors earlier study (Choung et al., 2012b), whilst the ultimate strengths predicted by CSR and NLFEA compare well, there are larger discrepancies found when using the strain energy concept. Zhang et al. (2013) compare nonlinear FEM and CSR to predict the ultimate strength of stiffened panels from an AFRAMAX tanker under combined compression and lateral pressure. This study finds that CSR can over-estimate the panel ultimate strength. Xu et al. (2013b) examine the effect of different boundary conditions and model extents for NLFEA of stiffened panels under biaxial in-plane load and lateral pressure. The results show that a panel spanning two bays in the longitudinal direction adequately represents a continuous stiffened panel.

The influence of shear on the compressive capacity of a plate or stiffened panel is studied by Fujikubo et al. (2013). The modelling approach, using multi point constraints, is described in detail and an example stiffened panel is analyzed. Shear of thin steel plates at non-uniform elevated temperatures is studied by

Salminen et al. (2014). A comparison of the buckling of stocky and slender plates under shear and bending is completed by Alinia et al. (2012) using nonlinear finite element analysis and a theoretical p-Ritz energy method. This shows inelastic buckling in the stocky plates at the ultimate strength. The interaction relationship between shear and compression for a series of square plates are derived using nonlinear finite element analysis by Syrigou et al. (2014). Two different in plane restraint boundary conditions on the edges of the plate are investigated.

4.2.5   Panels with openings, cut-outs or rupture damage

Stiffened panels may be perforated deliberately by openings for running pipework, access hatches and other design reasons. A panel may also be ruptured accidentally due to a gross damage event, which can be approximated by removing structure. In both cases, the opening may be represented by a simple cut-out from the otherwise intact panel. The reduction in the ultimate strength of a panel in this condition is the subject of several papers.

The ultimate strength of perforated plates typically placed in ship structure for surveyor inspection, pipe runs and weight reduction are investigated by Park et al. (P2013) using nonlinear FE analysis. Longitudinal compression, transverse compression and in-plane shear were tested. Regression analysis was employed on the results to develop empirical ultimate strength design formulations. The ultimate strength of stiffened panels with rectangular openings are presented by Lee (2012), Yu et al. (2012) and Chang et al. (2014) using nonlinear FE analysis approaches. Lee presents an empirical formula for estimating the reduction in ultimate strength due to the opening shows good agreement with the numerical results. Elastic buckling of skew plates loaded uniaxially and containing openings are presented by Tahmasebi et al. (2011). The ultimate strength of a series of stiffened panels with cut outs to represent rupture damage are analyzed parametrically by Benson et al. (2013e). The ultimate strength is shown to reduce as the cut out size is increased and the results are presented in the form of column collapse curves for use in practical structural design. The influence of the lengthwise and spanwise sizing of the cut-out is investigated. It is shown that the strength is strongly influenced by the span of the opening, and is sometimes marginally influenced by the opening length. Length is particularly important if the cut out removes.

Bayatfar et al. (2014) presented the results of a numerical study investigating the influence of cracks (in terms of length and location) on the ultimate compressive strength characteristics of imperfect unstiffened and stiffened plate elements, used in thin-walled structures such as ship hull girders. The cracks were presumed to be through-thickness, having no contact between their faces and no propagation was allowed. Flat-bar profile is the considered stiffener type in this study and materials are in the category of high strength steel alloys. This study indicates that the length of cracks and especially its location can significantly affect the ultimate strength characteristics of unstiffened and stiffened plate elements subjected to axial compressive action.

4.2.6   Welding effects

The welding process has a significant influence on the fabrication factors associated with distortion and residual stress of stiffened panels and thus on the ultimate strength. The welding process will create residual deformations (distortions) in the panel, in particular out-of-plane deformations. These imperfections are today included in numerical simulations of the ultimate strength, and often modeled as a double sinusoidal variation in the plane of the panel.

To find the influence of the welding residual stress field, the shape of the residual stress field can often be approximated (idealized) for a fillet welded stiffener to a panel if a single pass weld is performed. In the longitudinal direction, a high tensile value in the weld region (often close to the yield stress value) balanced by a lower compressive value away from the weld region.

Khan et al. (2011) studied axial compression of longitudinally stiffened plates, using such an idealized longitudinal residual stress field and with the weld imperfections modelled with the double sinusoidal field. It is seen that the decrease in the ultimate strength depends on the magnitude of the residual stress and the slenderness of the plates, i.e. moderate thick plates are the most sensitive. Paik et al. (2011) studied a similar panel geometry and found that the effect of residual stresses is larger for thicker plates. They also modelled transverse residual stresses but found that they are less important prior to buckling for the axial load situation.

Khedmati et al. (2013) studied curved stiffened panels in axial compression using the same approach, and found that including the residual stress field will marginally reduce the ultimate strength.

Paik et al. (2012c) studied welding and subsequent buckling collapse of an aluminum stiffened plate. Welding residual stresses (or rather strains) and deformations have been measured for a panel with three bays. The shape of the welding residual stress field was found to be similar to the idealized stress field often

used. Experimentally determined buckling loads were compared to numerical results, and it is found that even if agreement was good, it is essential to have a good model of the residual stress and deformation field and the softening (yield stress) in the heat affected zone.

Tekgoz et al. (2013b) have studied the influence welding residual stresses in stiffened panels using both the approach described above, with an idealized longitudinal residual stress field, and by modifying the elastic perfectly plastic stress-strain curve used in the FE-simulations (as originally proposed by Faulkner). They found this second approach to be fast and give good results.

Tekgoz et al. (2013a) studied a tee-stiffened plate, i.e. one stiffener fillet welded to a plane plate, and show how the welding sequence for a stiffened plate influences the residual stresses and has a subsequent effect on the ultimate strength of the plate. The welding residual deformations and residual stresses are determined from thermo-mechanical FE analysis for three alternative weld sequences (in all cases the both sides of the stiffener were welded simultaneously). It is shown that the welding sequence is the most influential parameter which affects the lateral displacement of the stiffener, which then leads to more ultimate load carrying capacity. The welding sequence also influences the displacement of the plate edges which then governs the buckling shape of the plate. The welding residual stress field is used to determine a modified stress-strain curve to be used for ultimate strength calculations.

Gannon et al. (2013) studied the influence of the welding residual stresses and deformation on the strength of tee-stiffened panels under axial compression. Welding residual stresses and deformations were obtained from a full thermo-mechanic FE analysis. Two weld passes were used for the stiffener, being deposited sequentially with a cooling period in between. The simulations showed that the reduction in ultimate strength varied between 5% to 18% for all models and decrease with increasing plate slenderness ratio. In Gannon et al. (2012b) the effect of axial shakedown was studied for the same tee-stiffened panel. Axial shakedown reduced the tensile welding stress peaks and the amplitudes of the welding deformations. It was found that a partial relief of welding stresses would increase the ultimate strength somewhat, although the amount of reduction depends on the failure mode as the residual stress reduction is not uniform. The residual stresses are relaxed during the first cycle of a constant amplitude load history.

The influence of weld stiffness on the buckling strength of web-core steel sandwich plates is studied by Jelovica et al. (2012). The study demonstrates that lower weld stiffness results in lower transverse shear stiffness and also shifts mode intersections towards higher aspect ratios.

4.2.7   In service degradation

A parametric study of ship plates with non-uniform corrosion represented by a nonlinear random field approach and then placed in axial compression are tested using nonlinear FE analysis by Teixeira et al. (2013b). The results show that the complex corrosion process, which is spatially distributed using random fields, produces an ultimate strength which is in most cases lower than the one obtained using a uniform corrosion model.

The ultimate tensile strength of corroded plates, with the corrosion surface modelled using a random field model, are tested using nonlinear FE analysis by Htun et al. (2013). The stochastic properties of the ultimate tensile strengths of the corroded plate are then estimated using a Polynomial Chaos Expansion (PCE) Method and also a Monte Carlo simulation. The study shows that PCE can be used to determine the stochastic response with fewer samples. However, unlike the findings of Teixeira et al. (2013b) (which test plates in compression rather than tension), the ultimate strength of the plates using random field corrosion modelling are shown to have less strength reduction than when using a uniform corrosion model.

Jiang et al. (2012b) investigate the effects of corrosion pits on the ultimate capacity of mild steel rectangular plates under uniaxial compression. The simulations show that the volume loss dominates the degradation of the compressive capacity of pitted mild steel plates in addition to plate slenderness. An empirical formula was proposed to predict the ultimate capacity of pitted plates under in plane compression. The comparison between results from the FEM simulation and the formula showed a satisfactory fit.

A finite element procedure to determine the buckling behaviour of a cracked stiffened panel using a mixed shell-solid mesh is proposed by Kimura et al. (2013). Shell element modelling is usually used in large deflection elasto-plastic analysis of thin plated structures. However, shell elements are less suitable for simulating the local behaviour of cracks or defects. Therefore a solid model is used in the local crack region and attached to a shell model using rigid body elements.

4.2.8   Experimental Testing

The ultimate strength of a column segment typically found in square cross-section columns of new large-size semi-submersible platforms was carried out by Estefen et al. (2012). The modelling approach for

introducing imperfections was initially verified from small scale physical experiments on flat stiffened panels which were repeated with nonlinear finite element analysis. A numerical model of the column segment, including representative geometric imperfections, was then tested. The influence of imperfection shape and amplitude is presented, comparing results to measured imperfections from a shipyard using a laser tracker. The results show that initial distortions have a significant influence on the displacement to failure but less influence on the axial load capacity.

4.2.9   Optimization

There is continued interest in the development and use of optimization methods to design plates and stiffened panels for greater reliability, efficiency and economy. Such methods involve the optimization of multiple geometric variables such as the material type, plate thickness, stiffener scantlings and the number of stiffeners and frames for a given panel. Efficient optimization approaches employ analytical methods which can quickly determine the strength of a panel and can therefore be employed in an optimization algorithm.

Ma et al. (2013) apply two multi objective optimization methods, Pareto Simulated Annealing (PSA) and Ulungu Multi-Objective Simulated Annealing (UMOSA), for a single panel optimization and then extend the method to concurrently optimize a system of stiffened panels such as found in a ship structure.

Farkas et al. (2014) demonstrate the optimization of a square cellular stiffened panel (also known as a sandwich plate) with an objective function of minimum fabrication cost, using an orthotropic plate method to predict the strength and a systematic search algorithm to find the optima.

4.2.10   Conclusions

Research into the ultimate strength of stiffened panels for ship and offshore structures continues to receive worthwhile attention. The parameters which affect the load shortening and strength of a stiffened panel in compression are numerous and include the geometry, the stiffener type, the material properties, the support conditions and the load components. Nonlinear FEM is used to conduct parametric studies to determine the influence of certain parameters of interest. A particular focus over the last three years has been on the ultimate strength formulations proposed in IACS CSR. Attempts at validating the formulas with the results from equivalent nonlinear FEM are inconclusive, with some studies showing much better correlation than others. This perhaps demonstrates the limitations of using a single rule formulation when applied to a complex and multi-parametric problem.

Future work should continue to apply rigorous methods for setting up and analyzing nonlinear FEM of stiffened panels with adequate consideration of the geometric and material imperfections which have a significant effect on the resulting ultimate strength prediction. Further research into the effect of multiple load combinations on stiffened panel ultimate strength is essential to enable a better treatment of complex load patterns in progressive collapse type methodologies.

4.3   Shells

The effect of geometric imperfection on the buckling strength is larger in shell structures than in flat plate structures. Figure 9 shows the schematic diagram which presents the post buckling behaviour of plate and shell structures, in which the material assumed to behaves elastically.

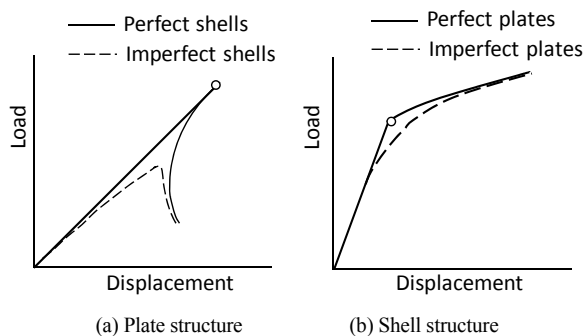(a) Plate structure   (b) Shell structure

Figure 9 Schematic diagram of post buckling behaviour

In the case of plate structures, the capacity does not reduce in the post buckling range although the rigidity after buckling is small compared to before buckling. On shell structures, the capacity reaches its

peak value at buckling and reduces sharply after buckling. The dotted lines in Fig. 1 show the behaviour of plate and shell with imperfection. A clear peak load at buckling is not apparent in plate structures, whereas the peak load of imperfect shells is much reduced in comparison with perfect shells. These are due to the difference of post buckling behaviour between plate and shell structures.

Koiter (1945) clarified the post buckling behaviour of shell structure. The Koiter formulation is based on the analysis of the potential energy of the loaded structure in buckled equilibrium configurations. Kotter initial postbuckling theory is a higher-order linearization that permits determination of slope and the curvature of the secondary path at the bifurcation point. After that, there are so many researches related to the effect of initial imperfection on the buckling strength of shells, such as Huchinson (1967) and Almroth (1966).

Shells are used for areas of ships with high curvature. The main structures of submersible vehicles, such as deep ocean research vehicles, deep sea rescue vehicles, and submarines, are constructed from shell structure. And also shell structures are used for the spherical tanks and cylindrical tank skirts in Moss type LNG carrier. In offshore floating platforms, critical parts are constructed from shell structures, which are curved or cylindrical panels which may also include additional stiffening for example ring stiffeners within a cylindrical shell. An example shell structure for an offshore structure is the column of a semi-submersible. Shells are also used for support structures used in the offshore environment such as piles, for offshore pipelines and for other submersible structures such as submarines.

As for the general buckling strength of ring-stiffened cylindrical shell under external pressure, Tokugawa and Bryant proposed a 'split-rigidity' method in which the formula for critical pressure consists of a shell term and a stiffener term.

$$P_c = \frac{Et}{R}\frac{\lambda^4}{\left(n^2+\lambda^2/2-1\right)\left(n^2+\lambda^2\right)^2}+\frac{EI_e(n^2-1)}{RR_S^2 L_s} \tag{5}$$

where, $\lambda = \pi R / L$, L; total length of cylinder, L_S; length between adjacent ring stiffeners, R; outer radius of cylinder, R_S; radius of neutral axis of ring-stiffener included effective breadth, E; elastic modulus, t; thickness of shell, n; circumferential buckling wave number, I_e; bending rigidity of ring-stiffener with effective breadth.

The main factor that determines the accuracy of eq. (6) is the effective breadth which is necessary for estimating the rigidity of ring stiffeners. Formerly, 2–3 times of shell thickness is adopted to coincide to the estimated collapse pressure to experimental results. These values are relatively smaller than actual ones because the experimental collapse pressures are reduced by initial imperfections. Pulos et al. (Pulos and Salerno, 1961) proposed the effective breadth of $1.56\sqrt{Rt}$ by considering the axi-symmetrical deformation of shell, but this value gives a little higher value. Yoshikawa et al. (2006) (2008) proposed the estimating procedure for effective breadth by considering both of axis-symmetrical and asymmetrical deformation. Further studies and verifications in this field are required.

The other buckling modes of ring stiffened cylinder under external pressure are shell buckling and torsional buckling of ring stiffener. As for the shell buckling, there are so many researches, such as Windenburg et al. (Windenburg and Trilling, 1934) and Yamamoto (Yamamoto, 1965), are found. The formulae for shell buckling strength have been proposed and the accuracy of formulae is confirmed by experiments, although there still have existed some errors in the cases with large size of ring stiffeners. On the other hand, there are few researches related to torsional buckling of ring stiffeners.

The buckling strength of ring stiffened cylinders under external pressure is investigated by Sawada et al. (2012). Specifically, formulae to estimate the torsional buckling strength of the ring stiffener are derived and validated with equivalent finite element analyses. The torsional buckling mode may occur if a large stiffener height is used for the ring stiffening. The analytical formulae are derived by assuming the cylinder as an equivalent flat panel and considering the stiffener web and attached plate as a spring. The method is adapted to account for the reduction in bending stiffness of the plate under compressive stress and the different spring stiffness of the plate and web. The resulting formulae correspond well to equivalent FEM analyses of a series of cylinders considering a range of stiffener heights.

As mentioned above, researches on the simple formulae for estimating the elastic buckling strength of ring stiffened cylinders under external pressure have been performed. To account for yielding, the equation of Johnson-Ostenfeld and φmethod can be adopted to estimate the elastic buckling strength, but there still remains the problem of what kind of stress must be considered as a reference stress.

Some research has compared numerical calculations for the buckling strength with FE analysis to experimental results.

An investigation into the use of nonlinear FE analysis for determining the collapse pressure of submarine pressure hulls is completed by MacKay et al. (2013). Results from 47 experimental tests on small-scale ring stiffened cylinders, with slenderness parameters equivalent to submarine pressure hulls, are compared to numerical results using ANSYS. Consideration is given to the material model, the out of circularity, artificially induced corrosion damage and boundary conditions. The accuracy of the numerical analysis is shown to be within 10% of experimental results with a 95% confidence interval, which is a significant improvement when compared to conventional design methods.

The effect of residual stresses on the buckling and ultimate strength of stiffened cylinders was numerically investigated by Cerik et al. (2013) with an emphasis on shakedown which might occur during the service, and the results of numerical calculation were compared with experimental results. They showed that yield level tension stresses induced by welding have a significant effect on strength and stiffness, and also that cyclic compressive loading does not cause any significant increase in ultimate strength although the compressive stresses at shell midbay locations are reduced by external loading.

Offshore pipelines experience significant axial, bending and pressure stresses during installation and operation on the seabed. Growing use of pipelines in deeper waters increases the bending deformation and pressure loading on the pipe, which can cause buckling and collapse if not correctly accounted for. Buckling modes include lateral (snaking) buckling, upheaval buckling and propagation buckling.

Gong et al. (2012) investigated how a buckle can propagate along a pipeline due to the combination of high external pressure and bending deformation at one point in the pipe. Experimental tests are completed in a hyperbaric chamber and are then compared to equivalent finite element analyses with good correlation observed.

Propagation buckling is also investigated by Albermani et al. (2011). Quasi-static propagation buckling tests in a hyperbaric chamber are completed and compared to a modified analytical solution and nonlinear finite element analysis.

Faceted pipe geometry is proposed to increase the propagation buckling capacity of the pipeline. The interaction between upheaval, lateral and propagation buckling is investigated numerically by Karampour et al. (2013).

Yudo et al. (2012) investigated the mechanical behaviour of pipe under pure bending load considering the oval deformation of the section. The study shows how nonlinear finite element analysis is required to account properly for the oval deformation in the pipe, which has the effect of reducing the buckling strength. The authors also investigate buckling of straight and curved pipes Yudo et al. (2014).

There are some investigations on how the production process used for pipes affects their buckling strength.

Large scale four point bending tests on spirally welded tubes for combined wall piles were performed by Van Es et al. (2013). Two tests are documented showing the performance of different steel grades and wall thickness. The tests show the buckling behaviour of the tubes and provide some verification of equivalent numerical analyses. Measurements of imperfection in the tubes were taken and compared to the eventual buckling location. These show that dimples created during cold forming play an important role in the location of the buckle.

Thick-walled steel pipes manufactured though the UOE process are used in deep-water pipeline applications. The UOE manufacturing process steps includes crimping U-ing, O-ing, and expansion. Chatzopoulou (2014) simulated the production process and also calculate the bending response of externally-pressurized pipe. The analysis showed that the increase of the total expansion value leads to minimization of the out-of-roundness of pipe, but at the same time it increases the hoop strain and consequently it reduces the collapse pressure resistance of the pipe due to the influence of Bauschinger effect. For combined pressure-bending loading condition, for relatively low external pressure levels, UOE pipes exhibit higher bending deformation capacity compared to seamless pipes. On the contrary, as the pressure level increases, the UOE pipes are less resistant to bending loads.

4.4   Ship structures

The research on ultimate strength of ships in the last years has been concentrated in few main topics. Following the publication of the new Classification Societies Rules designated as Common Structural Rules (CSR) concerning to ultimate strength, several works were dedicated to the comparison between the CSR and different methods of evaluating the ultimate strength of ships as presented in previous ISSC-Committee III.1 reports.

In the present period, special attention has been dedicated to progressive collapse methods, FE analysis and their applicability to intact ship integrity assessment, and degradation of the ultimate strength by corrosion or local structural damage. Also, some work was done on the effects of interaction between different types of loading and between vertical and horizontal bending.

4.4.1   *Progressive collapse methods*

Several researchers have been developing their own in house software for evaluating the behaviour of the hull girder under applied bending moment, covering intact and damage conditions, combined bending and corrosion, based on approximate progressive collapse methods. The original Smith's method consists of a tangent or differential method and the secant or direct method. The direct method is the one used by the CSR (Gordo and Guedes Soares, 1996) and may be represented by a simple equation as follows:

$$\overline{M} = \sum_i \overline{P}_i \times \overline{F}_i(\kappa) \tag{6}$$

where the position of the stiffened element is P_i, and the load in each element is F_i which depends on the curvature κ and the position of the neutral axis at each curvature, which requires an iterative procedure to balance the cross section. The above equations become the followings when horizontal and vertical bending are made explicit:

$$M_V = \sum_i (y_i - y_{na}) \sigma_i A_i \tag{7}$$

$$M_H = \sum_i (x_i - x_{na}) \sigma_i A_i \tag{8}$$

The secant method itself is not a progressive collapse method but the moment curvature relationship is obtained by calculating successive points of the curve and an incremental curvature procedure facilitates the convergence of the method at each step. With a linearization of the load shortening curves of the elements, the method may be used for ultimate strength assessment (Paik et al., 2013) .
The tangent method (Smith, 1977) (Yao and Nikolov, 1992) is a real progressive method and its potentialities are well and systematically described by Fujikubo et al. (F2012b). The governing equation is:

$$\overline{M}_{i+1} = \overline{M}_i + [D_i] \cdot \overline{\Delta\kappa}_i \tag{9}$$

The tangent stiffness matrix $[D_i]$ uses the slope of the load-shortening curves of the individual structural elements at each curvature. This first order method allows the 'differential' neutral axis, defined as the axis of zero variation of strain due to an increment of curvature, to be determined, which is not possible in the direct method.
   Recently several in-house implementations of the method prescribed by IACS CSR have been presented. Andric et al. (2014) compare some of them with their own software OCTOPUS and FEA for five different hull girder structures. A coefficient of variation of between 4 and 10% was found for the prediction of the different methods in the different types of structure. They concluded that differences among calculated ultimate bending moments are much higher for double hull tankers and bulk carrier than for container ship and single hull tanker.
   A comparison of several methods to predict the longitudinal bending moment-curvature relationship for a series of box beams representative of aluminum structures is made by Benson et al. (2013c), accounting for compartment-level, gross panel buckling effects of the orthogonally stiffened structure. The extended progressive collapse method is shown to compare favorably to the equivalent finite element analysis when overall buckling modes dominate.
Chenfeng et al. (2013) proposed an approximate approach by combining the progressive collapse mechanism and hull's beam theory. Similar work have been done by Li et al. (2013a).
   A method based on the kinematic displacement approach is proposed by Tayyar (2012) where the deflection of the hull is evaluated by the assembly of circular arcs by solving the differential equations of the beam theory. The same method was used by Choung et al. (2013) in conjunction with the formulas of the CSR.
   One of the most important part of information required by progressive collapse analysis if the definition of the load-shortening of stiffened elements. Gannon et al. (2012a) generated such curves simulating by FE the three-dimensional distribution of welding-induced residual stress and distortion, and applying it in Smith's method. Comparison with CSR and experimental data they concluded for a good agreement of the procedure with experiments. The same methods were used by Gui-Jie et al. (2012) for comparison with experimental data of a model of container ship' hull.
   The ultimate strength of composite ship hulls was studied by Misirlis et al. (2013) by developing a progressive failure model based on the finite element method. The analysis of the study leads to the

conclusion that differences failure criteria and modes of collapse result in significant differences due to interaction of local and global effects.

Makouei et al. (2014) developed software based on progressive collapse that uses as input the behaviour of large stiffened panels under compression instead of the discretized stiffened elements. The method is compared with the analytical incremental-iterative method proposed by the IACS CSR.

The effects of damage severity and location on the residual strength of a patrol vessel made with aluminum are investigated Taylor et al. (2013) using ISFEM (Intelligent Supersize Finite Element Method) and damage scenarios from DNV.

Toh et al. (2012) present a typical procedure of incremental-iterative method for the estimation of the ultimate strength of damaged ships. The stress-strain relations (σ-ε curve) for damaged members are obtained by FE analysis for tension and compression. Comparisons with the intact hull are used to establish the reduction rates of hull girder ultimate strength by damage.

4.4.2   Damaged structures

Benson et al. (2013f) used the progressive collapse method to assess the strength of several box girder models with different levels of ruptured damage applied and compare the results with FE analysis. The effect of the transverse and longitudinal extent of the rupture is investigated by changing the area and location of the damage.

Choung et al. (2012a) provide two convergence criteria to find translational and rotational locations of the neutral axis and relates it to the heeling angle of ship considering different asymmetries due to material, load and damage. It is concluded that the ultimate bending moment is correlated with the area reduction due to damage. The method was extended with a probabilistic approach to define the extension and location of damage applied to a VLCC (Choung et al., 2012a) (Nam and Choung, 2012).

Similarly an incremental formulation of the progressive collapse behaviour of hull girders with damage subjected to longitudinal bending is presented by Zubair et al. (2012) and Fujikubo et al. (2012b) based on the tangent method. Taking as examples bulk carriers and a tanker with collision damage in the side structures, the movement of neutral axis and biaxial bending response were analyzed. The effect of the side damage in the ultimate biaxial bending of the hull is shown for a different level of side damage.

Yamada (2014) proposes a numerical methodologies using FEA in assessing residual ultimate hull girder strength after collision simulation.

Makouei et al. (2015) also takes into account the influence of the rotation of the neutral axis on the residual hull girder strength of asymmetrically damaged ships under longitudinal bending to obtain a set of simple design formula to predict the residual strength of a damaged AFRAMAX tanker from its intact strength.

The hull girder is modeled as a beam with asymmetric cross section subjected to biaxial bending. The explicit expression of the rotation and translation of the neutral axis due to the buckling and yielding of structural elements is given. The proposed formulation is applied to the residual strength analysis of bulk carriers and a tanker having collision damages at the side structures. Particular focus is placed on the influence of the rotation of neutral axial on the residual hull girder strength and the solution procedures to obtain the residual strength including the case of biaxial bending.

Pollalis et al. (2013) present an investigation regarding the influence of modeling parameters in FE codes on the ultimate strength of intact and damage hulls. The rotation of the neutral axis and the bi-axial bending are studied to identify their effect on the reduction of the ultimate strength in comparison to the intact hull.

A simple model for predicting the ultimate strength of cracked box beams under torsional loads is proposed by Shi et al. (2012a) based on a FEA study considering different crack sizes and locations.

4.4.3   Corrosion

The effect of cracking and corrosion on ultimate strength of ships is analyzed by Gao et al. (2012). NLFEM and ISUM are used on container ships structures and simple equations are derived to correlate the ultimate strength with level of cracking and corrosion.

The effect of time-dependent corrosion wastage on the ultimate hull girder strength and geometric properties of the cross section is studied by Kim et al. (2012a) (2012b) both for different sizes of double hull oil tankers and container ships. The main objective of the study was to contribute to better definition of the corrosion addition on rules.

4.4.4   Complex ship structural components and complex loading

The ultimate strength of a Capesize bulk carrier hull girder under combined global and local loads in the hogging and AHL condition is performed by Shu et al. (2012) using FE software ABAQUS.
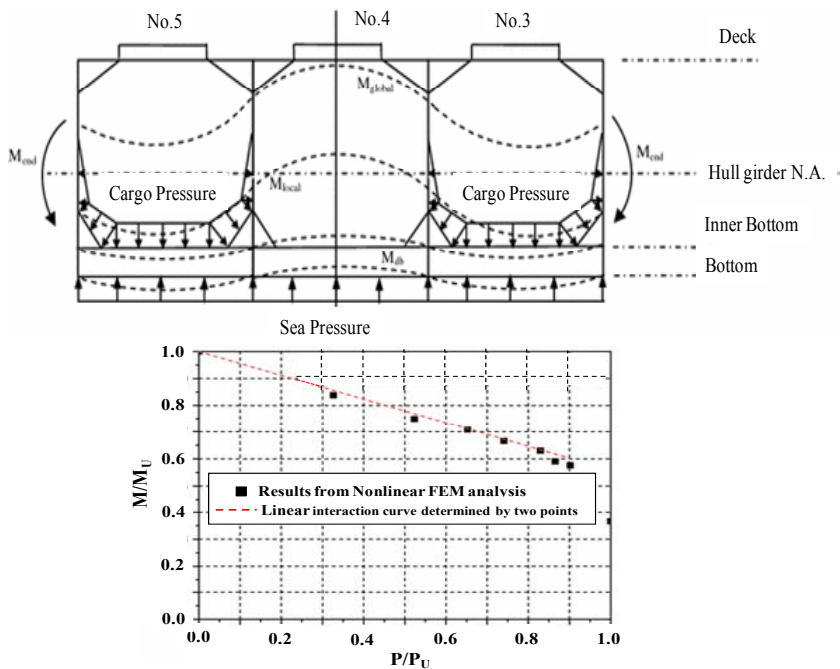
Figure 11. Interaction equation in AHL conditions and FE results. Ultimate pressure determined by FE analysis.

The effect of modifying the geometry of the existing ship to satisfy the new regulations was evaluated using design modification factor, which was determined to be 1.4. The research leads to the presentation of a practical interaction equation between global hogging bending capacity and average external sea pressure over the bottom in the form of:

$$M / M_u + \eta\, P / P_u = 1 \tag{10}$$

Toh et al. (2014) performed similar study for a Panamax bulk carrier under AHL condition but considering different levels of initial imperfections and found significant reductions on the ultimate strength due to both effects of about 25% which compares with the 37% found in the previous study.

Pei et al. (2013) noted that the double bottom of an empty hold is subjected to both longitudinal thrust due to hull girder bending in hogging and local bending caused by high pressure loads on bottom plating and applied different methods to this case of alternate loading condition. A new method was presented based on the Singularity Distribution Method and progressive collapse analysis by ISUM/FEM. The study concluded that the ultimate hull girder strength is reduced by roughly 20% due to local bending from secondary loads.

Some others (Kim et al., 2013b) pointed for a reduction of less than 10% due to the effect of the lateral pressure on the ultimate vertical bending moment of a double-hull oil tanker.

Related to the same subject, Gordo (2012) performed a study on the behaviour and ultimate compressive axial strength of a double-bottom subject to alternate lateral loading considering levels of lateral pressure.

Estefen et al. (2012) analyzed the behaviour of a complex part of the column of a new generation of semi-submersible platform up and beyond collapse. The buckling mechanism was related to the measured initial geometric imperfections. Different imperfection shapes generate different sequences of collapse deformations but the ultimate load does not change much, Figure 12. However a significant variation occurred in the displacement at collapse depending on the number of half-waves of imperfections.

Underwood et al. (2012a) investigated the influence of a damage-hole on the ultimate collapse strength of steel grillage arrangements. The influence of variations in geometrical arrangement of the structure is investigated through the use of FE analysis and the size and dimension of damage is represented by a hole

on the structure. Results indicate that the damage aperture may influence the type of collapse depending on the slenderness of the plate. The need to assess both interframe and overall collapse modes is pointed out as necessary to ensure a good prediction of the ultimate strength of a damaged structure.
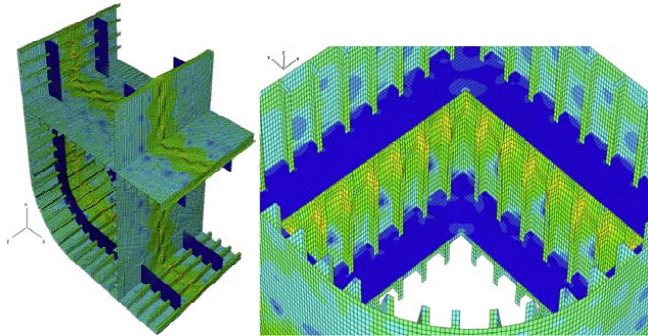

Figure 12. Different collapse deformations due to different shape of initial imperfections.

4.4.5   Reviews and applications

Zhang (2013) presents a review of buckling and ultimate strength assessment methods comparing them with FE analysis results for existing oil tankers and bulk carriers.

Gordo et al. (2011) consolidated the research done by the Portuguese marine center (CENTEC) on the ultimate strength of ship structures and components.

Geometrically and materially nonlinear finite element method and various incremental-iterative methods based on Smith's approach are benchmarked against the results of experimental testing of various stiffened box girders submitted to extreme pure bending by Kitarovic et al. (2013). The influence of various relevant aspects of the employed methods is evaluated and discussed considering global and local of structural response.

Li et al. (2013) analyzes the structural behaviour of a double skin bulk carriers by comparing FE results from elastic direct analysis with the nonlinear analysis in order to evaluate the safety margin of the ship.

The identification of the main parameters that influence the ultimate strength of welded aluminum ship structures and the validation of rapid assessment tools are dealt by Magoga et al. (2012), using ISFEM (Intelligent Supersize Finite Element Method) available in ALPS/HULL module of the MAESTRO to examine the ultimate hull-girder strength in vertical bending of a generic aluminum midship section. The results are compared with the UltSAS (Ultimate Strength Assessment) program.

Nikolov (2012) studied the progressive collapse behaviour of box girder models by FE analysis considering the effect of initial deflections and welding residual stresses. Unloading and reloading in the pre-collapse range are carried out to simulate the welding stress relief in experiments, and concluded that the ultimate strength was not affected by such alternate pre loading.

Saad-Eldeen et al. (2012) (2013a) (2013c) (2014) performed a series of simulations with FE to compare with the experimental results of corroded box girders under pure bending. Different elasto-plastic material models have been developed. Similar approach has been used by Xu et al. (2013a) to evaluate the ultimate strength of a tanker considering that the stress-strain curves of panels obtained in small scale tests are representative to the ones of stiffened panels of the compressive zone of a tanker hull.

The influence of different structural configurations of a river-sea container ship on the ultimate strength is evaluated by Zhang et al. (2013) and the limit state in combined action of bending and torsion is estimated by numerical and experimental evaluation (2013).

4.5   Offshore structures

Evaluation of the ultimate strength and history of collapse of structures in their intact and damaged conditions is one of the key issues in advanced design techniques based on explicit safety evaluation and collective optimization. The ultimate strength of an offshore structure is evaluated by using non-linear finite analysis of the structural model, where gravity loading is applied as an initial load step, then the ocean design loads for a chosen direction is incrementally applied until the ultimate strength of the structure is reached (Ueda and Rashed, 1991). As an important attribute that affects the life expectancy, requalification and life extension of the facility, the ultimate capacity of offshore structure can significantly influence the reliability levels and operational costs.

Studies on ultimate strength of offshore structures are rather limited compared with considerable number of documents on ships and ship-shaped structures. However, recent publications shed light on

effect of material property, aging factors (corrosion and fatigue), residual strength after collision with supply vessels, and ultimate limit state based design and evaluation.

Arjomandi et al. (2012) investigated the response of sandwich pipe systems subject to pure bending through a set of numerical parametric studies. The buckling response of the systems was evaluated by using the linear eigenvalue buckling analysis method, while nonlinear analysis was used to calculate the pre-buckling, buckling and post-buckling response. By employing nonlinear finite element analysis, the effect of significant geometrical parameters, material properties and the intra-layer interaction mechanism on the characteristic response of the systems was established. Ye et al. (2012) evaluated the ultimate strength of a typical drilling semisubmersible platform. The progressive collapse of the object platform was investigated using nonlinear finite element analysis with ANSYS. The analysis accounted for material nonlinearities but excluded geometrical nonlinearities and imperfections. The simulation results were compared with theoretical predictions by DnV rules and ABS rules and finally the corresponding ultimate limit state formulations were developed. An et al. (2014) investigated the collapse behaviour of sandwich pipe (SP) with strain hardening cementitious composites (SHCC) core under external pressure by both experiment and modelling. The SHCC preparation and the SP fabrication process are described in detail. Three SPs are tested using a hyperbaric chamber to obtain the very similar collapse pressure, demonstrating the reliability of the experimental results. A quarter-ring model is adopted to perform the FE analysis of structural behaviour of SPs under external pressure, where SHCC is modelled by a concrete damaged plasticity model. The accuracy of the model is verified by the good agreement between the numerical and experimental results.

Khedmate et al. (2012) calculated the ultimate strength of locally corroded tubular members under axial compressive loads in order to provide an initial estimation. To carry out this, a parametric finite element study was performed and the obtained results were examined against available experimental test. Then, validated models were used to derive a semi-empirical formula as a function of some parameters such as slenderness of the tubes and location of patch corrosion. It was found that location of corrosion has great effect on reduction of ultimate strength. Also, the study on the effect of corrosion geometry showed that tubes with different corrosion dimensions have different behaviours under compressive loads. Zhang et al (2012) investigated the effect of corrosion damage on ultimate strength of semi-submersible platform deploying a 3000m deep sea semi-submersible platform, see Figure13.

Their research indicated that corrosion damage has a significant influence on the ultimate bearing capacity of typical component and node on platform. The ultimate bearing capacity approximately decreases linearly with the increase of service years considering corrosion damage. Strength of typical component and node will be reduced and load will be enlarged under the combined effects of corrosion damage and various kinds of loads. Hence, long-term and regular anticorrosion of platforms is of great importance to improve the ultimate strength in the whole life cycle. Cerik et al. (2013) investigated the ultimate strength of damaged stiffened cylinders (by collision impact) subjected to combined axial compression and radial pressure, using the commercial FE code ABAQUS. After validating the numerical modelling strategy, a series of FE analyses were carried out for both damaged ring-stiffened and stringer-stiffened cylindrical shells, varying the extent of damage and the slenderness of the cylinders. This was done to derive formulas for predicting the residual strength of the damaged stiffened cylinders which can be useful for reliability-based studies for risk evaluation.
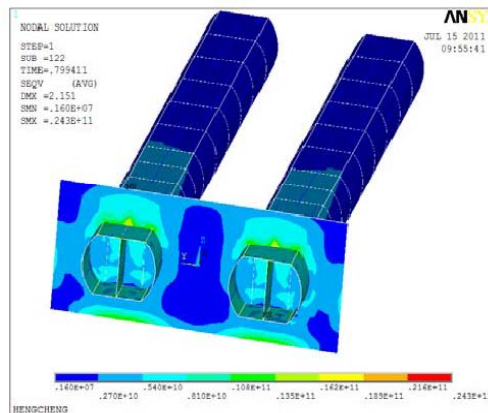

Figure 13. Stress distribution of typical component of semi-submersible platform (Zhang et al., 2012)

Nezamian et al. (2014) overviewed the ultimate strength assessments and their role in understanding the structural system response and failure modes to extreme loads for requalification and life extension of an oil field and for demonstrating fitness for purpose. An assessment of the structural integrity of thirteen identified platforms under existing conditions was undertaken as these platforms are nearing the end of their design life. This paper also describes an efficient method, the idealized structural system, to evaluate the failure modes in ultimate strength of structures. Its application to offshore frame structures was presented taking account of the nonlinear behaviour of members, joints, piling foundation and the structure as a whole.

Storheim et al. (2014) investigated the damage to offshore platforms subjected to ship collisions, see Figure 14. The effect of the ship–platform interaction on the distribution of damage is studied by modelling both structures using nonlinear shell finite elements. A supply vessel of 7500-ton displacement with bulbous bow is modelled. A comprehensive numerical analysis program is conducted. It was indicated that simplifying one body as rigid quickly leads to overly conservative and/or costly solutions, and is in some cases non-conservative. Current design guidelines for ship collisions with offshore structures need to be revised in view of significant increases in the supply vessel sizes and a wide variety of bow configurations that can exert significant collision forces over small areas on platforms.
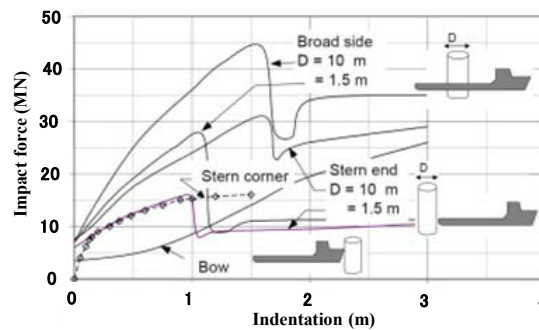

Figure 14. Force–deformation curves for a 5000-DWT supply vessel (Storheim and Amdahl, 2014)

Moreover, ultimate limit state based global structural analysis is addressed as well. Park et al. (2014) developed a hybrid substructure for a 5MW offshore wind turbine in order to reduce the wave forces. The fluid domain is divided into two regions to calculate the wave forces acting on the hybrid substructure with multi-cylinder and the scattering wave in each fluid region is expressed by an Eigen-function expansion method. The comparison between the mono pile and the hybrid substructure is made for wave forces. Using the wave forces obtained from this study, the structural analysis of hybrid substructure is carried out through ANSYS mechanical. It is found that the hybrid substructure system satisfy structural safety in respect of ultimate limit state (ULS). Lee et al. (2014) introduced a procedure of global structural analysis for a semi-submersible drill rig in accordance with DNV offshore rules. ULS of the unit was analysed with LRFD method for operating and survival condition.

It can be noted that available documented publications on the ultimate strength of offshore structures is rather limited compared with considerable numbers of publication on ship/ship shaped structures. Offshore structure is a huge assembly of various components depending on the required function and working conditions. Much efforts has been made on the ultimate strength at the level of specific components, i.e., stiffened panels, tubular members or joints; and on the effect of various parameters, i.e., composite material, initial imperfection, aging factors (corrosion and fatigue), less efforts have been made on the ultimate strength of the offshore structure globally and systematically. In this regard, systematic assessment of ultimate strength of offshore structures deserves further efforts.

4.6   Composite structures

Traditionally the use of composite materials in the shipbuilding industry was limited to pleasure crafts and small workboats. Nevertheless, in recent years there has been a reduction in the cost of composites structures mainly due to improved design tools, new fabrication procedures and reduction in the cost of high end materials. Furthermore, the need to achieve higher operational speeds and to reduce the maintenance costs is currently leading shipyards and naval architects to use composites in the design of larger vessels (Anyfantis and Tsouvalis, 2012). Mouritz et al. (2001) reports a steady increase in length of full composite vessels in the naval industry particularly outlining patrol boats, mine countermeasure vessels and corvettes and predicts that this trend could see warships between 120m-160m being built by 2020.

The increase in size of composite vessels has however uncovered new design and analysis challenges. Chen et al. (2007) (2008) state that the analysis of a composite ship structure should not be restricted to local structure, but that it should also include ultimate longitudinal strength assessment for ships over 60m. In fact, Chen et al. (2003) were the first authors to developed an analysis methodology for the evaluation of the ultimate strength of a composite vessel. Following a Smith's type approach Chen et al. calculated the ultimate strength of ship cross section using load shortening curves determined from composite column theory. This approach was later modified (Chen and Guedes Soares, 2007) (Chen and Guedes Soares, 2008) to include a progressive failure finite element model in the calculation of the ultimate strength of the ship panels.

In a progressive failure model the ultimate strength of the composite structure is determined by coding a suitable composite failure criterion within an incremental loading algorithm. Once failure is detected the degradation model is used to reduce the properties of the laminate to account for the material damage and to effectively weaken the panel. This iterative process, illustrated in Figure 15, is repeated until equilibrium is no longer possible. At this point the structure is deemed to have completely failed.
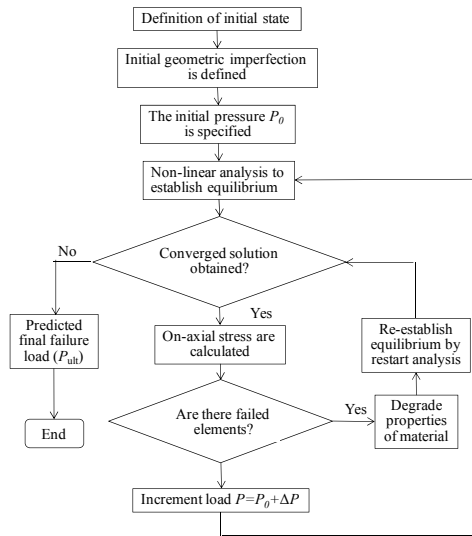

Figure 15. Typical flow chart of a composite progressive failure algorithm (Yang et al., 2011)

A recent example of a progressive failure analysis is the work by Yang et al. (2011) on the ultimate strength and reliability of laminated composite panels under axial compression. These authors used Tsai-Wu interactive failure criterion to identify the failure of the composite material combined with Engelstad failure terms to establish if the failure was caused by matrix fracture, fibre breakage or shearing failure. The material damage was represented using a limited, but constant, stiffness reduction specific for each one of the three previously listed composite failure modes. Good agreement between experimental and numerical predictions was obtained for thin and moderately thick plates however poor agreement was obtained for thick plates.

4.6.1   Failure identification and material degradation models

The accuracy and efficiency of a progressive failure finite element simulation hinges on two crucial components: an accurate composite failure criterion, used to identify the load that causes the initiation of failure, and a degradation model, used to represent the material damage progression until the ultimate failure.

Philippidis et al. (2013) introduced an anisotropic non-linear elastic constitutive model as well as failure onset criteria and degradation strategies in order to calculate the ultimate strength of thin to moderately thick composite structures under static loads. Puck and Schürmann, Lessard and Shokrieh as well as combined Puck/Chang-Lessard failure criteria were used in three models to predict the inception of failure in multi-directional (MD) laminates. Depending on the type of damage predicted by the respective failure criteria, two different degradation strategies were adopted. In case of matrix cracking a gradual degradation model was adopted whilst a total ply discount was used for fibre breakage. The

model accuracy was measured against simple experimental tensile coupon tests. Good agreement was found in all cases.

In a similar line, Moncada et al. (2012) evaluated the capabilities of the of two micro-mechanics theories, i.e. the generalized method of cells (GMC) and the high fidelity method of cells (HFGMC), for the progressive failure prediction of polymer matrix composites and also evaluated the influence of four different failure criteria (maximum strain, maximum stress, Tsai-Hill and Tsai-Wu) applied at the microscopic level. The results indicate that the choice of failure criteria has a significant effect on accuracy of the ultimate strength predictions with the maximum strain criterion showing the best agreement with the experiments. The differences in results obtained by switching between the GMC and HFGMC theories were small compared to those found among the four failure criteria.

The model allows the determination of the ultimate strength of laminates under complex tri-axial loadings. The model uses the macroscopic (laminate level) loading to calculate the state of stress at a microscopic (fibre-matrix level) level which allow to establish the failure and damage progression at the mesoscopic level.

The model was successfully implemented to provide predictions of failure envelopes and non-linear stress–strain curves of isotropic, unidirectional and mutli-directional laminates made of glass/epoxy and carbon/epoxy materials and subjected to 3D loadings, including through-thickness stresses.

Chamis et al. (2013) also present a MS progressive failure model to provide theoretical predictions of the ultimate strength of composite laminates. The critical damage events/indexes predictions tracked trans-laminar and inter-laminar composite failures. Composite laminates, with and without a central hole, were subjected to uniaxial tension and compression, bending and thermal load cases. Good agreement was found in all cases. It is noted that although accurate, due to its inherit complexity, the MS method proposed by both Chamis et al. and Carrere et al. are not yet suitable for design work.

It can be noted that all the investigations discussed so far have established the ultimate strength of the composite structures using a mesa-scale (lamina level) damage progression model. Gan et al. (2011) presented an investigation aimed at modelling the initiation and evolution of damage within a Glass Fibre Reinforced Plastic (GFRP) by including real geometric variability. The investigation implemented 3D textile modelling instead of classical laminate theory. Good agreement was observed between predicted and actual stress-strain curve, however the final failure was poorly predicted.

All damage material models used in the investigations discussed so far fall into the elastic damage category, limiting their application to laminates that exhibit and elastic-brittle behaviour. Nevertheless, some thermoset and thermoplastic composites exhibit a plastic response under transverse and shear loads. In order to establish the ultimate strength of composite structures with such characteristics, Chen et al. (2011) developed a combined plastic damage model for composites which accounts for both the plasticity effects and material properties degradation. The material model was verified by performing progressive failure analysis of composite laminated unstiffened panels with a central hole. The model showed sufficient accuracy in the prediction of failure loads.

4.6.2   Ultimate strength of composite stiffened panels and box girders

All the works discussed so far have focused on investigation of the ultimate strength of simple coupon type samples or unstiffened laminated panels. Anyfantis et al. (2012) state that the ultimate strength of composite stiffened panels has not been sufficiently studied. These authors proposed and validated a progressive failure methodology for the calculation of the ultimate strength of longitudinally, blade stiffened composite panels loaded in compression. The progressive failure methodology was incorporated into the commercial FE code ANSYS. It can be appreciated from Figure 16 that good agreement was achieved for test cases were the panels exhibit an abrupt failure mode. However it was found that the proposed methodology was less effective in panels that exhibit mode switch prior to failure. For these panels, it was recommended that inertial effects should be considered in the framework of a non-linear dynamic analysis.

The review of literature shows that very little work has been done on simplified models for the calculation of the ultimate strength of composite panels. Yang et al. (2013) have recently address this by presenting a modifying Brubak et al. (2007) (2008) semi-analytical ultimate strength models for isotropic stiffened models in an attempt to represent laminated composite panels. It is important to note that the model is still limited to the analysis of unstiffened panels only. Thin panels simulations show reasonable accuracy whilst thick panels show overly conservative results.

Recently, Sayyar et al. (2013) investigated the ultimate strength of pre-stressed composite box girders. These authors state that experimental results on aircraft stiffened thin-sheet composite structures, as used on aeroplane wings, indicate that the effective buckling strength is generally less than the tensile strength. The reversible nature of the stress systems in thin walled wing structures thus leads to a design solution governed by compression that leaves the superior tensile strength of the composite material under-

utilized. Experimental carbon composite box girder models pre-stressed using titanium rods were tested to destruction using a cantilever bending load case. It was found that the pre-stressing of the box girder increased the ultimate strength by 89% while adding only 15% to the weight of the structure.
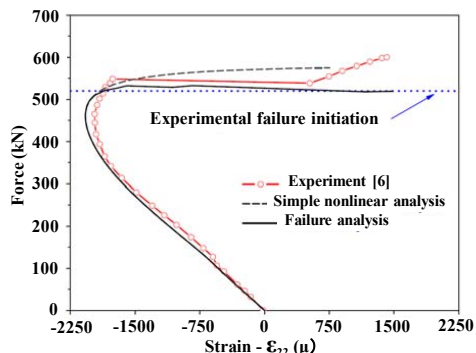

Figure 16. Force versus axial strains measured at the web of the blade stiffeners (Anyfantis and Tsouvalis, 2012)

4.6.3   Environmental effects

It is common knowledge that composite laminates are not affected by corrosion in the same way as metal structures do. Nevertheless, recent work (Kant et al., 2010) suggests that carbon fibres under prolonged exposure to sea water and elevated temperature have their mechanical properties, specifically elastic modulus, reduced. Based on this evidence, Kant et al. (2011) reported on an ongoing investigation aimed at establishing the effects of sea water on the ultimate tensile strength of carbon fibres using nano-tensile testing. Based on limited experimental data available at the time of the publication of results, the authors concluded that the fibres soaked with sea water did not show a clear trend of variation in measured properties such as failure stress and modulus variation with strain as a function of exposure conditions, and the potential degradations seems to occur for fibres with poor mechanical properties quantified by a value corresponding to the storage modulus with respect to axial strain.

4.6.4   Compression after Impact

An area that has received attention in the last years is the ultimate Compression After Impact (CAI) strength of composite structures.CAI strength is widely used as a damage tolerance threshold value for composite structures in the aerospace industry but has potential applications in the shipbuilding industry to the evaluation of the ultimate strength of composite structures damaged by ballistic impacts and grounding.

Nettles and Jackson (2013) conducted an investigation into the CAI strength of out-of-autoclave (OOA) processed laminates. OOA laminates are gaining much attention due to the elimination of needing a costly autoclave large enough to hold the part to be cured. The CAI strength of two commercially available OOA systems (IM7/8552 & IM7/MTM-45) was compared using a conventional autoclave laminate (T40-800/5230) as a baseline. Three different levels of impact severity were investigated and compared with undamaged control specimens as presented in Figure 17.
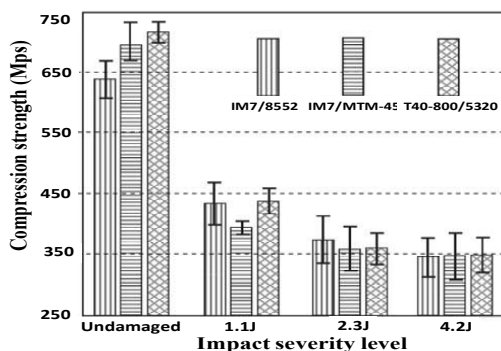

Figure 17. Compression strength versus impact severity (Nettles and Jackson, 2013)

Information on damage, size and morphology were assessed along with the CAI ultimate strength values. The results of the investigation showed that the two OOA laminates tested have similar damage tolerance characteristics to the autoclave processed laminate. This is important for the composite shipbuilding industry where the large size of the structure may preclude the use of an Autoclave.

Lee et al. (2011) investigated the CAI strength of MD laminates using the Soutis-Fleck model, that mathematically replaces micro-buckling/kinking damage with a through thickness line crack. The model requires a damage area, reduced properties in the damage site and in-plane stress distribution near the damage site. The damage site was model as an equivalent hole and as a soft inclusion. From the comparison of the theoretical predictions and experimental measurements for CAI strength, it was found that when fibre breakage occurs at certain plies, the equivalent hole model was more suitable for the prediction that the soft penetration model. The differences between the theoretical and experimental strength results were found to be less than 10%.

4.7   Aluminum structures

4.7.1   Introduction

Aluminium structures are used in a variety of marine applications such as hull and decks in high-speed boats and catamarans and superstructures for ships. Other applications are box-girder bridges, walls and floors in offshore modules and containers. The use of aluminium is primarily being driven by the demand for reduced structural weight, increased payload, higher speed and reduced fuel consumption. Compared to steel structures, the ultimate strength and collapse behaviour of aluminium structures are significantly affected not only by initial imperfections (i.e. residual stresses and initial deformations), but also by the material nonlinearity and the deterioration of mechanical strength in the heat-affected zones (HAZ) caused by welding in assembly and fabrication. The level of the mechanical strength decrease in the HAZ is dependent on alloy type, temper, welding process and welding parameters. This reduction can be typically between 30%–50% of the strength of the base material for 5xxx and 6xxx-series alloys, most commonly considered for ship construction, joined by fusion welding (Sensharma et al., 2011). Such a material strength decrease in HAZ may lead to a serious reduction of the aluminium structural strength. The application of ultimate limit-state (ULS) for aluminium ships requires adapted ultimate strength methods which take into account the influences of the alloy type, material softening in the HAZ, strain hardening and loading type. However, the available literature is relatively limited over the last three years when compared with the studies on steel structures.

4.7.2   Weld-induced effects

Extensive work was carried out by Sensharma et al. (2011) concerning the effect of welded properties on aluminium structures. This study intended to provide a basis for modification to design standards by analysing the impact of HAZ on the load-carrying capacity of aluminium stiffened panels under compressive, tensile and bending loads. To that end, fine mesh finite element models were developed and analysed for a range of tee bar-stiffened panels along with 5083-H116 and 6082-T6 aluminium alloys. For each panel, three comparative FE models were made: the first consisting of all base metal throughout the model with no separate HAZ regions, the second with all HAZ metal throughout the model, and the third with HAZ regions adjacent to welded edges. Based on the analysis conducted, it appeared that there is a significant advantage for modelling aluminium marine stiffened panels by explicitly considering the HAZ extent, location, and strength rather than applying a uniform knock-down factor to the strength of the HAZ material.

A parametric series of nonlinear finite element analyses of unstiffened plates with 5083-H116 and 6082-T6 material properties in uniaxial compression are presented by Benson et al. (2013b). The study demonstrates the effect of the material model, imperfection parameters, residual stress and heat affected zone on the plate load shortening curve. A series of plate load shortening curve datasets are presented, accounting for three severity levels of imperfection and including effects of HAZ and residual stress. These curves are proposed as suitable for direct implementation in a Smith type progressive collapse method. As an example, two load shortening curve datasets are shown below. These are representative of typical plates and use the ''base case'' material and geometric properties (defined within the text). The aluminium alloy results use a HAZ ratio of 0.125 with HAZ located at the four plate edges.

Paulo et al. (2013) carried out a set of finite element analyses (FEA) to reproduce the mechanical behaviour of integrally stiffened aluminium panels under axial compression. The aim was to assess the sensitivity to initial geometrical imperfections and material properties. Two different types of 6082-T6 panels used in high-speed catamaran ferries, equivalent to previous experimental tests, were taken into consideration as FEM models (Figure 19).
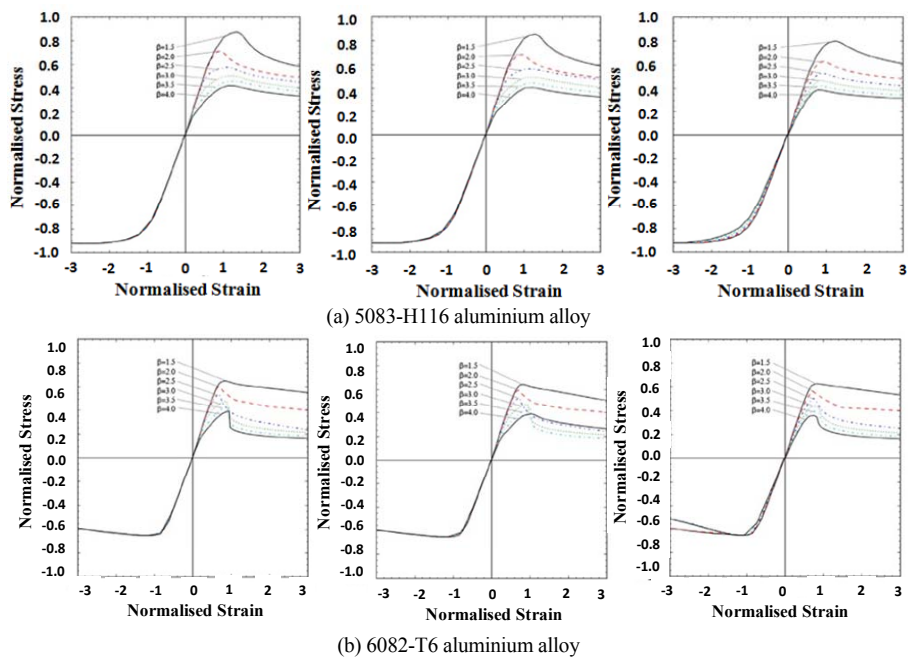
(a) 5083-H116 aluminium alloy

(b) 6082-T6 aluminium alloy

Figure 18. Plate load shortening curves with slight (left), average (centre) and severe (right) imperfections

a) with L-shaped stiffeners
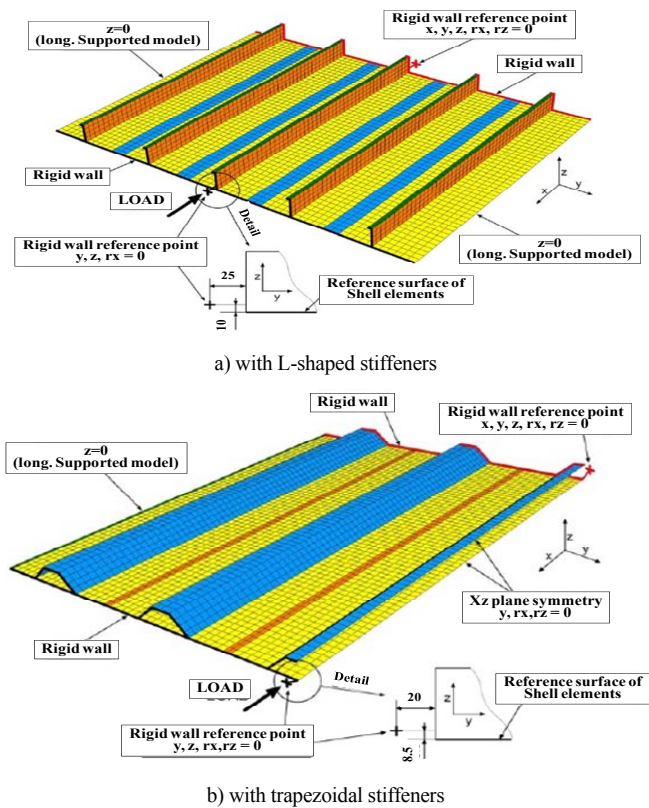

b) with trapezoidal stiffeners

Figure 19. Detailed description of FEM models for analysis

Panels with L-shaped stiffeners were MIG welded whilst panels with trapezoidal closed-section were joined using a friction stir welding (FSW) technique. In the numerical simulation models, particular attention was given to the correct reproduction of the boundary conditions and the configuration of the loading edges. As an overall conclusion, it was demonstrated that a reliable ultimate load prediction in the presence of compressive loads should be preceded by a careful assessment of geometric imperfections that are used in the initial model, with their influence more significant than that coming from the effective stress vs. equivalent plastic strain curve in the HAZ of the studied panels.

A nonlinear FEA-based numerical study was done by Khedmati et al. (2014) in order to investigate the effects of various geometrical imperfections types on the ultimate strength of aluminium stiffened plates under different combined axial compression and lateral pressures. The finite element models taken into consideration were triple-span panels stiffened by either extruded or non-extruded angle-bar profiles (proposed by the Committee III.1 'Ultimate Strength' of ISSC'2003). These models were made of Aluminium alloy 6082-T6, by different arrangements of heat-affected zone (HAZ). The main outcomes of this study confirmed the need for a subtle identification of the real shapes of the initial deformations, especially in structures like catamarans and ferries that are designed to operate in severe sea conditions. In a continuation study, Pedram et al. (2014) numerically investigated the effects of welding on the strength of the aluminium stiffened plates under different combined uniaxial compression and lateral pressures. In this study, the softening of the heat affected zone (HAZ) and the residual stress were taken into consideration for all FE models. Based on the extensive finite-element investigations, different aspects of the effect of welded induced initial imperfections on aluminium panels were outlined and some design-oriented conclusions were drawn to which may make reference.

4.7.3 Formulation Development

Collette (2011) developed a series of rapid semi-analytical methods for predicting the compressive and tensile response of aluminium plates and stiffened panels. These methods were designed to allow Smith-type progressive collapse approaches to be implemented for aluminium vessels. Unlike existing steel ultimate strength methodologies, particular attention was paid to capturing aluminium-specific response features, such as round material stress-strain curves and the weakening effect of fusion welds. In limited comparison of the results to FEA studies and published experiments the methods generally performed well, and represented a rapid aluminium-specific approach to ultimate strength calculations.
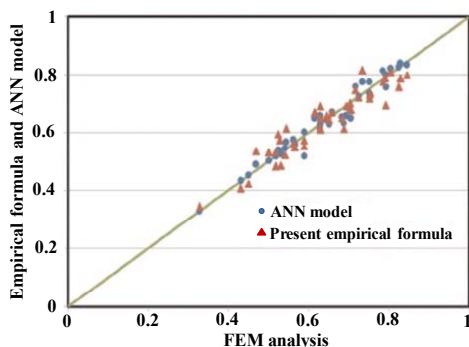

Figure 20. Comparison of the non-dimensional ultimate strength values obtained using the FEM versus those values predicted using the present empirical formula and the ANN model

4.7.4 Experimental Investigation

An experimental and nonlinear FEA-based numerical study on buckling collapse of a fusion-welded aluminium stiffened plate structure was carried out by Paik et al. (2012c). A set of aluminium stiffened plate structures fabricated via gas metal arc welding in which the test structure was equivalent to a full scale deck of an 80m long high speed vessel. The plate part of the test structure was made of 5383-H116 aluminium alloy, and extruded stiffeners were made of 5083-H112 aluminium alloy. A good agreement was found between the nonlinear FEM computations and the experimental results. It was concluded that the nonlinear FEM computations significantly depend on the structural modelling technique applied. In particular, the welding-induced initial imperfections in terms of initial distortions, residual stresses, and softening in the heat-affected zone need to be modelled as appropriate for the nonlinear FEA of welded aluminium structures.

4.7.5   Fiber-Reinforced Polymer Strengthened

Zahurul Islam et al. (2011) presented an experimental investigation of fibre-reinforced polymer (FRP) strengthened aluminium square and rectangular hollow sections experiencing web crippling failure due to localised concentrated loads or reactions.
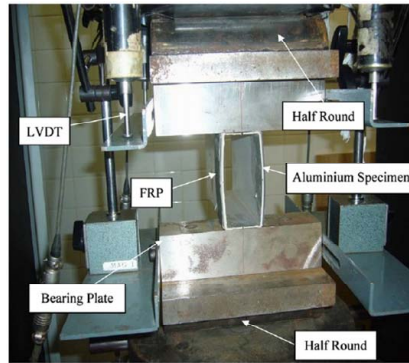

Figure 21. Test setup of End-Two-Flange loading condition

The work was mainly focused on the effects of different adhesive and FRP for the strengthening of 6061-T6 heat-treated aluminium alloy tubular sections against web crippling (Figure 21).

The influence of different widths of FRP plate strengthening against web crippling subjected to end-two-flange and an interior-two-flange loading condition was also investigated in this study. In general, the test results revealed that the FRP strengthening significantly enhances the web buckling capacity of aluminium tubular sections, especially for those sections with large value of web slenderness ratio. It was also shown that the increases of FRP width do not provide much improvement in the strengthening of the aluminium sections. Hence, the FRP strengthening against web crippling was found to be effective when the FRP width is having the same width as the bearing length for aluminium tubular sections.

4.7.6   Sandwich Panels

There is significant and growing interest in using aluminium sandwich panels in the shipbuilding industry, as an attractive and interesting solution to the increasing environmental demands. Crupi et al (2013) made a comparison of static and impact response for aluminium foam and honeycomb sandwich constructions. A combined experimental and theoretical approach was applied to investigate the static and impact response. The obtained results confirmed that the capacity of energy dissipation under bending loading is affected by the collapse mechanism, and also by the face-core bonding and the cell size for foam and honeycomb panels, respectively.

4.7.7   Hull Girder

Benson et al. (2013d) completed nonlinear FE analysis to determine the ultimate strength response of several example aluminium ship-type structures under vertical bending moment. Firstly a series of four square box girders were analysed, with scantlings similar to equivalent large aluminium ships. A nominal aluminium multihull midsection was also analysed. The FE models were extended over multiple frame spaces to capture both interframe and overall grillage buckling effects. The FE analyses were compared to results from an extended Smith-type progressive collapse method, which has the ability to predict hull girder ultimate strength including both interframe and overall grillage collapse. Additional nonlinear FE analyses of the flat panels making up the box girders are presented by Benson et al. (2013c). These are compared to results from the adapted large deflection orthotropic plate method, which is the approach used to develop the panel load shortening curve including overall buckling effects. The results from both papers show relatively close agreement between analysis methods and demonstrated a significant effect from overall buckling in reducing the ultimate strength of the section when compared to equivalent interframe results.

The effect of damage severity and location on the residual strength of a generic aluminium hull structure with scantlings typical of a patrol vessel are investigated by Taylor et al. (2013) using ISFEM. Different damage scenarios as defined in classification guidance by DNV and Lloyd's Register are considered.

Magoga et al. (2014) presented ALPS/HULL ISFEM (intelligent supersize finite element method) results of ultimate hull girder strength analysis under vertical and horizontal bending applied independently. The aim was to quantify the degree to which weld-induced imperfections (i.e. initial plate and stiffener deflection, plate and stiffener residual stress, HAZ breadth and HAZ yield stress softening) reduce ultimate global bending load capacity of a patrol boat midship section and to determine if certain imperfection parameters contribute more to the reduction than others. This investigation was based on a one-bay hull girder ISFEM model containing only longitudinal stiffener fillet welds made by metal inert gas welding process. All longitudinal stiffeners and girders included in the model are T-section profiles made of aluminium alloys 6351-T6, 5083-H116 and 6082-T6. The obtained results of the analysis cases illustrated that severe levels of HAZ-related imperfections (includes yield stress reduction, tensile residual stress and HAZ breadth) and plate initial deflection are the most influential parameters in the reduction of the ultimate strength of the aluminium patrol boat studied. The effect of plate and stiffener compressive residual stress and stiffener column type initial deflection were found to be relatively small. The results also showed that the ultimate strength of the patrol boat studied is more affected by imperfections under sagging loads compared with hogging and horizontal bending loads.

4.7.8   Summary and Recommendation for Future Works

In summary, based on the literature review, it seems the research studies on the buckling/ultimate strength of aluminium marine structures are rather limited. There is a growing continuation for using aluminium alloy structures in marine applications. In particular, such a trend can be seen in the case of large high-speed crafts operating in deep ocean environments for which more rigorous ultimate strength based-design techniques and methodologies are required.

Following the studies made to date, attention should still be given to more numerically and experimentally investigate the influences of alloy type, material nonlinearity, welding location along with its parameters, HAZ characteristics and weld-induced imperfections on the ultimate strength of aluminium plate and stiffened panels as well as ultimate global bending load capacity of aluminium midship sections subjected to different types of loadings and its combinations. By such a contribution, much more reliable buckling and ultimate strength formulations are developed which can, in turn, provide a more suitable basis for modifications to aluminium design standards.

Other point of interest can be the study on the effects of some in-service damages like openings and cracks which must be diagnosed accurately in security and safety considerations. Also, it would be interesting to more investigate the structural behaviour of the structures consist of extruded integral stiffened panels like deck and superstructure elements. Furthermore, it should be noted that due to increasing environmental demands, more study on aluminium sandwich structures used in maritime industries can be interesting research topic to carry out.

5.   BENCHMARK STUDY

5.1   Small box girder

5.1.1   Introduction

The purpose of this benchmark study is to demonstrate the level of uncertainty in an ultimate strength calculation using NLFEM due to the effect of various physical parameters which are necessary for nonlinear analysis. These parameters include the initial geometric imperfection definition, the material plasticity model, the boundary conditions used to restrain the model, the mesh density, the element type and the choice of finite element solver. The study also makes an attempt to quantify the magnitude of uncertainty in the finite element solution which could be expected in the ultimate strength prediction of a box girder using NLFEM. This is done by making a statistical evaluation of all the "baseline" results from the benchmark study participants and producing a confidence band above and below an "averaged" bending-moment curvature plot.

In ISSC Committee III.1 2012 it was concluded that results from ultimate strength analyses "can still be affected by large uncertainties that must at least be identified and then possibly estimated" (Paik et al., 2012b). The 2012 ISSC report divides the source of uncertainties into physical aspects (such as the uncertainty in defining the material properties or imperfections) and modelling aspects (uncertainty in the ability of the numerical model to adequately approximate the physics of a structural collapse).

Confidence in NLFEM for ultimate strength analysis comes from having a detailed understanding of both these sources of uncertainty. There is not much information currently available to properly quantify the expected uncertainty in the results from a particular ultimate strength assessment. Classification rules do provide some guidance; for example IACS CSR uses a partial safety factor of 1.1 to account for both modelling and physical uncertainties in an ultimate strength calculation. However, previous benchmark studies including those by ISSC have shown larger differences between analyses. For example, results

from the hull girder vertical bending moment benchmark studies in ISSC 2012 showed differences in ultimate strength predictions of over 30% for some of the ship hulls tested. This disparity indicates a current need for research to better identify and quantify the influence of different modelling and physical parameters on an ultimate strength analysis using NLFEM.

A common theme within many of the papers reviewed in this report is that the successful use of NLFEM still relies on analysts having a high degree of expertise in constructing the finite element model, sound engineering judgement to evaluate the uncertainty of the results and knowledge regarding the limitations for a given finite element program. Analysts may try to gain confidence in their NLFEM approach by comparing their results to a benchmark – either from a previous numerical analysis or physical experiment. For example, a well-used experimental test is the 1/3 scale frigate model tested by the UK Admiralty Research Establishment (Dow, 1991). Previous benchmark studies by ISSC Ultimate Strength committees have also provided excellent sources of numerical benchmarks for plates, stiffened panels and hull girders. However, any comparison made by an analyst with a previous study can also be clouded by the modelling and physical uncertainties within the original test results, which are often poorly understood and documented. If it is unclear what the uncertainty is within an existing ultimate strength result for a ship, it is difficult to judge the comparative success of a new result.

To produce a reliable result, ultimate strength analyses using NLFEM frequently need to quantify physical uncertainties for inclusion. An analyst often makes recourse to a statistical "average" to adequately represent the actual structure within the numerical model – for example by specifying average imperfection levels. The influence of any parameter can then be tested by running a parametric study – carefully varying the parameter within certain bounds and evaluating its effect on the ultimate strength.

A common example which is often tested is the magnitude and shape of the geometric imperfections within a plate or stiffener. It is normally essential to include some form of geometric imperfection within the NLFEM mesh to enable the formation and nucleation of buckling, which often precipitates the collapse of the structure and hence governs the ultimate strength. However, the exact shape of the geometric imperfection for a given structure is rarely known and, as shown by numerous studies, the shape and magnitude of the imperfection is known to affect the ultimate strength behaviour to some extent. Therefore the analyst must make a proper consideration of the imperfection to ensure the resulting ultimate strength prediction is reasonable.

Modelling uncertainties are much harder to estimate, specifically because the analyst will not normally know what the "real" result should be and so the magnitude of the error in any calculation method is impossible to realize. This is often true even when comparing with a physical experiment because the modelling uncertainty of the test setup is often unknown and, especially for large-scale hull girder type experiments, repeat tests are rare.

Efforts to improve the quantification of both physical and modelling uncertainties will lead to improved confidence in ultimate strength analysis using NLFEM. This benchmark study hopes to contribute progress in this regard.

5.1.2 Model Parameters

The benchmark study replicates physical experiments completed by Gordo et al. (2009) on three box girders built from high tensile steel. These were tested to collapse under pure bending moment using a 4-point bending rig. A schematic of the test rig is shown in Figure 22.

Each model has a cross section of 600 mm × 800 mm (Figure 22). The length varies according to the number of spans and the spacing between frames, and is 0.8 m, 0.9 m or 1.2 m (These are the lengths considered within the simulations). All Box girders and stiffeners are modeled with 4 mm thickness. The transverse frames are 'L' stiffeners L50 × 28 × 6 made of mild steel. The longitudinal stiffeners are continuous through the models.
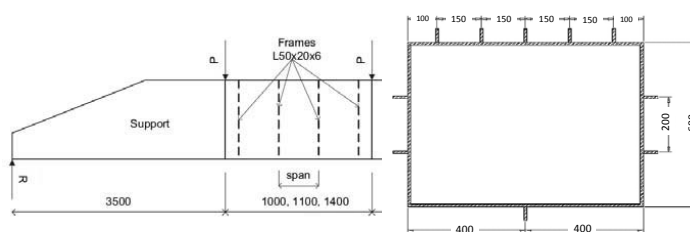

Figure 22. Schematic of the test rig used for the experimental tests of the three box girders (left) and cross section of box girders (right). All plate and stiffeners are 4mm thick. Stiffeners are 20mm height (Gordo and Guedes Soares, 2009).

The girders have a relatively small and simple cross section, which enabled the initial specification for the baseline studies attempted by all participants to be carefully defined. Typical meshes are of the order of 10,000 elements, which means solutions are reached in a relatively short time. The simple dimensions of the box enables the geometric imperfection to be defined in the mesh using either Eigenvalue buckling mode shapes or direct translation of the nodes. The specification is available separately for those who wish to validate or practice their own NLFEM approach.

Baseline calculations for all three box girders were attempted by all participants. Sub studies to investigate the parametric influence of different characteristics were then completed by different participants using the H300 box girder.

5.1.3   Baseline Calculations

The baseline calculations were completed by all participants using an issued specification which described the model geometry, the material yield strength and plasticity characteristics, initial imperfection characteristics and required boundary conditions. The full specification is available separately. A summary of the key characteristics is given here.

Geometric imperfection consists of a superposition of 3 different mode shapes: plate imperfection, stiffener lateral imperfection and column imperfection. The imperfection shapes and amplitudes have been chosen to represent an "average" level of imperfection typically found on ship structures as defined in several previous studies (Smith et al., 1991). The mode shapes have been chosen to be relatively conservative whilst retaining some realism. For example the plate imperfection shapes are assumed to alternate direction, rather than form a hungry horse pattern. The plate imperfection is defined using a two mode Fourier series in calculations.

$$\frac{w}{w_{0pl}} = \left(0.8\sin\frac{\pi x}{a} + 0.2\sin\frac{m x \pi}{a} \right).\sin\frac{\pi y}{b} \tag{11}$$

where w is the imperfection amplitude at a given coordinate position (x, y) from a plate corner. Each plate has length a and breadth b. The maximum imperfection amplitude, w_{opl}, is 0.4 mm for all plates.

The stiffener lateral-torsional imperfection describes the "tilt" of the stiffener from upright and is defined using a single half wave between frames:

$$v_s = \frac{w}{h_w}\sin\left(\frac{\pi x}{a} \right)v_{os} \tag{12}$$

where v_s is the imperfection amplitude at a given coordinate position (x, w) from a stiffener-frame intersection. The stiffener has a total web height h_w of 20mm in this study. For the baseline studies the maximum imperfection amplitude, v_{os}, is specified as $0.015 \times h_w = 1.5$ mm for all stiffeners. The tilt direction runs consistent with the corresponding plate imperfection (see Figure 22).

The column imperfection is a global mode shape and describes the distortion of the plate and stiffeners as a single unit. The shape is applied to both plate and stiffener nodes using the following equation:

$$v_s = \frac{w}{h_w}\sin\left(\frac{\pi x}{a} \right)v_{os} \tag{13}$$

where A is the length between frames (200,300 or 400 mm) and B is the breadth of the panel (600mm or 800 mm). The column imperfection is directed outward in the central bay of the box girder (see Figure 22) with maximum magnitude, w_c, of 1.5 mm.
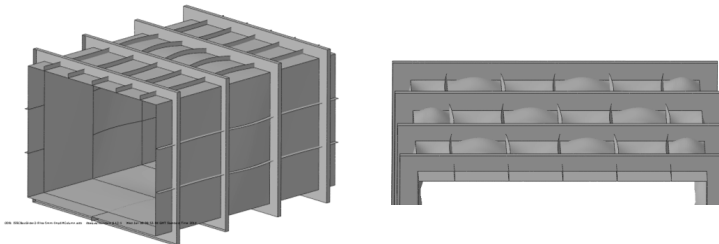

Figure 22. Magnified column imperfection (left), plate imperfection and stiffener lateral Imperfection (right). Magnification ×20

A bilinear material model is used with E = 210 GPa, σ_o = 732 MPa and a 1% post yield hardening (engineering stress-strain curve). The stress-strain values for use in the FEM plasticity model are as follows:

Table 5. Material Properties for HTS690 as used for numerical analyses.

	ε_{nom}	σ_{nom} (MPa)	ε_{true}	σ_{true} (MPa)	$\varepsilon_{plastic}$
Yield	3.49E–03	7.32E+08	0.00348	7.35E+08	0.00E+00
Ultimate	3.97E–02	8.08E+08	0.038909	8.40E+08	3.49E–02

The specification asked for the model extents to only include the test section as used in the original experiments. A pure vertical bending moment is applied through rigid body constraints at each end of the girder. Benchmark participants were free to set the exact boundary conditions appropriate to their own modelling approach and the particular requirements of the software package used. A typical approach uses a reference node to constrain all nodes at each end using a rigid body constraint. Incremental load or rotation is then applied through the reference node. The resulting bending moment and rotation results can be outputted directly from the reference node. Curvature is measured using the total relative rotation between each end of the box girder for convenience and to ensure standardized results. The best method to use for measurement of curvature is debatable to compare accurately with the experiment. A recent paper by Gordo et al. (2014) discussing similar box girder tests to those used in this benchmark study demonstrates the difference between measuring curvature from the ends of the model and measuring curvature from adjacent frames to the nucleated buckling.

The rigid body boundary condition typically used in ANSYS, ABAQUS and other software packages does not require the reference node to be placed on the neutral axis of the section. The reference node position is irrelevant because it is used purely to control the rotation at the box girder end.

Participants were free to choose software package and solver type used, as shown in Table 6.

All participants were asked to conduct a mesh refinement study to determine an appropriate characteristic element length which gives a converged prediction of the progressive collapse curve. An example convergence study is shown in Figure 23. Participants typically found a characteristic length of 10mm to be sufficient. Some participants further refined the element length in the stiffeners to give an increased number of elements through the depth. The mesh should have at least two elements in the web height. A mesh with 1 element in the web height gives a conservative result.

Table 6. Summary of participants in benchmark study

Participant	FEM Package	Solver	Element Type
1	Trident / VAST 9.1	Orthogonal Trajectory	Shell
2	ANSYS Workbench v11.0	Newton-Raphson	Shell181
3	ABAQUS v6.13	Arc Length (Riks)	Shell S4R
4	ANSYS APDL v14.5	Newton-Raphson	Shell181
5	ANSYS APDL v14.5	Newton Raphson	Shell181
6	LS-Dyna v971d r 6.0.0	Dynamic-Explicit	Shell ELFORM2
7	ABAQUS v6.13	Arc Length (Riks)	Shell S4R
8	NX-NASTRAN	Newton-Raphson	Shell
9	ABAQUS v6.13	Newton-Raphson	Shell S4R
9	ANSYS APDL 14.5 and 15.0	Arc Length	Solid 95
10	Smith Method (HullColl)	N/A	N/A

Participants 1-9 used shell elements in the baseline calculations. Results for the three box girders are presented in Figure 24 to Figure 26. A mean progressive collapse curve is also presented for each box girder together with an upper and lower curve one standard deviation away from the mean. These are provided to give some indication as to the statistical uncertainty of the numerical analyses.

The mean curve is formulated using a point by point averaging method. At each specified interval of curvature (increment of 0.0002m^{-1}), the resultant bending moment from each participants result is used to calculate a mean BM. Because the raw data from the finite element analyses is not given with fixed curvature increments, all the datasets were first made consistent using a standard curvature increment of 0.0002m^{-1} and applying linear interpolation. The standard deviation curves are also calculated on a point by point averaging basis.

The differences between the numerical results are relatively minor. A comparison of the predicted ultimate strengths between participants is shown in Table 7. It should be noted that the peak of the mean

curves from the figures differ slightly from the mean ultimate strength reported in the table. This is because the peak of each curve does not occur at the same curvature value. The point by point averaging method will not distinguish the peak. Which is the most statistically significant "average" ultimate strength from these results remains questionable.

Also, it should be noted that the experiment results from Gordo et al. (Gordo and Guedes Soares, 2009) have been adjusted to fit the initial stiffness of the FEM models. The difference is due to difficulties in accurately measuring rotation.
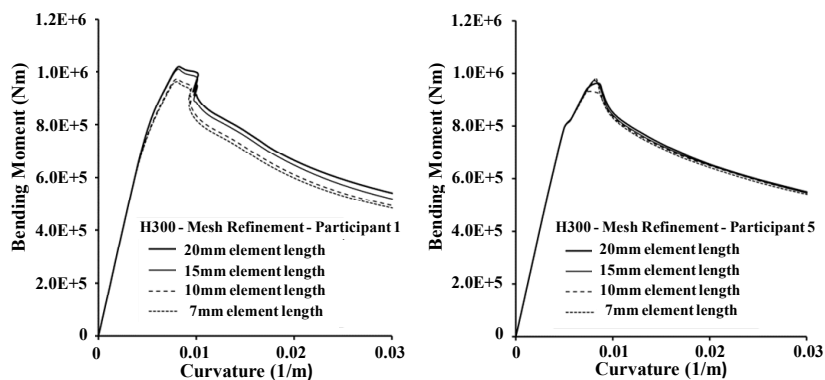
Figure 23. Mesh refinement study by participant 1 (left) and participant 5 (right).
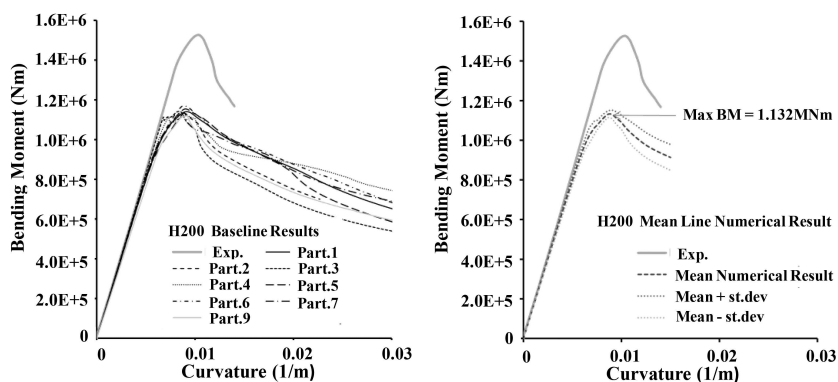
Figure 24. H200 bending moment – curvature baseline results from all participants (left) and mean numerical results (right)
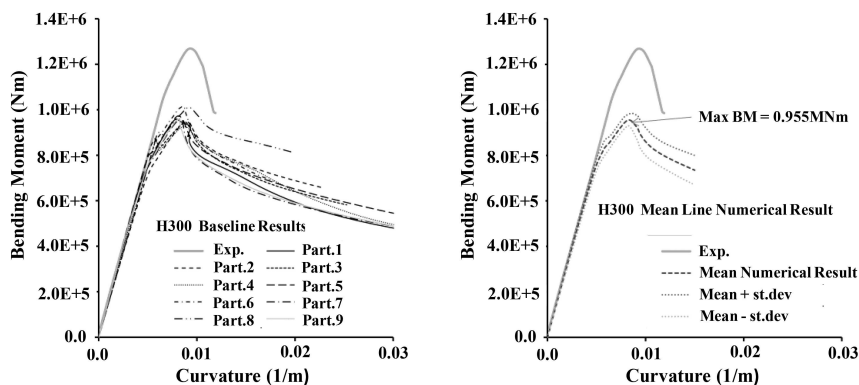

Figure 25. H300 bending moment – curvature baseline results from all participants using shell elements (left) and mean numerical results (right).
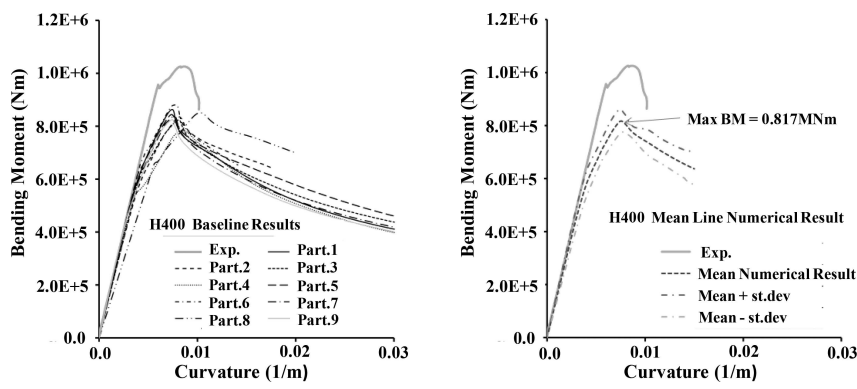
Figure 26. H400 bending moment – curvature baseline results from all participants (left) and mean numerical results (right).

The most notable finding of the baseline study is that numerical results using shell elements predict a significantly lower strength than the experimental test for all three girders. This suggests that one or more parameters from the specification of the experiment differ from the reality. The additional parametric studies investigating the influence of geometric imperfection, material model and plate thickness in the sub sections below give some indication as to where differences between the NLFEM and experiment may produce such disparity. Another possible reason for the large differences between NLFEM and experiment, which is not tested here, is differences in the boundary conditions and load application. A previous study by Benson et al. (2013a) showed that friction between the strips connecting the load to the four point bending rig could inhibit buckling in the top flange of the box and increase the ultimate strength capacity of the girder. However, it is not possible to verify whether this is indeed a cause of the discrepancy between results.

The mean numerical results with standard deviation curves above and below show the approximate bounds of a 95% confidence level between datasets, assuming a normal distribution about the mean curve and a population sample of 8. Although the sample size is small this provides some clarity in judging the correlation between different participants. At the curve peak the uncertainty is between 3.3% (H200) and 10.6% (H400). This is equivalent to the uncertainty suggested by the IACS CSR partial safety factor and suggests that the safety factor is reasonable. It must be pointed out that this conclusion is only inferred from a relatively small cross section box girder.

Table 7. Ultimate strength results of baseline box girder benchmark analyses.

	Ult. Str. H200 (MN.m)	Ult. Str. H300 (MN.m)	Ult. Str. H400 (MN.m)
Experiment	1.527	1.269	1.026
Participant 1	1.139	0.958	0.863
Participant 2	1.134	0.947	0.835
Participant 3	1.139	0.944	0.823
Participant 4	1.119	0.956	0.783
Participant 5	1.154	0.969	0.844
Participant 6	1.170	1.015	0.880
Participant 7	1.134	0.961	0.836
Participant 8	-	1.011	0.850
Participant 9	1.120	0.958	0.824
Participant 10 (Solid elements)	1.651	-	1.091
Participant 11 (Smith method)	1.291	1.175	0.913
Ave. Ult. Str. (shell elements only)	1.139	0.966	0.838
St. Dev. (shell elements only)	0.017	0.029	0.028

5.1.4 Comparison with Solid Element Mesh

Participant 10 investigated the use of solid elements for the analysis. The cases H200 and H400 were studied using meshes with an average element length of 30 – 40 mm, giving a total number of elements of some 85000 (both tetrahedral and cubic). The resulting aspect ratio for elements in the plate parts is high,

but believed to have a minor influence on the results as quadratic elements were used. The current meshes used 1–2 elements over the height on the webs of the stiffeners. Differences compared with the parallel simulations using shell elements were the use of only one imperfection mode, here plate imperfection, the use of a mild steel, with yield stress 250 MPa in the transverse frames (as indicated in the report from the manufacturing of the box beams used for the experiments) and also the use of a trilinear stress-strain curve for both materials. The simulations were performed using a prescribed rotation of one end section or using the arc-length method, though in the latter cases it was found sometimes difficult to obtain convergent results.

Figure 27 (left) shows the moment curvature relationship for the H200 Box girder. It is seen that the maximum moment is overestimated using a bilinear stress strain curve, whereas a trilinear stress strain curve will give a lower maximum bending moment. The material used for the transverse stiffeners is seen to have a small effect. Figure 27 (right) shows the influence of material model for the H400 box girder with transverse stiffeners modelled as mild steel. Uses of a more realistic trilinear material model will also here give a lower maximum bending moment.

Compared to the use of shell elements, use of solid elements slightly overestimate the maximum moment. It has not been possible to quantifiably explain this difference in results, or the difference seen in elastic stiffness for the solid element meshes compared to the experimentally obtained elastic stiffness. Note though that contrary to the shell element simulations, no adjustment of the elastic stiffness to match the experimental results were made.
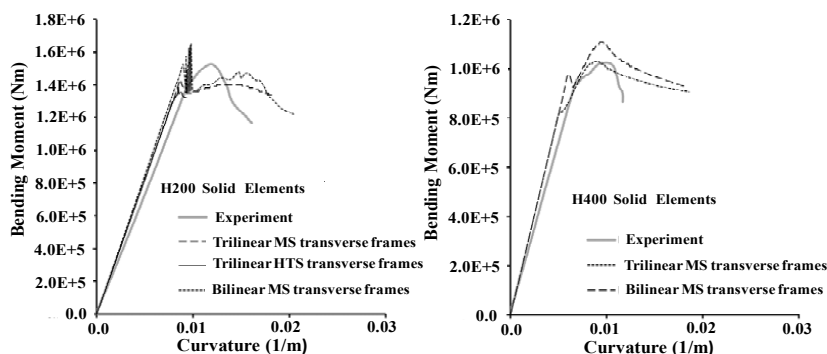

Figure 27. Bending moment – curvature results for participant 10 using solid elements, H200 (left) and H400 (right).

5.1.5   Comparison with Smith method

Participant 11 completed a Smith method progressive collapse calculation for each box girder using the same geometry and material information as for the finite element experiments. Hard corners are assumed at the corners of the box girder extending 60mm in both directions. The panel load shortening curves are developed using the method described by Gordo et al. (1996).
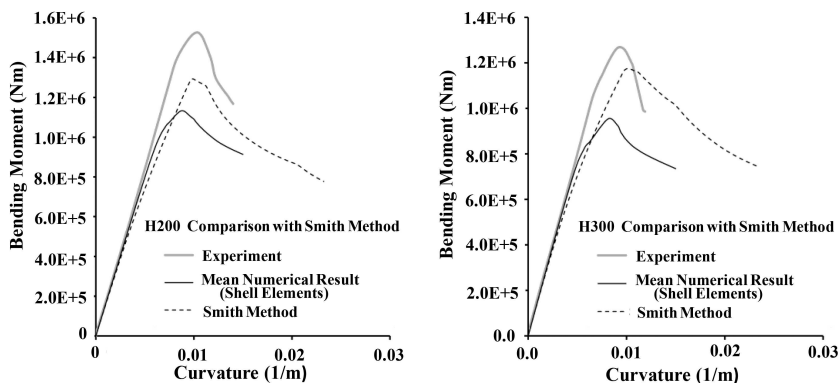

Figure 28. Bending moment-curvature results from Smith method. Comparison with experiment and mean curve shell of finite element analysis. H200 (left) and H300 (right)

The resulting bending moment-curvature plots for are shown in Figure 28 and compared to the mean numerical result from shell finite element analysis and the original experimental result. The results show that the Smith method gives an optimistic prediction of ultimate strength in comparison to NLFEM for these particular cases. The small scale of the box girders makes the Smith method highly sensitive to the definition of the panel load shortening curve for the top flange of the box. It is also sensitive to the extent of the hard corners. This sensitivity is more pronounced than found for a ship sized model. It suggests that Smith method is less appropriate for use on very small cross section.

5.1.6 Effect of Imperfection Amplitude and Shape

Several participants analyzed the effect of changing the parameters governing the geometric imperfections. No information was available to describe the exact imperfections in the experimental model, although it is noted in the experiment reports that the panels were relatively flat with minimal level of imperfection amplitudes. Therefore all imperfection parameters used in this benchmark study are nominal and based on statistical levels appropriate to ship type plating.

Participant 1 investigated the effect of parametrically changing the plate imperfection and column imperfection independently. The other imperfection parameters are kept at baseline amplitudes in each parametric study. The results are shown in Figure 29. This demonstrates insensitivity to both plate and column imperfection amplitude.
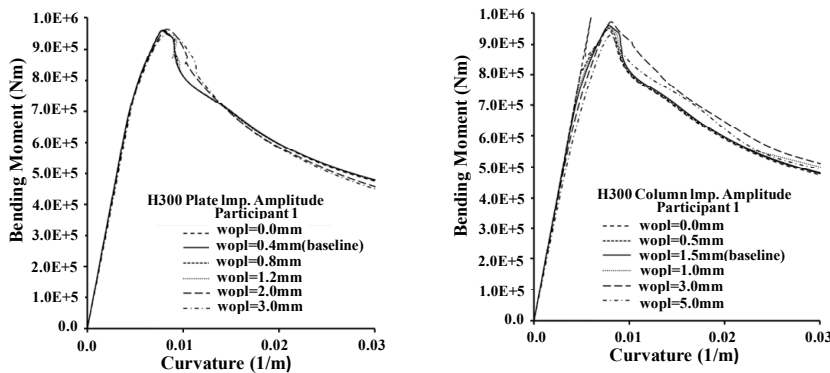

Figure 29. Effect of Imperfection Amplitude (participant 1). Parametric change of plate imperfection (left) and column imperfection (right)

Participant 4 also investigated the effect of changing the imperfection amplitude for the H300 box girder. The study considered different amplitudes of the stiffener lateral-flexural imperfection. Plate imperfection was kept at constant amplitude of 4mm. The initial deflection was applied in two directions, as shown in Figure 30. Three values for amplitudes of this initial deflection have been used:

$v_{os} = 0.00025 \times a = 0.075$mm
$v_{os} = 0.0015 \times a = 0.45$mm
$v_{os} = 0.005 \times a = 1.5$mm (baseline imperfection)

where 'a' is the distance between frames. In addition a case with no initial imperfection was completed. All other parameters, such as the material model and mesh size, used baseline settings.
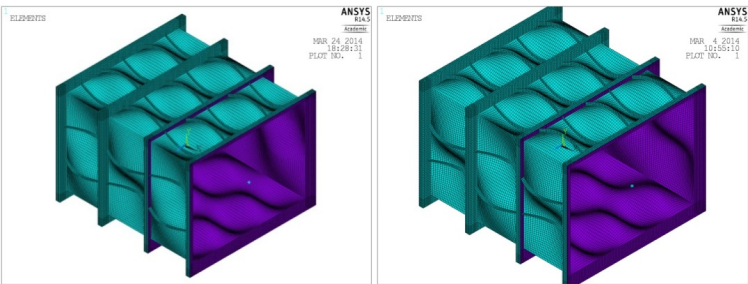

Figure 30. H300 with scaled initial imperfection, +ve up (left), −ve down (right)

Figure 31 shows the bending moment–curvature plots for the variant models. With values of initial deflection 0.00025×a and 0.0015×a almost no difference is detected between positive and negative initial deflection models. However, when the maximum initial deflection value (0.005×span) has been considered, negative initial deflection model shows about 6% larger ultimate strength than positive initial deflection model.

Considering the first two values for the initial deflection amplitude (0.00025×a and 0.0015×a) reduces the ultimate strength 2.86% and 4.29% respectively. However, initial deflection increases it 2.72% considering the maximum value (0.005×a), all in positive case. In negative case, it reduces it 3.12% and 4.98% for 0.00025×a and 0.0015×a respectively and only 3.1% for 0.005×a.

All considered values of initial deflection have not more than 5% influences on the ultimate strength. This indicates that the box girder is relatively insensitive to the magnitude of imperfection applied.
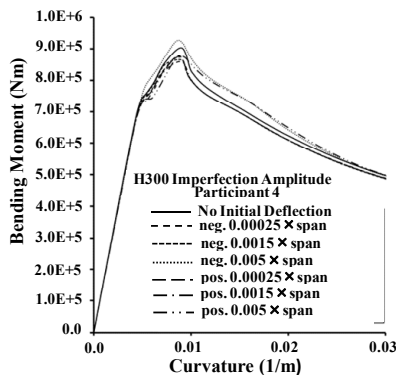

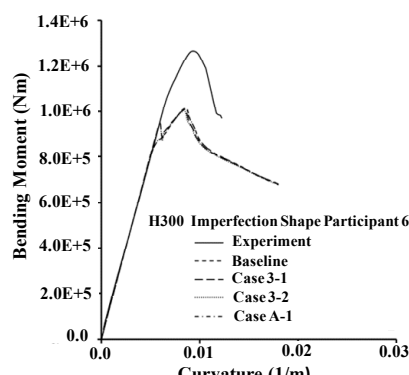Figure 31. Effect of Imperfection Amplitude (participant 4)

Figure 32. Effect of Imperfection Shape (participant 6)

Participant 6 investigated the effect of changing each imperfection parameter whilst keeping the remaining imperfections at the baseline level. The ultimate strength of the box girder for 9 cases is summarized in Table 8. The study found the model relatively insensitive to all three imperfection components. The largest effect was found on altering the column imperfection. With zero column imperfection amplitude, the ultimate strength approached the zero imperfection value, which is about 7.7% higher than the baseline result. However, increasing the imperfection magnitude in any parameter caused a relatively insignificant reduction on the ultimate strength and in some instances actually increased it.

Participant 6 investigated the effect of different imperfection shapes and directions in the plating. The plate imperfection lobes alternate direction in the baseline model. In case 3-1 and case 3-2 the plate imperfection is changed to a hungry horse type pattern with all lobes directed inwards (3-1) or outward (3-2). For Case A-1 the plate imperfection is modelled with two half waves along the length. The load shortening curves (Figure 32) show minimal effect on the ultimate strength and the mode of collapse.

Table 8. Ultimate strength of H300 box girder with different imperfection amplitudes (Participant 6).

		Plate wopl [mm]	Lateral-Torsional vos [mm]	Column woc [mm]		Ult. Strength (N.m)	Difference to baseline (%)
				Central bay	End bays		
Baseline		0.4	1.5	1.5	0.375	1015800	N/A
CASE 2-1	Lateral-Torsional	0.4	0	1.5	0.375	1016300	0.05
CASE 2-2		0.4	0.75	1.5	0.375	1015300	-0.05
CASE 2-3			3.0			1015800	0.00
CASE 2-4	Plate	0	1.5	1.5	0.375	1016400	0.06
CASE 2-5		0.2				1005900	-0.97
CASE 2-6		0.8				1018000	0.22
CASE 2-7	Column	0.4	1.5	0	0	1093500	7.65
CASE 2-8				0.75	0.1875	1005500	-1.01
CASE 2-9				3.0	0.8	1016700	0.09
Zero Imp.		0	0	0	0	1094400	7.74

Based on these studies, we can conclude that including some imperfection in the model is important as the resulting ultimate strength can be over predicted by up to 8%. The most important parameter is the column imperfection. However, so long as some imperfection is present, the amplitude has a relatively insignificant effect on the ultimate strength. The column imperfection is the most significant parameter with influence on the ultimate strength behaviour.

5.1.7   Effect of Material Model Parameters

A parametric study to show the effect of different yield strengths was completed by participant 3 and participant 5. The extent of the yield strength change was kept within realistic bounds of +-50MPa, which could be the expected variation in actual material properties compared to the nominal yield of 732MPa. Both studies (Figure 33) showed similar results, with the change in yield having only a moderate effect on the overall ultimate strength and no effect on the mode of collapse. Participant 5 completed additional parametric studies to compare the effect of different strain hardening models (Figure 34). Both studies show a minor effect on ultimate strength and no effect on the mode of collapse.
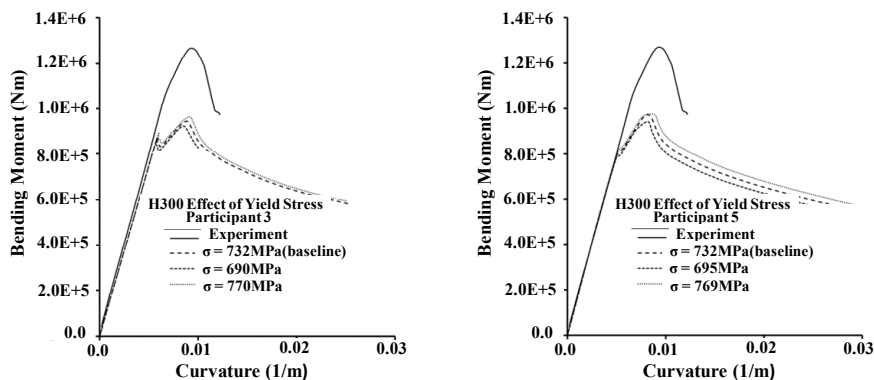

Figure 33. Effect of Material Yield Strength Participant 3 (left) and Participant 5 (right)
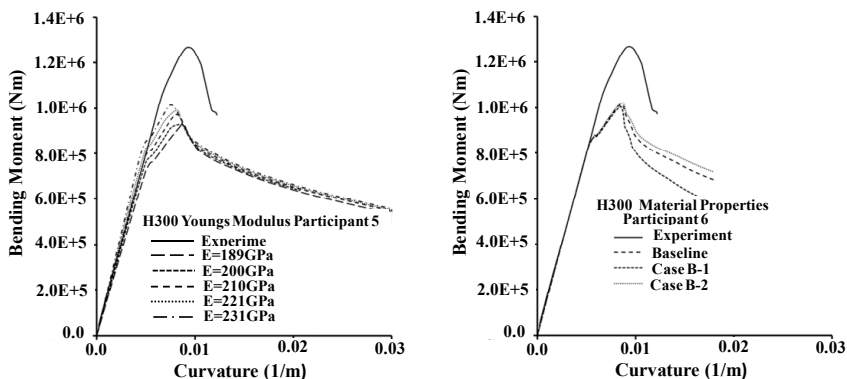

Figure 34. Effect of Material Young's Modulus (Participant 5) (left) and material properties (Participant 6) (right).

5.1.8   Effect of Plating Thickness

Participants 3, 5 and 11 investigated the effect of varying the plating thickness for the H300 box girder. The load shortening curves from participants 3 and 5 are plotted in Figure 35. The results indicate that changes in plate thickness have a significant effect on the ultimate strength of the box girder, but that the mode of collapse remains the same. Results from all participants show a similar relationship between ultimate strength and plate thickness (Figure 36). The load shortening curves also show that increasing the plate thickness causes a noticeable increase in the stiffness of the box girder. This is as expected because the radius of gyration increases with thicker plate. The results from participant 11, using the

Smith method, reflect the higher ultimate strength prediction found by using a simplified progressive collapse method.

The relationship between ultimate strength and plate thickness is linear for the range of thicknesses tested (3.8mm to 5.0mm), with a gradient of approximately 40%. For example, a 25% change in plate thickness from 4mm to 5mm produces a 40% change in the ultimate strength. This means that, for small scale cross sections, a relatively slight difference in plate thickness has a significant effect on the ultimate strength.

Nominal plating thickness as stated by the steel supplier may differ from the actual measured thickness. These experiments demonstrate the need for accurate measurements of plate thickness for a given cross section to enable an accurate representation in the numerical model.
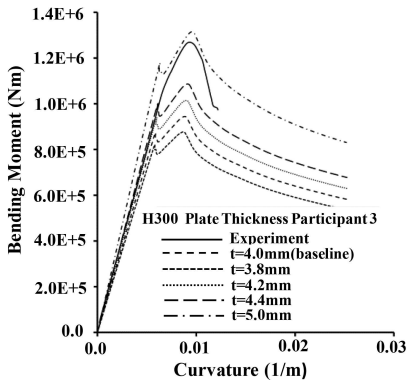

Figure 35. Effect of changing the plating thickness (participant 3).
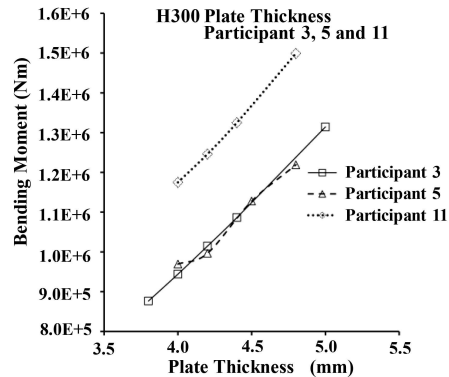
Figure 36. Relationship between plating thickness and ultimate strength

5.1.9   Summary/Conclusions

The box girder benchmark study demonstrates that, given a relatively strict problem definition, a set of experienced users of commercial nonlinear finite element analysis packages will produce consistent results for a small scale ultimate strength problem. The range of ultimate strengths predicted within the baseline calculations for the benchmark fall within the IACS CSR partial safety factor for strength prediction uncertainty ($\gamma_m = 1.1$). This provides good validation of the partial safety factor value, although this conclusion is only made when considering a relatively small and simple box girder structure.

The benchmark also demonstrates clear variation between experimental results and equivalent baseline numerical results. The baseline calculations were completed using nominal values for material and geometric parameters. The variation suggests that one or more parameters from the specification of the experiment differ from the reality. The boundary conditions in the experiment and numerical analyses may also differ. To evaluate some of these potential differences, specific material and geometric parameters were varied in the finite element models and the influence on the ultimate strength was evaluated. These results show that the material stress-strain model, imperfection shape and imperfection amplitude have only minor influence on the ultimate strength. Varying the plate thickness has a more significant influence on the ultimate strength. The finite element analyses are also compared to a simplified progressive collapse analysis using the Smith method. The Smith method predicts ultimate strengths closer to the experimental results but still lower in magnitude. In this instance, the Smith method is highly sensitive to the extent of the hard corner because of the small size of the cross section.

5.2   Three hold model of hull girder

The main purpose of this benchmark study using three hold model are to investigate the influence of initial imperfections and lateral load on hull girder ultimate strength and also to clarify the differences of calculation results provided by several researchers.

5.2.1   Calculation cases

As shown in Table 9, eight cases varying the initial imperfections and the lateral loads will be calculated. The effect of initial imperfections and/or lateral loads on the hull girder ultimate strength will be investigated. The mid-ship section of the modelled Capesize bulk carrier is shown in Figure 36. The longitudinal stiffener space and the transverse frame space are also shown in Figure 36. The principal

particulars and the dimensions of longitudinal stiffeners are summarized in Tables 10 and 11, respectively. The Young's modulus (E) of longitudinal members in the mid-ship section is 206,000 [MPa] in the elastic region, and the bi-linear relation between stress and strain is assumed with the strain hardening rate of $E/50$. The yield stress is also shown in Figure 36.

In actual ships, initial geometrical imperfections and residual stresses caused by welding exist in plates and stiffeners, and these initial imperfections will reduce the ultimate strength of both stiffened plate structures and the entire hull girder.

Only geometrical imperfections are considered in the calculations of case_3, 4, 7 and 8 as shown in Table 9. The local buckling mode given by Eq. (14) is considered in panels, and both the flexural buckling mode and torsional buckling mode given by Eq. (15) are considered in stiffeners. The initial imperfections are also given to flange so as to maintain right angles between flange and web. The schematic diagram and an example of initial imperfections are shown in Figure 37 and 38, respectively.

$$w_{0p} = A_0 \sin\frac{m\pi x}{a} \sin\frac{\pi y}{b} + B_0 \sin\frac{\pi x}{a} \tag{14}$$

$$w_{0w} = B_0 \sin\frac{\pi x}{a}, \quad v_{0w} = C_0 \sin\frac{\pi x}{a} \tag{15}$$

where:

A_0 ($= 0.1\beta^2 t_p$): Maximum deflection of the local buckling mode
B_0 ($= 0.0015a$): Maximum deflection of the flexural buckling mode
C_0 ($= 0.0015a$): Maximum deflection of the torsional buckling mode

β ($= \frac{b}{t_p}\sqrt{\frac{\sigma_Y}{E}}$): Slenderness ratio

m ($= a/b$): Aspect ratio t_p: Panel thickness
a: Transverse frame space E: Young's modulus
b: Longitudinal stiffener space σ_Y: Yield stress

Table 9. Calculation cases

	Condition	Initial imperfections	Lateral loads	Object hold
Case_1	Hogging	Without	Without	—
Case_2	Sagging			—
Case_3	Hogging	With		—
Case_4	Sagging			—
Case_5	Hogging	Without	With	Empty
Case_6	Sagging			Loaded
Case_7	Hogging	With		Empty
Case_8	Sagging			Loaded

Table 10. Principal particulars.

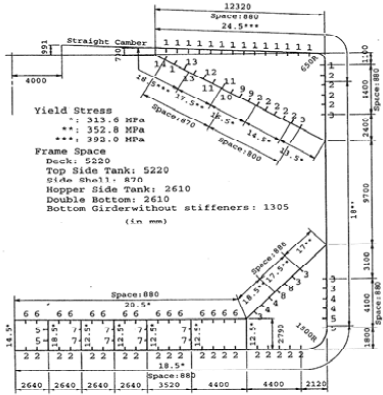|	
Length [m]	285.0
Breadth [m]	50.0
Depth [m]	26.9
Draft [m]	19.83
Number of cargo holds	9
Hold length [m]	26.1

Figure 36. Mid-ship section of Capesize bulk carrier.

Table 11. Dimensions of longitudinal stiffeners.

No.*	Dimensions [mm]	Type	Yield stress [MPa]
1	390×27	Flat-bar	392
2	333×9+100×16	Tee-bar	352.8
3	283×9+100×14	Tee-bar	352.8
4	283×9+100×18	Tee-bar	352.8
5	333×9+100×17	Tee-bar	352.8
6	283×9+100×16	Tee-bar	352.8
7	180×32.5×9.5	Bulb-bar	235.2
8	283×9+100×17	Tee-bar	352.8
9	333×9+100×18	Tee-bar	352.8
10	333×9+100×19	Tee-bar	352.8
11	383×9+100×17	Tee-bar	352.8
12	383×10+100×18	Tee-bar	352.8
13	383×10+100×21	Tee-bar	352.8
14	300×27	Flat-bar	392

* Numbers correspond to those indicated in Figure 36.
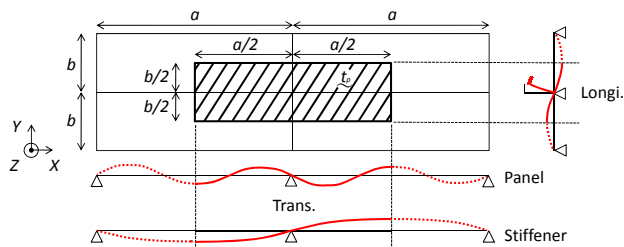
Figure 37. Schematic diagram of initial imperfections.

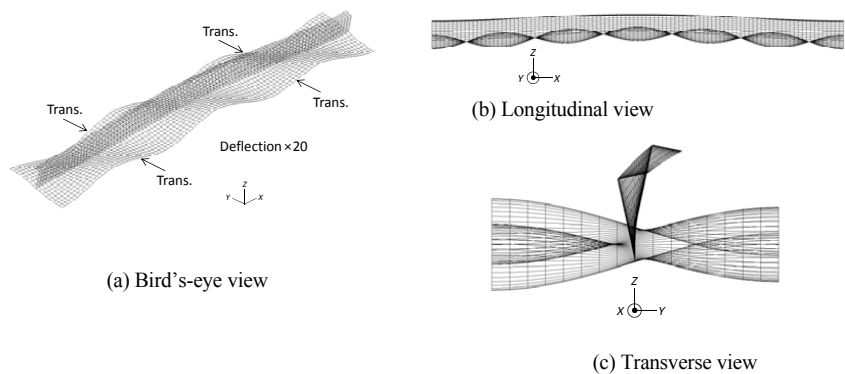(a) Bird's-eye view

(b) Longitudinal view

(c) Transverse view

Figure 38. Example of initial imperfections (deflection × 20).

This calculation is performed on the assumption that the bulk carrier has nine holds, with the odd numbered holds heavily loaded with internal cargo under the alternate loading condition shown in Figure 39. Therefore, the double bottom structure is subjected to the global vertical bending moment as well as local lateral pressure loads caused by external sea pressure on outer bottom plate and internal cargo pressure on inner bottom plate in cargo holds. The internal cargo pressure and external sea pressure are considered in the calculations of Case_5, 6, 7 and 8 as shown in Table 9.

In accordance with the requirements for the direct strength assessment in CSR-BC, the alternate loading condition shown in Table 12 is considered, i.e., heavy cargo alternate loading condition (LC_10). Although this is the only load case that must be considered for the direct strength assessment, the effect of lateral loads on the hull girder ultimate strength in the sagging condition is also investigated in this calculation.

In the hogging condition, i.e., the calculations of Case_5 and 7 as shown in Table 9, the hull girder ultimate strength in the empty hold is calculated by utilizing the No. 3 ~ No. 5 holds model as shown in Figure 39. On the other hand, in the sagging condition, i.e., the calculations of Case_6 and 8 as shown in Table 9, the hull girder ultimate strength in the cargo hold is calculated by utilizing the No. 4 ~ No. 6 holds model as shown in Figure 39.

The boundary conditions are shown in Figure 40. The symmetry conditions were applied to all members in the center plane. A center point of the FE model was constrained X displacement. Rigid bodies were attached at both ends of the FE model, and constrained Y and Z displacements and X and Z rotations. Moreover, rigid bodies were also used for applying the global bending moment by the rotation control (enforced rotation) on the FE model.
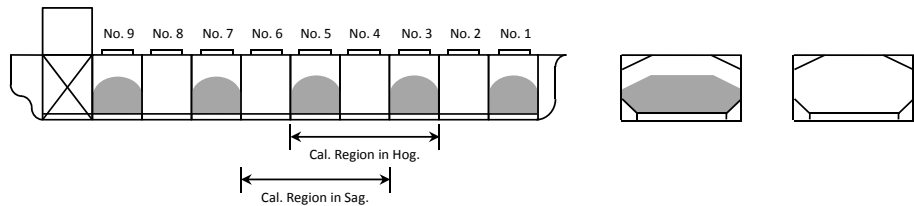

Figure 39. Alternate condition and calculation region.

Table 12. Calculating loading condition.

No.	Description	Draft	Loading pattern	Aft Mid Fore	Load case
LC_10	Alternate load (heavy cargo)	T_S			F2*

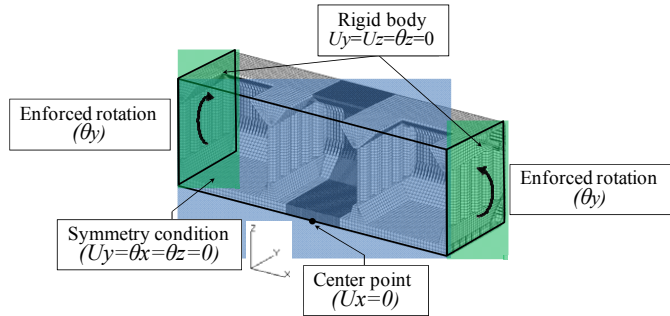* F2: Following sea in hogging.

Figure 40. Boundary conditions.

5.2.2 Calculation results

Participants for this benchmark calculations and the mesh division of FE model are summarized in Table 13.

The effect of initial imperfections

At first, participants investigated the effect of initial imperfections on the hull girder ultimate strength. Figure 41 shows the relationships between the vertical bending moment and the curvature from all participants by utilizing the 3 holds model. Figure 41 (a) and (b) show the results without and with imperfections, respectively. Table 14 shows the peak moment obtained by FE analysis.

Participants 1 and 2, who used the static implicit FEA code, obtained the mostly linear moment-curvature relationships and failed to get the post-buckling behaviour of stiffened panel. Static analysis can simulate the post buckling behaviour of simple stiffened panel by utilizing the enforced displacement procedure or Riks method, and can get the ultimate strength of it. But, for the complicated structure, such as actual hull girder structure which is composed with many stiffened panels, it is difficult to calculate the post buckling behaviour of each buckled panel, because there are so many nodes with negative stiffness after buckling.

Participant 2 also investigated the effect of modeling region on the hull girder ultimate strength. Figure 42 shows the relationships between the vertical bending moment and the curvature varying the modeling region. The obtained peak moments are summarized in Table 15. From Table 15, the peak moment obtained by using the 3 frames model was highest in all cases (Case_1-4). Furthermore, the results of the 3 hold models show the significantly low peak moment except for Case_1. In the case of small calculation region, especially in hogging condition with imperfection, both ultimate strength and post ultimate strength can be obtained, but the others cases seems to fail. The reason that the ultimate strength can be obtained only for the 3 frames model with imperfection under hogging condition, is thought to be follows.

In the small region model, the number of elements with negative stiffness by buckling is relatively small, and the change of stiffness after buckling is smaller in an imperfect model than in a perfect model, and the effect of buckling on ultimate strength is smaller in hogging condition than sagging condition.

On the other hand, participants 3 and 4, who used the dynamic explicit FEM, can obtain not only the ultimate strength but also the post ultimate behaviour. The calculation can be continued in stable at post buckling and post ultimate region due to the inertia effect. The results of ultimate strength by both participants show a small difference but same tendencies. Participant 4 also calculated with an implicit procedure, and could obtain the ultimate strength only for Case_4 utilizing Riks method by trial-and-

errors changing the loading steps, but failed for another cases as shown in Figure 41 with the blue dotted line. Overall, it seems that it is difficult to obtain the ultimate strength for actual ship hull girder by static procedure even if using Riks method.

Table 13. Summary of participants in benchmark study.

	Participant 1	Participant 2	Participant 3	Participant 4
FEA code	Trident	ANSYS	LS-DYNA	ANSYS
Solver	Implicit	Implicit	Explicit	Explicit Implicit
Plate*	Bottom part:10 × 29 Deck part :7 × 42	10 × 10 (10 × 30)**	Bottom part:4 × 12 Deck part :4 × 24	Bottom part: 6×12 Deck part: 6 ×25
Web depth	Deck, 3; Bottom, 4	3 (6)**	2	2
Flange breadth	2	2 (4)**	2	2

*Plates bounded by longitudinal stiffeners and transverse web frames (breadth × length).

**Figures between brackets indicate the number of elements only for the 3 frames model.

From results by participant 3, the effect of initial imperfections on the hull girder ultimate strength was more remarkable under the sagging condition than under the hogging condition.

Under hogging moment, the deck part first reaches the yield stress in tension, and keeps its loading capacity, and then the bottom part reaches its ultimate strength in compression. In this case, the yielding load at the deck is not much affected by initial imperfections, and the reduction of ultimate strength due to imperfection is small.

Under sagging condition, the deck part first reaches to its buckling strength, and reduces its loading capacity after buckling. Redistribution of stress in the deck takes place, but the whole section reaches ultimate strength because the reduction of capacity of buckled parts is large. The effect of imperfection on ultimate strength in compression is larger than in tension, therefore the reduction of ultimate strength due to imperfection is larger in sagging condition than in hogging condition.

The reduction of load carrying capacity after ultimate strength in sagging condition is larger than in hogging condition.

The effect of lateral loads

Participant 3 investigated the effect of lateral loads on the hull girder ultimate strength. Figure 43 shows the relationships between the vertical bending moment and the curvature of all cases. The calculation results obtained by the Smith's method are also shown in Figure 43. The hull girder ultimate strength is summarized in Table 16. Participant 1, 2 and 3 also tried to calculate the effect of lateral loads, and their results are shown in Figure 44 and Table 17. But, many of the calculations failed to find ultimate strength due to the same reason for case 1 to 4.

The effect of lateral loads on the hull girder ultimate strength was more remarkable under the hogging condition than under the sagging condition. At the bottom plates at mid span of the empty hold under the hogging condition, the compressive stress is introduced by the hogging moment, and the compressive stress is also produced by the lateral pressure loads. Therefore, the buckling of bottom plates and its stiffeners takes place earlier than the tensile yielding at deck plates. Under the hogging condition, it is found that the calculation result by the Smith's method agree with the FEA results without considering the lateral loads, and the FEA results including the effect of lateral loads show the safety value compared with the value of M_{CSR-H} as shown in Table 16. Under the sagging condition, however, differences between the calculation result by the Smith's method and the FEA results are observed. This is because the initial imperfections much affect the hull girder ultimate strength under the sagging condition, and the buckling mode of imperfection in FEA seems to be safety side assumption compared to the actual imperfection in real ship structure.

Table 14. Hull girder ultimate strength using 3 holds model   (unit; GN・m)

|	Participant 1	Participant 2	Participant 3	Participant 4
Case_1	17.57	14.37	18.54	17.67
Case_2	-14.59	-10.26	-17.02	-16.24
Case_3	15.74	15.15	17.57	17.57
Case_4	-14.44/-14.54	-11.04	-12.88	-12.88

Table 15. The difference of peak bending moment changing model region (unit; GN m).
(participant 2 with implicit static calculation)

|	3 frames	5 frames	7 frames	9 frames	1 hold	3 holds
Case_1	14.82	—	—	—	13.03	14.73
Case_2	-16.26	—	—	—	—	-10.26
Case_3	17.94	17.83	17.58	17.58	17.56	17.49
Case_4	-15.97	-14.37	-14.75	-13.15	-14.92	-14.74

Table 16. Hull girder ultimate strength varying initial imperfections and lateral loads (unit; GN m).
(participant 3)

	Initial imperfections / Lateral loads	FEA		Smith's method (M_u)	CSR-H* (M_{CSR-H})
		Without	With		
Hogging	Without	18.54	17.57	18.31	13.32
	With	13.68	13.39		
Sagging	Without	-17.02	-12.88	-14.73	-13.39
	With	-17.00	-12.83		

*According to CSR-H, the reduction of hull girder ultimate strength due to lateral loads is considered as follows: $M_{CSR-H} = M_u / (\gamma_M \gamma_{DB})$, where, $\gamma_M = 1.1$, $\gamma_{DB} = 1.25$ (Hog.), 1.0 (Sag.),
γ_M: Partial safety factor covering material, geometric, and strength prediction uncertainties,
γ_{DB}: Partial safety factor covering the effect of double bottom bending
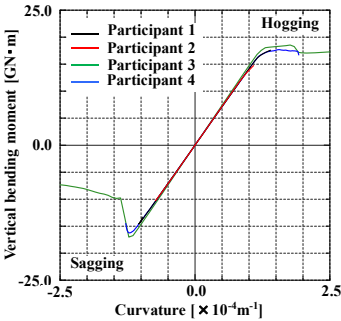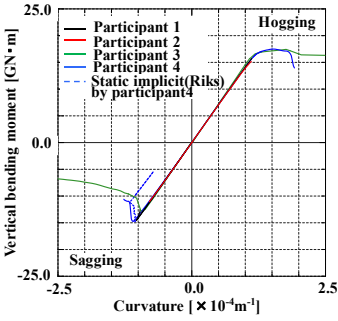
(a) Case_1 (hog.) and Case_2 (sag.)   (b) Case_3 (hog.) and Case_4 (sag.)

Figure 41. Relationships between vertical bending moment and curvature using 3 holds model

(a) Case_1 (hog.) and Case_2 (sag.)   (b) Case_3 (hog.) and Case_4 (sag.)

Figure 42. Relationships between vertical bending moment and curvature varying modeling region
(participant 2)

Table 17: Hull girder ultimate strength
using 3 holds model (unit; GN·m)

	Participant 1	Participant 2	Participant 3
Case_5	7.39	−	13.68
Case_6	-14.54	−	-17.00
Case_7	7.48	−	13.39
Case_8	-14.37/-14.32	-10.40	-12.83

Figure 43. Relationships between vertical
bending moment and curvature varying initial
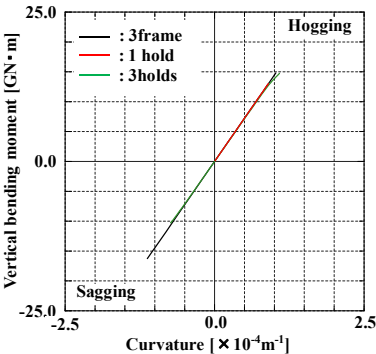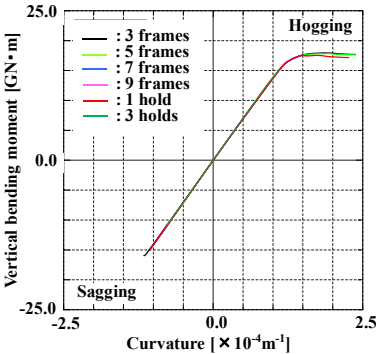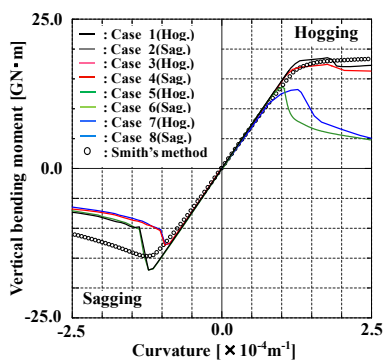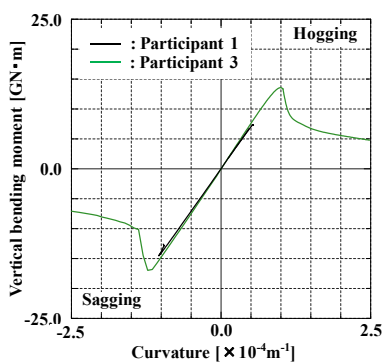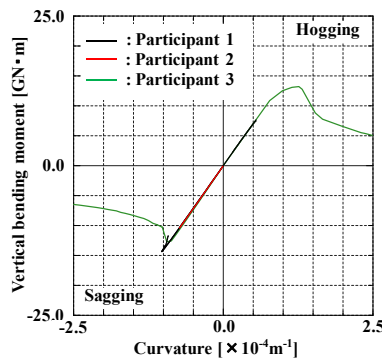imperfections and lateral loads (participant 3)

(a) Case_5 (hog.) and Case_6 (sag.)

(b) Case_7 (hog.) and Case_8 (sag.)

Figure 44. Relationships between vertical bending moment and curvature using 3 holds model,

5.3   Summary and Recommendation for Future Works

In the calculation of three hold model of a bulk carrier hull girder (section 5.2), the influence of initial imperfections and lateral load on hull girder ultimate strength are investigated. The differences in calculation results provided several researchers are clarified.

Unlike the box girder model in section 5.1, it is difficult to obtain the ultimate strength of a full scale hull girder by using a static FE solver, because there are so many elements with negative stiffness after buckling. However, by using time dependent dynamic analysis, it is easy to obtain the ultimate strength of large size of model, such as three hold model.

As for the effect of initial imperfections on the hull girder ultimate strength, it was more remarkable under the sagging condition than under the hogging condition. Under hogging moment, the deck part first reaches yield stress in tension, and keeps its loading capacity, and then the bottom part reaches ultimate strength in compression. Under sagging condition, the deck part first reaches buckling strength, and reduces its loading capacity after buckling. The redistribution of stress at deck part takes place, but the whole section reaches ultimate strength because the reduction of capacity of buckled parts is large. The effect of imperfection on ultimate strength in compression is larger than in tension, therefore the reduction of ultimate strength due to imperfection is larger in sagging condition than in hogging condition.

As for the effect of lateral loads on the hull girder ultimate strength, it was more remarkable under the hogging condition than under the sagging condition. Under the hogging condition, compressive stress is introduced in the outer bottom plates by both the hull girder bending moment and the lateral pressure loads. Therefore, the buckling of outer bottom plates and its stiffeners takes place earlier than the tensile

yielding at deck plates. But under the sagging condition, the ultimate strength mainly depends on the buckling of deck, and therefore the effect of lateral pressure on the hull girder strength is small under sagging moment.

The hull girder ultimate strength by FEM considering initial imperfection and lateral loads shows good agreement with predicted value by CSR-H. The newly introduced partial safety factor covering the effect of double bottom bending γ_{DB} seems to be reasonable from the results of benchmark study.

6.   CONCLUSION AND RECOMMENDATION

This report describes the results of literature survey and benchmark calculations related to buckling and ultimate strength of components and systems of ships and offshore structures, which have been conducted during the last three years. The report consists of six chapters.

In chapter 1, the history of assessment of buckling and ultimate strength of ships and offshore structures are briefly reviewed. Recent developments led by marine industry authorities on the buckling and ultimate strength of ships and offshore structures, including GBS (Goal-based New ship Construction Standard) in IMO, CSR (Common structural rules) by IACS and CSR-H (Harmonized Common Structural Rule) by IACS are introduced.

In chapter 2, the two criterions for ultimate assessment, the partial safety approach and the probabilistic approach, are briefly described, and the fundamentals and general characteristic of ultimate strength are also discussed.

In chapter 3, the results of literature survey for assessment procedure for ultimate strength, such as 1) Empirical and analytical methods, 2) Numerical methods, 3) Experimental methods, 4) Reliability assessment, 5) Rules and regulations are shown.

For empirical and analytical methods, modifications and extensions of simplified progressive collapse methods for predicting the ultimate strength of hull structures are investigated. The investigations of empirical formula for ultimate residual strength of damaged hull due to collision and corrosion are also performed.

For numerical methods, the numerical problem using static FEA in calculation of ultimate strength of large size of model, such as a three hold actual ship model, is highlighted. The needs of development of more valid ISUM elements, from the viewpoint of modeling effort and computing time, are also noted.

For experimental methods, experiments for stiffened panels, box girder models have been performed in these three years, but the specimen sizes and scantlings are limited. More experiments are desired to be performed and the detail information of experiments is expected to be opened for validation of analytical and numerical calculations.

Reliability assessment of ultimate strength of various items, such as ships damaged by collision/ grounding and corrosion, are recently performed by many researchers. By accumulation of results of reliability assessment of ultimate strength, it will be expected to be used more for confirming and modifying the regulations.

For rules and regulations, the changes in CSR-H from CSR are mainly described. The scantlings according to CSR-H are somewhat more conservative than CSR. This is mainly due to using the more conservative formula in both CSR rules sets when a theoretical back ground is not clear. It is desired to perform a further study in order to clarify the theoretical background, with modification of rules as necessary. Some of the technical background documents are not sufficient. We understand that this is unavoidable because not all been clarified yet. It is recommended that the unknown and unapparent items be clearly stated in background documents.

In chapter 4, the results of literature survey for ultimate strength of various structures, such as 1) Tubular members and joins, 2) Steel plate and stiffened plates, 3) Shells, 4) Ship structures, 5) Offshore structure, 6) Composite structures and 7) Aluminum structures are described.

For tubular members and joins, many researchers have examined two type of reinforcement on the strength of tubular members, i.e., using the fiber reinforce polymers and the steel- concrete composite structure. As recent research efforts have examined the resistance of tubular member subjected lateral impacts. The various reinforcement schemes for tubular joints have been investigated to extend the operating life of existing offshore platform. Recent research efforts have also covered the strength of complex tubular joints e.g. the elliptical joints, multi-planar joints, for which the existing design codes do not provide explicit strength equations.

Moreover, many researchers have examined the strength of tubular joints under accidental loading to develop the basis for engineering guidelines in such limit states.

For study of ultimate strength of steel plate and stiffened plates continues to be important for improving code based design formulas and direct strength analysis procedures. The analytical formulation for ultimate strength of stiffened panels have continued to study under compressive loading and multiple

loading, such with shear loading and lateral loading. And the behaviour of the panel with opening, rupture damage and service degradation are also investigated by numerical procedures.

For shells, the ultimate strength can be calculated by numerical methods considering initial imperfections and the effect of yielding, but the simple formulas for estimating the ultimate strength of shells, such as stiffened shells under the external pressure, is desired to be investigated more.

For ship structures, the special attention have been dedicated to progressive collapse methods, FEA and their applicability on intact ship integrity assessment, degradation by corrosion or reduction of the ultimate strength of the ship girder by structural local damage. Also some work was done on the interaction between different types of loading and their effect on the ultimate strength or interaction between vertical and horizontal bending.

Available publications on the ultimate strength of offshore structures are rather limited compared with considerable numbers of publication on ship/ ship-like structures. Offshore structures are huge assemblies of various components depending on the required function and working conditions. Much effort has been made on the ultimate strength at the level of specific components, i.e., stiffened panels, tubular members or joints; and on the effect of various parameters, i.e., composite material, initial imperfection, aging factors (corrosion and fatigue). Less effort has been made on the ultimate strength of the offshore structure globally and systematically. In this regard, systematic assessment of ultimate strength of offshore structures deserves further efforts.

The ultimate strength of composite structure is determined by coding a suitable composite failure criterion within an incremental loading algorithm. Once failure is detected the degradation model is used to reduce the properties of the laminate to account for the material damage and to effectively weaken the panel. Recent research focused on failure identification and material degradation models. The very little work has been done on simplified models for the calculation of ultimate strength of composite panels, and an area that has received attention is the ultimate strength after impact.

For aluminum structures, the available literature is relatively limited over the last three years when compared with the studies on steel structures. Compared to steel structures, the ultimate strength and collapse behaviour of aluminium structures are significantly affected not only by initial imperfections, but also by the material nonlinearity and the deterioration of mechanical strength in the heat-affected zones (HAZ) caused by welding in assembly and fabrication. Therefore, weld-induced effects have been then main focus of research on aluminium structures.

In chapter 5, the results of benchmark calculation for ultimate strength of small box girder model and three hold model of bulk carrier are shown.

For the benchmark calculation of small box girder model, the discrepancy of results between participants is in the range of uncertainly suggested by the IACS CSR partial safety factor. It should be noted that the numerical results are significantly lower than the experimentally measured strength. There is a possibility of difference of boundary condition between calculations and experiment, especially friction effect at loading and supporting positions.

For the benchmark calculation of three hold model of bulk carrier, it is hard to obtain the ultimate strength of hull girder by using the static FE solver, because there are so many elements with negative stiffness after buckling. By using the time dependent dynamic analysis, it is easy to obtain the ultimate strength of large size of model, such as three hold model. The hull girder ultimate strength by the dynamic explicit FEM considering initial imperfection and lateral loads shows good agreement with predicted value by CSR-H. The newly introduced partial safety factor covering the effect of double bottom bending ; γ_{DB} seems to be reasonable from the results of benchmark study.

REFERENCES

Aalberg, A., Langseth, M. & Larsen, P. K. 2001. Stiffened aluminium panels subjected to axial compression. *Thin-walled structures,* 39, 861–885.

Abs 2014. ABS guide for Buckling and Ultimate Strength Assessment for Offshore Structures. ABS.

Abubakar, A. & Dow, R. S. 2013. Simulation of grounding damage using the finite element method. *Int J Solids Struct.,* 50, 623–636.

Alagusundaramoorthy, P., Sundaravadivelu, R. & Ganapathy, C. 1999. Experimental study on collapse load of stiffened panels with cutouts. *Journal of Constructional Steel Research,* 52, 235–251.

Albermani, F., Khalilpasha, H. & Karampour, H. 2011. Propagation buckling in deep sub-sea pipelines. *Eng. Struct.,* 33, 2547–2553.

Alinia, M. M. & Dibaie, A. 2012. Buckling and failure characteristics of slender web I-column girders under interactive compression and shear. *comp. Meth. Civil Eng.,* 3, 15–34.

Alinia, M. M., Hosseinzadeh, S. a. A. & Habashi, H. R. 2007. Influence of central cracks on buckling and post-buckling behaviour of shear panels. *Thin-Wall Struct.,* 45, 422–431.

Alinia, M. M., Hosseinzadeh, S. a. A. & Habashi, H. R. 2008. Buckling and post-buckling strength of shear panels degraded by near border cracks. *J. Construct Steel Res.,* 64, 1483–1494.

Almroth, B. O. 1966. Influence of imperfections and edge restraint on the buckling of axially compressed cylinders. NASA CR-432, Prepared under contract No. NAS 1–3778 by Lockeheed Missile and Space Company.

Alps/Scol 2006. A computer program for progressive structural crashworthiness under collisions and grounding. Proteus Engineering S: MD, USA: Stevensville.

Amlashi, H. K. K. & Moan, T. 2008. Ultimate strength analysis of a bulk carrier hull girder under alternate hold loading condition–a case study Part 1: nonlinear finite element modelling and ultimate hull girder capacity. *Marine Structures,* 21, 327–352.

An, C., Duan, M. L., Filhoc, R. T. & Estefen, S. F. 2014. Collapse of sandwich pipes with PVA fiber reinforced cementitious composites core under external pressure. *Ocean Engineering,* 82, 1–13.

Andric, J., Kitarovic, S. & Bicak, M. 2014. IACS incremental-iterative method in progressive collapse analysis of various hull girder structures. *Brodogradnja/Shipbuilding,* 65, 65–78.

Anyfantis, K. N. & Tsouvalis, N. G. 2012. Post buckling progressive failure analysis of composite laminated stiffened panels. *Applied Composite Materials,* 19, 219–236.

Arjomandi, K. & Taheri, F. 2012. Bending Capacity of Sandwich Pipes. *Ocean Engineering,* 48, 17–31.

Bayatfar, A., Khedmati, M. R. & Rigo, P. 2014. Residual ultimate strength of cracked steel unstiffened and stiffened plates under longitudinal compression. *Thin-Walled Structures* 84, 378–392.

Benson, S. 2011. *Progressive Collapse Assessment of Lightweight Ship Structures,* Newcastle University.

Benson, S., Abubakar, A. & Dow, R. S. 2013a. A comparison of computational methods to predict the progressive collapse behaviour of a damaged box girder. *Eng Struct.,* 48, 266–280.

Benson, S., Downes, J. & Dow, R. 2013b. Load shortening characteristics of marine grade aluminium alloy plates in longitudinal compression. *Thin-Walled Structures,* 70, 19–32.

Benson, S., Downes, J. & Dow, R. S. 2013c. A Comparison of Numerical Methods to Predict the Progressive Collapse of Lightweight Aluminium Vessels. *J. Ship Prod. Des.,* 29, 117–126.

Benson, S., Downes, J. & Dow, R. S. 2013d. Compartment level progressive collapse analysis of lightweight ship structures. *Marine Structures,* 31, 44–62.

Benson, S., Leelachai, A. & Dow, R. S. 2013e. Ultimate strength of stiffened panels with circular cut-outs under in-plane compression *12th International Conference on Fast Sea Transportation.*

Benson, S., Syrigou, M. & Dow, R. S. 2013f. Longitudinal strength assessment of damaged box girders. Collision and Grounding of Ships and Offshore Structures. *Proceedings of the 6th International Conference on Collision and Grounding of Ships and Offshore Structures.*

Brubak, B., Andersen, H. & Hellesland, J. 2013. Ultimate strength prediction by semi-analytical analysis of stiffened plates with various boundary conditions. *Thin-Walled Structures,* 62, 28–36.

Brubak, L. & Hellesland, J. 2008. Strength criteria in semi-analytical, large deflection analysis of stiffened plates in local and global bending. *Thin-Walled Structures*.

Brubak, L., Hellesland, J. & Steen, E. 2007. Semi-analytical buckling strength analysis of plates with arbitrary stiffener arrangements. *Journal of Constructional Steel Research,* 63, 532–543.

Bryan, G. H. 1891. On the stability of a plane plate under thrust in its own plane with application to the buckling of side of a ship. *London Math. Soc.,* 22, 54–67.

Bs7910 2013. Guide to methods for assessing the acceptability of flaws in metallic structures. British Standards Institute.

Caldwell, J. B. 1965. Ultimate longitudinal strength. *Trans RINA,* 107, 411–30.

Cerik, B. C. & Cho, S. R. 2013. Residual strength of damaged stiffened cylinders under combined axial compression and radial pressure. . *The 12th Int. Symp. on Practical Design of Ships and Other Floating Structures (PRADS'13).* Changwon City: Korea.

Chalmers, D. W. 1993. *Design of Ship's Structures,* London.

Chamis, C. C., Abdi, F., Garg, M., Minnetyan, L., Baid, H., Huang, D., Housner, J. & Talagani, F. 2013. Micromechanics-based progressive failure analysis prediction for WWFE-III composite coupon test cases. *Journal of Composite Materials,* 47, 2695–2712.

Chan, T. M., Gardner, L. & Law, K. H. 2010. Structural design of elliptical hollow sections: a review. *Proc. ICE Struct. Build.*

Chang-Li, Y. & Lee, J. 2014. Formulation of reduction rate for ultimate compressive strength of stiffened panel induced by opening. *China Ocean Eng.,* 28, 557–568.

Chatzopoulou, G., Varelies, G.E. & Karamanos, S.A. 2014. Finite element analysis of UOE pipes under external pressure and bending. *In:* Conference, P. O. T. I. O. a. P. E. (ed.).

Chen, J. F., Morozov, E. V. & Shankar, K. 2011. Plastic damage model for progressive failure analysis of composite structures. *ICCM International Conferences on Composite Materials.*

Chen, N. Z. & Guedes Soares, C. 2007. Longitudinal Strength Analysis of Ship Hulls of Composite Materials under Sagging Moments. *Composite Structures,* 77, 36–44.

Chen, N. Z. & Guedes Soares, C. 2008. Ultimate longitudinal strength of ship hulls of composite materials. *Journal of Ship Research,* 52, 184–193.

Chen, N. Z., Sun, H. H. & Guedes Soares, C. 2003. Reliability analysis of a ship hull in composite material. *Composite Structures,* 62, 59–66.

Chenfeng, L., Huilong, R., Zhongqiu, Z., Xiaodong, Z., Ji, Z. & Donghao, X. 2013. An approximate calculation approach for the ultimate strength of ship hull girder. *OMAE 2013.* San Francisco.

Chiew, S. P., Zhang, J. C., Shao, Y. B. & Qiu, Z. H. 2012. Experimental and Numerical Analysis of Complex welded Tubular DKYY-Joints. *Advances in Structural Engineeing,* 15.

Cho, S. R., Kim, H. S., Doh, H. M. & Chon, Y. K. 2013. Ultimate strength formulation for stiffened plates subjected to combined axial compression, transverse compression, shear force and lateral pressure loadings. *Ships and Offshore Structures,* 8, 628–637.

Choung, J., Nam, J. & Ha, T. 2012a. Assessment of residual ultimate strength of an asymmetrically damaged tanker considering rotational and translational shifts of neutral axis plane. *Marine Structures,* 25, 71–84.

Choung, J., Nam, J. M. & Ha, T.-B. 2012b. Slenderness ratio distribution and load-shortening behaviours of stiffened panels. *Mar. Struct.,* 26, 42–57.

Choung, J., Nam, J. M., Tayyar, G. T., Yoon, S. W. & Lee, K. 2013. Assessment of Ultimate Longitudinal Strength of a VLCC considering Kinematic Displacement Theory. *Journal of the Society of Naval Architects of Korea,* 50, 255–261.

Choung, J., Park, J. B. & Song, C. Y. 2014. Lateral pressure effect on average compressive strength of stiffened panels for in-service vessels. *Ships Offshore Struct.,* 9, 110–118.

Collette, M. D. 2011. *Rapid analysis techniques for ultimate strength predictions of aluminium structures,* Taylor & Francis, London: UK.

Cook, R. D., Malkus, D. S., Plesha, M. E. & Witt, R. J. 2002. *Concepts and applications of finite element analysis,* New York: Wiley.

Crupi, V., Epasto, G. & Guglielmino, E. 2013. Comparison of aluminium sandwiches for lightweight ship structures: Honeycomb vs. foam. *Marine Structures* 30, 74–96.

Cui, S., Cheong, H. K. & Hao, H. 2000. Experimental study of dynamic post-buckling characteristics of columns under fluid–solid slamming. *Engineering structures* 22, 647–656.

Cui, S., Kiat Cheong, H. & Hao, H. 1999. Experimental study of dynamic buckling of plates under fluid–solid slamming. *International Journal of Impact Engineering,* 22, 675–691.

Dai, X. H. & Lam, D. 2012. Shape effect on the behaviour of axially loaded concrete filled steel stub columns at elevated temperature. *J. Constr. Steel Res.,* 73, 117–127.

Dai, X. H., Lam, D., Jamaluddin, N. & Ye, J. 2014. Numerical analysis of slender elliptical concrete filled columns under axial compression. *Thin Wall Struct.,* 77, 26–35.

Deco, A. & Frangopol, D. M. 2013. Risk-informed optimal routing of ships considering different damage scenarios and operational conditions. *Reliability Engineering and System Safety,* 119, 126–140.

Deco, A., Frangopol, D. M. & Zhu, B. 2012. Reliability and redundancy assessment of ships under different operational conditions. *Ocean Engineering,* 42, 457–471.

Dnv-Os-J101 2014. Design of Offshore Wind Turbine Structures.

Dow, R. S. 1991. Testing and analysis of a 1/3 scale frigate model. *Adv. Mar. Struct.,* 2, 749–773.

Dyanati, M. & Huang, Q. 2014. Seismic Reliability of a fixed offshore platform against collapse. *Proceedings of the ASME 2014 33rd International Conference on Ocean, Offshore and Arctic Engineering.* San Francisco: California: USA.

El-Hanafi, A. S., Badran, S. F. & Leheta, H. W. 2013. Design of Y stiffened panels in double hull tanker under axial compressive loads. *Analysis and Design of Marine Structures,* CRC Press, 291–300.

Ergin, A. & Ozdemir, M. 2013. Ultimate Strength Analysis of Ship Structural Panels. *TEAM 2013.* Keelung: Taiwan.

Espinos, A., Gardner, L., Romero, M. L. & Hospitaler, A. 2011. Fire behaviour of concrete-filled elliptical steel columns. . *Thin Wall Struct.,* 49, 239–255.

Estefen, T. P. & Estefen, S. F. 2012. Buckling propagation failure in semi-submersible platform columns. *Mar. Struct.,* 28, 2–24.

Farkas, J. & Jármai, K. 2014. Optimization of welded square cellular plates with two different kinds of stiffeners. *J. Constr. Steel Res.,* 101, 61–65.

Fujikubo, M. & Kaeding, P. 2002. New simplified approach to collapse analysis of stiffened plates *Mar Struct. 15,* 15, 251–283.

Fujikubo, M., Muis Alie, M. Z., Takemura, K., Iijima, K. & Oka, S. 2012a. Residual Hull Girder Strength of Asymmetrically Damaged Ships. *Journal of the Japan Society of Naval Architects and Ocean Engineers,* 16, 131–140.

Fujikubo, M., Uda, S., Tatsumi, A., Iijima, K., Ogawa, H. & Takami, T. 2013. Finite Element Modeling of a Continuous Stiffened Panel under Combined Inplane Shear and Thrust. *TEAM 2013.* Keelung: Taiwan.

Fujikubo, M., Zubair, M. A., Takemura, K., Iijima, K. & Oka, S. 2012b. Residual Hull Girder Strength of Asymmetrically Damaged Ships. *Journal of the Japan Society of Naval Architects and Ocean Engineers,* 16, 131–140.

Gan, J. M., Bickerton, S. & Battley, M. 2011. Modelling the initiation and evolution of damage within GFRP by including real geometric variability. *ICCM International Conferences on Composite Materials.*

Gannon, L., Liu, Y., Pegg, N. & Smith, M. J. 2012a. Effect of welding-induced residual stress and distortion on ship hull girder ultimate strength. *Marine Structures,* 28, 25–49.

Gannon, L., Liu, Y., Pegg, N. & Smith, M. J. 2013. Effect of three-dimensional welding-induced residual stress and distortion fields on strength and behaviour of flat-bar stiffened panels. *Ships Offshore Struct.,* 8, 565–578.

Gannon, L. G., Pegg, N. G., Smith, M. J. & Liu, Y. 2012b. Effect of residual stress shakedown on stiffened plate strength and behaviour. *Ships Offshore Struct. ,* 8, 638–652.

Gao, D. W., Shi, G. J. & Wang, D. Y. 2012. Residual ultimate strength of hull structures with crack and corrosion damage. *Engineering Failure Analysis,* 25, 316–328.

Gaspar, B. & Guedes Soares, C. 2013. Hull girder reliability using a Monte Carlo based simulation method. *Probabilistic Engineering Mechanics,* 31, 65–75.

Gaspar, B., Teixeira, A. P., Guedes Soares, C. & Wang, G. 2011. Assessment of IACS-CSR implicit safety levels for buckling strength of stiffened panels for double hull tankers. *Mar. Struct.,* 24, 478–502.

Ghavami, K. & Khedmati, M. R. 2006. Numerical and experimental investigations on the compression behaviour of stiffened plates. *Journal of Constructional Steel Research,* 62, 1087–1100.

Gong, S., Sun, B., Bao, S. & Bai, Y. 2012. Buckle propagation of offshore pipelines under external pressure *Mar. Struct.,* 29, 115–130.

Goode, C. D., Kuranovas, A. & Kvedaras, A. K. 2010. Buckling of slender composite concrete-filled steel columns. *J. Civ. Eng. Manag.,* 16, 230–237.

Gordo, J. M. 2012. *Ultimate compressive strength of double-bottom under alternate lateral loading* SOARES, C. G. & SANTOS, N. A. (eds.) Engenharia e Tecnologia Marítima, Lisboa: Salamandra.

Gordo, J. M. & Guedes Soares, C. 1996. Approximate method to evaluate the hull girder collapse strength *Mar. Struct.,* 9, 449–470.

Gordo, J. M. & Guedes Soares, C. 2004. Experimental evaluation of the ultimate bending moment of a box girder. *Marine Systems & Ocean Technology,* 1, 1–14.

Gordo, J. M. & Guedes Soares, C. 2008a. Compressive tests on short continuous panels. *Marine Structures,* 21, 113–137.

Gordo, J. M. & Guedes Soares, C. 2008b. Experimental evaluation of the behaviour of a mild steel box girder under bending moment. *Ships and Offshore Structures,* 3, 347–358.

Gordo, J. M. & Guedes Soares, C. 2009. Tests on ultimate strength of hull box girders made of high tensile steel. *Marine Structures 22(4),* 22, 770–790.

Gordo, J. M. & Guedes Soares, C. 2011. Compressive tests on stiffened panels of intermediate slenderness. *Thin-Walled Structures,* 49, 782–794.

Gordo, J. M. & Guedes Soares, C. 2012. Compressive Tests on Long Continuous Stiffened Panels. *Journal of Offshore Mechanics and Arctic Engineering,* 134, 021403–021403–8.

Gordo, J. M. & Guedes Soares, C. 2014. Experimental analysis of the effect of frame spacing variation on the ultimate bending moment of box girders. *Marine Structures,* 37, 111–134.

Gordo, J. M., Teixeira, A. P. & Guedes Soares, C. 2011. Ultimate strength of ship structures. *Marine Technology and Engineering.*

Gui-Jie, S. & De-Yu, W. 2012. Ultimate strength model experiment regarding a container ship's hull structures. *Ships and Offshore Structures,* 7, 165–184.

Han, L. H., He, S. H., Zheng, L. Q. & Tao, Z. 2012. Curved concrete filled steel tubular (CCFST) built-up members under axial compression: experiments. *J. Constr. Steel Res.,* 74, 63–75.

Han, L. H., Hou, C. C., Zhao, X. L. & Rasmussen, K. J. R. 2014. Behaviour of high-strength concrete filled steel tubes under transverse impact loading. *J. Constr. Steel Res.,* 92, 25–39.

Han, L. H., Zheng, L. Q., He, S. H. & Tao, Z. 2011. Tests on curved concrete filled steel tubular members subjected to axial compression. *J. Constr. Steel Res.,* 67, 965–976.

He, S. B., Shao, Y. B., Zhang, H. Y., Yang, D. P. & Long, F. L. 2013. Experimental study on circular hollow section (CHS) tubular K-joints at elevated temperature. *Eng. Fail. Anal.* , 34, 204–216.

Hibbitt, H., Karlsson, B. & Sorensen, P. 2010. *Abaqus analysis user's manual version 6,* RI, USA: Dassault Systemes Simulia Corp Providence.

Hou, C., Han, L. H. & Zhao, X. L. 2013. Concrete-filled circular steel tubes subjected to local bearing force: Experiments. *Journal of Constructional Steel Research,* 83, 90–104.

Htun, M. M. & Kawamura, Y. 2013. A Study on the Method to Estimate the Stochastic Property of the Strength of Corroded Plate by Response Surface Method with Polynomial Chaos Expansion. *In:* Ceco (ed.) *Proceedings of the PRADS2013.* Changwon City: Korea.

Hu, S. Z. & Jiang, L. 1998. A finite element simulation of the test procedure of stiffened panels. *Mar Struct.,* 11, 75–99.

Hu, Y., Cui, W. C. & Pedersen, P. T. 2004. Maintained ship hull girder ultimate strength reliability considering corrosion and fatigue. *Mar Struct.,* 17, 91–123.

Huchinson, J. W. 1967. Imperfection sensibility of external pressurized spherical shells. *JournalofApplied Mechanics* 34.

Iacs 2006a. *Common Structural Rules for Bulk Carriers*, International Association of Classification societies.

Iacs 2006b. *Common Structural Rules for Double Hull Oil Tankers,* International Association of Classification Societies.

Iacs 2010a. Common Structural Rules for Bulk Carriers. International Association of Classification Societies.

Iacs 2010b. Common Structural Rules for Double Hull Oil Tankers. International Association of Classification Societies.

Iacs 2014a. *Common Structural Rules for Bulk Carriers and Oil Tankers*, International Association of Classification Societies.

Iacs 2014b. *Technical Background Documents for CSR*, International Association of Classification societies.

Ibekwe, A. U., Pu, Y., Ham, W. L. & Dow, R. S. 2014. Progressive collapse analysis and reliability of a damaged hull girder. *Proceedings of the ASME 2014 33rd International Conference on Ocean, Offshore and Arctic Engineering.* San Francisco, California: USA.

Imo. Goal-Based Standards. International Maritime Organization. November 2006 London.

Iso. Requirements for Their Ultimate Limit State Assessment. International Organization for Standardization. *In:* 2, I. C.-S. a. M. T.-S. S.-P., ed., November 2006 Geneva.

Jelovica, J., Romanoff, J., Ehlers, S. & Varsta, P. 2012. Influence of weld stiffness on buckling strength of laser-welded web-core sandwich plates. *J. Constr. Steel Res.,* 77, 12–18.

Jiang, X. & Guedes Soares, C. 2012a. A closed form formula to predict the ultimate capacity of pitted mild steel plate under biaxial compression. *Thin-Walled Structures,* 59, 27–34.

Jiang, X. & Guedes Soares, C. 2012b. Ultimate capacity of rectangular plates with partial depth pits under uniaxial loads *Marine Structures,* 26, 27–41.

Jin, M., Zhao, J. C., Chang, J. & Zhang, D. X. 2012. Experimental and parametric study on the post-fire behaviour of tubular T-joint. *J. Constr. Steel Res.   ,* 70, 93–100.

Kant, M. & Penumadu, D. 2011. Sea water effects on ultimate tensile and fracture strength of carbon fibers with nano-tensile testing. *ICCM International Conferences on Composite Materials.*

Kant, M., Siriruk, A. & Penumadu, D. 2010. Sea water and temperature effects on the mechanical properties of single carbon fibers. *25th Technical Conference of the American Society for Composites and 14th US-Japan Conference on Composite Materials 2010.*

Karampour, H., Albermani, F. & Veidt, M. 2013. Buckle interaction in deep subsea pipelines. *Thin-Walled Struct.,* 72, 113–120.

Kenny, S., Taheri, F. & Pegg, N. 2002. Experimental investigations on the dynamic plastic buckling of a slender beam subject to axial impact. *International journal of impact engineering,* 27, 1–17.

Khan, I. & Zhang, S. 2011. Effects of welding-induced residual stress on ultimate strength of plates and stiffened panels. *Ships Offshore Struct.,* 6, 297–309.

Khedmati, M. R. & Edalat, P. 2013. Ultimate Strength Characteristics of a Ship's Deck Stiffened Plate Structure in the Presence of Camber Parabolic Curvature. *J. Offshore Mech. Arct. Eng.,* 135, 031601–031601.

Khedmati, M. R. & Nazari, M. 2012. A numerical investigation into strength and deformation characteristics of preloaded tubular members under lateral impact loads. *Mar. Struct.,* 25, 33–57.

Khedmati, M. R., Nazari, M. & Khalaj, A. F. 2012. A numerical investigation into ultimate strength and buckling behaviour of locally corroded steel tubular members. *The 31rd Int. Conf. on Ocean, Offshore and Arctic Engineering (OMAE2012).* Rio de Janeiro: Brazil: American Society of Mechanical Engineers (ASME).

Khedmati, M. R., Pedram, M. & Rigo, P. 2014. The effects of geometrical imperfections on the ultimate strength of aluminium stiffened plates subject to combined uniaxial compression and lateral pressure. *Ships and Offshore Structures,* 9, 88–109.

Kiat Cheong, H., Hao, H. & Cui, S. 2000. Experimental investigation of dynamic post-buckling characteristics of rectangular plates under fluid-solid slamming. *Engineering Structures,* 22, 947–960.

Kim, B. J., Seo, J. K., Park, J. H., Jeong, J. S., Oh, B. K., Kim, S. H., Park, C. H. & Paik, J. K. 2010. Load characteristics of steel and concrete tubular members under jet fire: an experimental and numerical study. *Ocean Eng.,* 37, 1159–1168.

Kim, D., Kim, B., Seo, J., Kim, H., Zhang, X. & Paik, J. 2014. Time-dependent residual ultimate longitudinal strength - grounding damage index (R-D) diagram. *Ocean Engineering,* 76, 163–171.

Kim, D. K., Park, D. K., Kim, H. B., Seo, J. K., Kim, B. J., Paik, J. K. & Kim, M. S. 2012a. The necessity of applying the common corrosion addition rule to container ships in terms of ultimate longitudinal strength. *Ocean Engineering,* 49, 43–55.

Kim, D. K., Park, D. K., Park, D. H., Kim, H. B., Kim, B. J., Seo, J. K. & Paik, J. K. 2012b. Effect of corrosion on the ultimate strength of double hull oil tankers - Part II: Hull girders. *Structural Engineering and Mechanics,* 42, 531–549.

Kim, D. K., Pedersen, P. T., Paik, J. K., Kim, H. B., Zhang, X. & Kim, M. S. 2013a. Safety guidelines of ultimate hull girder strength for grounded container ships. *Safety Science,* 59, 46–54.

Kim, K., Park, D. H., Kim, H. B., Kim, B. J., Seo, J. K. & Paik, J. K. 2013b. Lateral pressure effects on the progressive hull collapse behaviour of a Suezmax-class tanker under vertical bending moments. *Ocean Engineering,* 63, 112–121.

Kim, K. & Yoo, C. H. 2008. Ultimate strengths of steel rectangular box beams subjected to combined action of bending and torsion. *Eng Struct. ,* 30, 1677–1687.

Kimura, N., Tanaka, S. & Okazawa, S. Study of Buckling/Post-Bucklnig Behaviours of Plate Structures Using Shell-Solid Mixed Analysis. TEAM 2013, 2013 Keelung: Taiwan.

Kitarovic, S., Žanic, V. & Andric, J. 2013. Progressive collapse analyses of stiffened box- girders submitted to pure bending. *Brodogradnja,* 64, 437–455.

Koiter, W. T. 1945. Over de Stabiliteit van het elastche Evenwichi, Dissertation, Delft, Holland, Tarnslation. *On the Stability of Elastic Equilibrium,* NASA TTF-10833,1967,and AFFDL-TR-70–25,1970, Sec.7.7.

Kumar, M. S., Alagusundaramoorthy, P. & Sundaravadivelu, R. 2009. Ultimate strength of stiffened plates with a square opening under axial and out-of-plane loads. *Eng Struct.,* 31, 2568–2579.

Kutt, L. M., Piaszczyk, C. M., Chen, Y. K. & Liu, D. 1985. Evaluation of the longitudinal ultimate strength of various ship hull configurations. *Trans Soc Naval Archit Mar Eng.,* 93, 33–53.

Lam, D., Gardner, L. & Burdett, M. 2010. Behaviour of axially loaded concrete filled stainless steel elliptical stub columns. *Adv. Struct. Eng.,* 13, 493–500. .

Lee, C. H., Jang, C. H., Jun, S. H. & Oh, Y. T. 2014. Global Structural Analysis for Semi-submersible Drill Rig. *The Twenty-fourth International Ocean and Polar Engineering Conference,* . Busan: Korea.

Lee, J., Soutis, C. & Kong, C. 2011. Prediction of compression-after-impact (CAI) strength of CFRP laminated composites. *ICCM International Conferences on Composite Materials.*

Lee, J. S. 2012. On the Ultimate Compressive Strength of Stiffened Panels with Rectangular Opening. *Proceedings of 5th PAAMES and AMEC2012.* Taiwan.

Lesani, M., Bahaari, M. R. & Shokrieh, M. M. 2013a. Detail investigation on un-stiffened T/Y tubular joints behaviour under axial compressive loads. *J. Constr. Steel Res.,* 80, 91–99.

Lesani, M., Bahaari, M. R. & Shokrieh, M. M. 2013b. Numerical investigation of FRP-strengthened tubular T-joints under axial compressive loads. *Comp. Struct.,* 100, 71–78.

Li, C., Ren, H., Zhao, Z., Zhao, X., Zeng, J. & Xu, D. 2013a. An approximate calculation approach for ultimate strength of ship hull girder. *Proceedings of the International Conference on Offshore Mechanics and Arctic Engineering - OMAE.2013.*

Li, G. C., Yang, Z. J., Lang, Y. & Fang, C. 2013b. Behaviour of high strength concrete filled square steel tubular columns with inner CFRP circular tube under bi-axial eccentric loading. *Adv. Steel Constr.,* 9, 231–246.

Li, S. Q., Zhang, Q. J. & Zheng, J. J. 1993. Experimental investigation on dynamic buckling and plastic collapse of rectangular plates subjected to solid-fluid in-plane impact. *Acta mechanica sinica,* 25, 249–258.

Lie, S. T., Li, T. & Shao, Y. B. 2014. Plastic collapse load prediction and failure assessment diagram analysis of cracked circular hollow section T-joint and Y-joint. Fatigue Fract. Eng. *Mat. Struct.,* 37, 314–324.

Lindemann, T. & Kaeding, P. 2013. Investigations on the Influence of Particular Components of the Idealized Structural Unit Method (ISUM) for Collapse Analysis of Plate Structures. *Proceedings of the Twenty-Third (2013) International Offshore and Polar Engineering.* Anchorage: Alaska: USA.

Lindemann, T., Klostermann, L. & Kaeding, P. 2013. Approaches to the Improvement of the Applicability of the Idealized Structural Unit Method for Collapse Analysis of Plate Structures. *Proceedings of the Twenty-Third (2013) International Offshore and Polar Engineering.* Anchorage: Alaska: USA.

Liu, B. & Wu, W. 2013. Standardized nonlinear finite element analysis of the ultimate strength of bulk carriers. Wuhan Ligong Daxue Xuebao (Jiaotong Kexue Yu Gongcheng Ban). *Journal of Wuhan University of Technology (Transportation Science and Engineering),* 37, 716–719.

Liu, Z. & Amdahl, J. 2012. Numerical and simplified analytical methods for analysis of the residual strength of ship double bottom. *Ocean Engineering,* 52, 22–34.

Lloyd's 2014. *Lloyd's Registe Rules and Regulations for the Classification of Offshore Units, July 2014.*, Lloyd's Register.

Lohning, T. & Muuholm, U. 2013. Finite element-based design of grouted connections with shear keys for offshore wind turbines. *Struct. Eng.,* 23, 295–302.

Lu, H., Han, L. H. & Zhao, X. L. 2010. Fire performance of self-consolidating concrete filled double skin steel tubular columns: experiments. *Fire Saf. J.,* 45, 106–115.

Ma, M., Hughes, O. & Paik, J. K. 2013. Ultimate Strength based Stiffened Panel Design using Multi-Objective Optimization Methods and Its Application to Ship Structures. *Proceedings of the PRADS2013. CECO.* Changwon City: Korea.

Mackay, J. R. & Van Keulen, F. 2013. Partial safety factor approach to the design of submarine pressure hulls using nonlinear finite element analysis. *Finite Elem. Anal. Des.,* 65, 1–16.

Magoga, T. & Flockhart, C. 2012. Ultimate strength calculations of an aluminium patrol boat. *International Maritime Conference 2012, Pacific 2012.* RINA, Royal Institution of Naval Architects.

Magoga, T. & Flockhart, C. 2014. Effect of weld-induced imperfections on the ultimate strength of an aluminium patrol boat determined by ISFEM rapid assessment method. *Ships and Offshore Structures,* 9, 218–235.

Makouei, S. H., Teixeira, A. P. & Guedes Soares, C. G. 2014. An approach to estimate the ship longitudinal strength using numerical databases of stress-strain curves of stiffened panels Developments in Maritime Transportation and Exploitation of Sea Resources. *In:* 2013, P. O. I. (ed.) *15th International Congress of the International Maritime Association of the Mediterranea* Coruna: Spain.

Makouei, S. H., Teixeira, A. P. & Guedes Soares, C. G. 2015. *A study on the progressive collapse behaviour of a damaged hull girder,* Maritime Technology and Engineering. London, Taylor & Francis Group.

Misirlis, K., Downes, J. & Dow, R. S. 2013. Ultimate strength of composite hulls under vertical bending. *FAST 2013 - 12th International Conference on Fast Sea Transportation.*

Moncada, A. M., Chattopadhyay, A., Bednarcyk, B. A. & Arnold, S. M. 2012. Micromechanics-based progressive failure analysis of composite laminates using different constituent failure theories. *Journal of Reinforced Plastics and Composites,* 31, 1467–1487.

Mouritz, A. P., Gellert, E., Burchill, K. & Challis, K. 2001. Review of Advanced Composite Structures for Naval Ships and Submarines. *Composite Structures,* 53, 21–41.

Muis Alie, M. Z. 2012. Residual Longitudinal Strength Analysis of Ship's Hull Girder with Damages. *International Society of Offshore and Polar Engineers (ISOPE).* Proceedings of the Twenty-second (2012) International Offshore and Polar Engineering Conference.

Muis Alie, M. Z. 2013. *Residual hull girder strength of asymmetrically damaged ships. ,* Osaka University.

Nam, J. M. & Choung, J. 2012. Residual Longitudinal Strength of a VLCC Considering Probabilistic Damage Extents. *Proceedings of the Twenty-second (2012) International Offshore and Polar Engineering Conference.* Rhodes.

Nam, J. M., Choung, J., Park, S. Y. & Yoon, S. W. 2014. Progressive collapse analysis and reliability of a damaged hull girder. *Proceedings of the ASME 2014 33rd International Conference on Ocean, Offshore and Arctic Engineering.* San Francisco, California: USA

Nam, M. & Choung, J. 2013. Assessment of Average Compressive Strengths Effect of Stiffened Panels on Hull Girder Ultimate Longitudinal Strengths. *Proceedings of the PRADS2013. CECO.* Changwon City: Korea.

Nettles, A. T. & Jackson, J. R. 2013. Compression after impact strength of out-of-autoclave processed laminates. *Journal of Reinforced Plastics and Composites,* 32, 1887–1894.

Nezamian, A. & Nezamian, M. 2014. A Review of Failure Modes in Ultimate Strength Assessment for Re-qualification and Life Extension of an Oil Field. *The Twenty-fourth International Ocean and Polar Engineering Conference.* Busan: Korea.

Nikolov, P. I. 2012. Box girder strength under pure bending: Comparison of experimental and numerical results. Sustainable Maritime Transportation and Exploitation of Sea Resources. *Proceedings of the 14th International Congress of the International Maritime Association of the Mediterranean, IMAM 2011, 2012.*

Oliveira, D. Report of Committee III.1.Ductile Collapse. Proceedings of the 10th International ship and Offshore Structures Congress, 1988 Lynby, Denmark, . 315–404.

Ozdemir, M. & Ergin, A. 2013. *Nonlinear buckling behaviour of stiffened ship panels*, Taylor & Francis, Espoo: Finland.

Paik, J., Kim, D. K., Park, D. H., Kim, H. B. & Kim, M. 2012a. A new method for assessing the safety of ships damaged by grounding. *Trans. RINA., Part A1, Intl J Maritime Eng.,* 154, 1–20.   .

Paik, J. K. 2007. Ultimate strength of perforated steel plates under edge shear loading. *Thin-Wall Struct.,* 45, 301–306.

Paik, J. K. 2008. Ultimate strength of perforated steel plates under combined biaxial compression and edge shear loads. *Thin-Wall Struct.,* 46, 207–213.

Paik, J. K. 2009. Residual ultimate strength of steel plates with longitudinal cracks under axial compression–experiments. *Ocean engineering,* 35, 1775–1783.

Paik, J. K., A.K., T. & Che, J. S. 1996. Ultimate strength hulls under combined vertical bending, horizontal bending, and shearing forces. *Trans SNAME,* 104, 31–59.

Paik, J. K., A.K., T., Pedersen, P. T. & Y., P. 2001. Ultimate strength of ship hulls under torsion. *Ocean Eng.,* 28, 1097–1133.

Paik, J. K., Amlashi, H., Boon, B., Branner, K., Caridis, P., Das, P. & Fujikubo, M. 2012b. Report of ISSC Technical Committee III.1 - Ultimate Strength. *18th International Ship and Offshore Structures Congress.*

Paik, J. K., Andrieu, C. & Cojeen, H. P. 2008a. Mechanical collapse testing on aluminum stiffened plate structures for marine applications. *Marine Technology,* 45, 228–240.

Paik, J. K. & Kim, B. J. 2008. Progressive collapse analysis of thin-walled box columns. *Thin-Wall Struct.,* 46, 541–550.

Paik, J. K., Kim, B. J. & Seo, J. K. 2008b. Methods for ultimate limit state assessment of ships and ship-shaped offshore structures: Part III hull girders. *Ocean Eng.,* 35, 281–286.

Paik, J. K., Kim, B. J., Sohn, J. M., Kim, S. H., Jeong, J. M. & Park, J. S. 2012c. On buckling collapse a fusion-welded aluminium stiffened plate structure: An experimental and numerical study. *Journal offshore Mechanics and Arctic Engineering,* 134, 021402–021409.

Paik, J. K., Kim, D. K., Park, D. H., Kim, H. B., Mansour, A. E. & Caldwell, J. B. 2013. Modified Paik–Mansour formula for ultimate strength calculations of ship hulls. *Ships and Offshore Structures,* 8, 245–260.

Paik, J. K. & Mansour, A. E. 1995. A simple formulation for predicting the ultimate strength of ships. *J. Mar. Sci. Tech.,* 1, 52–62.

Paik, J. K. & Sohn, J. 2011. Effects of Welding Residual Stresses on High Tensile Steel Plate Ultimate Strength: Nonlinear Finite Element Method Investigations. *J. Offshore Mech. Arct. Eng.,* 134, 021401–021401.

Paik, J. K. & Thayamballi, A. K. 2003a. A concise introduction to the idealized structural unit method for nonlinear analysis of large plated structures and its application. *Thin-Wall Struct.,* 41, 329–355.

Paik, J. K. & Thayamballi, A. K. 2003b. An experimental investigation on the dynamic ultimate compressive strength of ship plating. *International Journal of Impact Engineering,* 28, 803–811.

Park, J., Chun, M., Jeon, S., Kim, B., Jang, K., Suh, Y., Kim, J. & Lee, J. 2013. Advanced Guideline to Predict the Ultimate Strength of Perforated Plate with Edge Reinforcement. *Proceedings of the PRADS2013. CECO.* Changwon City: Korea.

Park, M. S., Jeong, Y. J. & Y.J., Y. 2014. Structural analysis of a hybrid substructure with multi-cylinder for 5MW offshore wind turbines. *Proceedings of the ASME 2014 33rd International Conference on Ocean, Offshore and Arctic Engineering.* San Francisco, California: USA.

Paulo, R. M. F., Teixeira-Dias, F. & Valente, R. a. F. 2013. Numerical simulation of aluminium stiffened panels subjected to axial compression: Sensitivity analyses to initial geometrical imperfections and material propertie. *Thin-Walled Structures,* 62, 65–74.

Pedram, M. & Khedmati, M. R. 2014. The effect of welding on the strength of aluminium stiffened plates subject to combined uniaxial compression and lateral pressure. *International Journal of Naval Architecture and Ocean Engineering,* 6, 39–59.

Pei, Z., Iijima, K., Fujjikubo, M., Tanaka, Y., Tanaka, S., Okazawa, S. & Yao, T. 2013. Collapse behaviour of a bulk carrier under alternate heavy loading conditions. *International Journal of Offshore and Polar Engineering,* 23, 224–231.

Philippidis, T. P. & Antoniou, A. E. 2013. A progressive damage FEA model for glass/epoxy shell structures. *Journal of Composite Materials,* 47, 623–637.

Pollalis, C. & Samuelides, M. S. 2013. Ultimate strength of damaged hulls. Collision and Grounding of Ships and Offshore Structures. *Proceedings of the 6th International Conference on Collision and Grounding of Ships and Offshore Structures, ICCGS 2013.*

Prestileo, A., Rizzuto, E., Teixeira, A. P. & Guedes Soares, C. 2013. Bottom damage scenarios for the hull girder structural assessment. *Marine Structures,* 33, 33–55.

Pulos, J. G. & Salerno, V. L. (eds.) 1961. *Axisymmetric elastic deformation and stresses in a ring-stiffened perfect circular cylindrical shell under external hydrostatic pressure,* Office of Naval Research, Bethesda: MD.

Qi, E., Cui, W. & Wan, Z. 2005. Comparative study of ultimate hull girder strength of large double hull tankers. *Mar Struct.,* 18, 227–49.

Qian, X. 2013. Failure assessment diagrams for circular hollow section X- and K-joints. *Int. J. Press. Ves. Piping,* 104, 43–56.

Qian, X., Jitpairod, K., Marshall, P. W., Swaddiwudhipong, S., Ou, Z., Zhang, Y. & Pradana, M. R. 2014. Fatigue and residual strength of concrete-filled tubular X-joints with full capacity welds. *J. Constr Steel Res.,* 100, 21–35.

Qian, X., Li, Y. & Ou, Z. 2013a. Ductile tearing assessment of high-strength steel X-joints under in-plane bending. *Eng. Fail. Anal.,* 28, 176–191.

Qian, X., Ou, Z., Swaddiwudhipong, S. & Marshall, P. W. 2013b. Brittle failure caused by lamellar splitting in a large-scale tubular joint with fatigue cracks. *Mar. Struct.,* 34, 185–204.

Qian, X., Zhang, Y. & Choo, Y. S. 2013c. A load-deformation formulation with fracture representation based on the J-R curve for tubular joints. *Eng. Fail. Anal.,* 33, 347–366.

Qu, H., Huo, J., Xu, C. & Fu, F. 2014. Numerical studies on dynamic behaviour of tubular T-joint subjected to impact loading. *Int. J. Impact Eng.,* 67, 12–26.

Rønning, L., Aalberg, A. & Kristian Larsen, P. 2010. An experimental study of ultimate compressive strength of transversely stiffened aluminium panels. *Thin-Walled Structures,* 48, 357–372.

Saad-Eldeen, S., Garbatov, Y. & Soares, C. G. 2011. Experimental assessment of the ultimate strength of a box girder subjected to severe corrosion. *Marine Structures,* 24, 338–357.

Saad-Eldeen, S., Garbatov, Y. & Soares, C. G. 2012. Influence of weld toe shape and material models on the ultimate strength of a slightly corroded box girder. . *In:* Resources, S. M. T. a. E. O. S. (ed.) *Proceedings of the 14th International Congress of the International Maritime Association of the Mediterranean, IMAM 2011, 2012.*

Saad-Eldeen, S., Garbatov, Y. & Soares, C. G. 2013a. Effect of corrosion severity on the ultimate strength of a steel box girder. *Engineering Structures,* 49, 560–571.

Saad-Eldeen, S., Garbatov, Y. & Soares, C. G. 2013b. Experimental assessment of corroded steel box-girders subjected to uniform bending. *Ships and Offshore Structures,* 8, 653–662.

Saad-Eldeen, S., Garbatov, Y. & Soares, C. G. 2013c. Ultimate strength assessment of corroded box girders. *Ocean Engineering,* 58, 35–47.

Saad-Eldeen, S., Garbatov, Y. & Soares, C. G. 2014. Strength assessment of a severely corroded box girder subjected to bending moment. *Journal of Constructional Steel Research,* 92, 90–102.

Salminen, M. & Heinisuo, M. 2014. Numerical analysis of thin steel plates loaded in shear at non-uniform elevated temperatures. *J. Constr. Steel Res.,* 97, 105–113.

Sawada, Y., Izumi, N. & Yoshikawa, T. 2012. Torsional Buckling Strength of Ring Stiffener in External Pressurized Cylinder. *Proceedings of 5th PAAMES and AMEC2012.* Taiwan.

Saydam, D. & Frangopol, D. M. 2013. Performance assessment of damaged ship hulls. *Ocean Engineering,* 68, 65–76.

Sayyar, M., Soroushian, P. & Weerasiri, R. R. 2013. Prestressing effects on the ultimate flexural strength of composite box sections. *Composite Structures,* 106, 806–814.

Seifi, R. & Khoda-Yari, N. 2011. Experimental and numerical studies on buckling of cracked thin-plates under full and partial compression edge loading. *Thin-Walled Structures,* 49, 1504–1516.

Sensharma, P., Collette, M. D. & Harrington, J. 2011. Effect of welded properties on aluminum structures. *Ship Structure Committee Report 2011.*

Shanmugam, N. E., Zhu, D. Q., Choo, Y. S. & Arockiaswamy, M. 2014. Experimental studies on stiffened plates under in-plane load and lateral pressure. *Thin-Wall Struct.,* 80, 22–31.

Shariati, M. 2012. Experimental and numerical investigation of buckling in rectangular steel plates with groove-shaped cutouts. *Journal of Zhejiang University-Science A; Applied Physics & Engineering,* 13.

Sheehan, T., Dai, X. H., Chan, T. M. & Lam, D. 2012. Structural response of concrete filled elliptical steel hollow sections under eccentric compression. *Eng. Struct.,* 45, 314–323.

Shi, G. J. & Wang, D. Y. 2012a. Residual ultimate strength of cracked box girders under torsional loading. *Ocean Eng.,* 43, 102–112.

Shi, G. J. & Wang, D. Y. 2012b. Residual ultimate strength of open box girders with cracked damage. *Ocean Eng.,* 43, 90–101.

Shu, Z. & Moan, T. 2012. Ultimate hull girder strength of a bulk carrier under combined global and local loads in the hogging and alternate hold loading condition using nonlinear finite element analysis. *Journal of Marine Science and Technology,* 17, 94–113.

Silva, J., Garbatov, Y. & Soares, C. G. 2013. Ultimate strength assessment of rectangular steel plates subjected to a random localised corrosion degradation. *Engineering Structures,* 52, 295–305.

Smith, C. S. 1977. Influence of local compressive failure on ultimate longitudinal strength of a ship's hull. *3th Int. Symposium on Practical Design in Shipbuilding.* Tokyo.

Smith, C. S., Anderson, N., Chapman, J. C., Davidson, P. C. & Dowling, P. J. 1991. Strength of stiffened plating under combined compression and lateral pressure. *Trans. R. Inst. Nav. Archit.*, 131–147.

So, H. & Chen, J. T. 2007. Experimental study of dynamic crushing of thin plates stiffened by stamping with V-grooves. *International Journal of Impact Engineering,* 34, 1396–1412.

Storheim, M. & Amdahl, J. 2014. Design of offshore structures against accidental ship collisions. *Marine Structures 37,* 37, 135–172.

Sun, H. H. & Guedes Soares, C. 2003. An experimental study of ultimate torsional strength of a ship-type hull girder with a large deck opening. *Marine Structures,* 16, 51–67.

Sundarraja, M. C. & Prabhu, G. G. 2012. Experimental study on CFST members strengthened by CFRP composites under compression. *J. Constr. Steel Res.,* 72, 75–83.

Syrigou, M. S., Benson, S. & Dow, R. S. 2014. Strength of ship plating under combined shear and compression. *Proceedings of International Conference On Safety & Reliability of Ship, Offshore & Subsea Structures.* Glasgow: UK.

Tahmasebi Nejad, A. & Shanmugam, N. E. 2011. Elastic buckling of uniaxially loaded skew plates containing openings. *Thin-Walled Struct.,* 49, 1208–1216.

Tan, K. H., Fung, T. C. & Nguyen, M. P. 2013. Structural behaviour of CHS T-joints subjected to brace axial compression in fire. *J. Struct. Eng.-ASCE,* 139, 73–84.

Tanaka, S., Yanagihara, D., Yasuoka, A., Haradac, M., Okazawa, S., Fujikubo, M. & Yao, T. 2014. Evaluation of ultimate strength of stiffened panels under longitudinal thrust. *Mar Struct.,* 36, 21–50.

Taylor, S. C., Magota, T. & Aksu, S. 2013. Residual strength assessment of an aluminium naval platform. *In:* Rina, R. I. O. N. A. (ed.) *International Conference on Damaged Ship II.*

Tayyar, G. T. & Bayraktarkatal, E. 2012. A new approximate method to evaluate the ultimate strength of ship hull girder. *In:* Resources, S. M. T. a. E. O. S. (ed.) *Proceedings of the 14th International Congress of the International Maritime Association of the Mediterranean.* Genova: Italy.

Teixeira, A. P., L.D., I. & Soares, C. G. 2013a. Assessment of characteristic values of the ultimate strength of corroded steel plates with initial imperfections. *Engineering Structures* 517–527.

Teixeira, A. P., Soares, C. G. & Wang, G. 2013b. Probabilistic modelling of the ultimate strength of ship plates with non-uniform corrosion. *J. Mar. Sci. Technol.,* 18, 115–132.

Tekgoz, M., Garbatov, Y. & Soares, C. G. 2013a. Advanced Guideline to Predict the Ultimate Strength of Perforated Plate with Edge Reinforcement. *Proceedings of the PRADS2013. CECO.* Changwon City: Korea.

Tekgoz, M., Garbatov, Y. & Soares, C. G. 2013b. Finite element modelling of the ultimate strength of stiffened plates with residual stresses. *Analysis and Design of Marine Structures.* Espoo: Finland: Taylor & Francis.

Toh, K., Maeda, M. & Yoshikawa, T. 2012. The effect of initial imperfection on the hull girder ultimate strength of intact and damaged ships. *Proceedings of the International Offshore and Polar Engineering Conference.*

Toh, K., Maeda, M. & Yoshikawa, T. 2014. The Effect of Initial Imperfections and Lateral Loads on the Hull Girder Ultimate Strength of Intact and Damaged Ships. *22th International Offshore and Polar Engineering Conference.*

Tran, K. L., Davaine, L., Douthe, C. & Sab, K. 2012. Stability of curved panels under uniform axial compression. *J. Constr. Steel Res.,* 69, 30–38.

Turner, M. J., Clough, R. W., Martin, H. C. & Topp, L. J. 1956. Stiffness and deflection analysis of complex structure. *J. Aeronautical Science,* 23, 805–823.

Ueda, Y. & Rashed, S. M. H. 1974. An ultimate transverse strength analysis of ship structure. *J Soc Naval Arch Japan,* 13, 87–104.

Ueda, Y. & Rashed, S. M. H. 1991. Modern Method of Ultimate Strength Analysis of Offshore Structure. *Int J Offshore and Polar Eng., ISOPE*

Ueda, Y., Rashed, S. M. H., Nakacho, K. & Sasaki, H. 1983. Ultimate strength analysis of offshore structures-application of idealized structural unit method. *J Kansai Soc Naval Architects Japan,* 190, 131–42.

Ueda, Y. & Yao, T. 1985. The influence of complex initial deflection modes on the behaviour and ultimate strength of rectangular plates in compression. *J. Constructional Steel Research,* 5, 265–302.

Uenaka, K. 2014. Experimental study on concrete filled elliptical/oval steel tubular stub columns under compression. *Thin Wall Struct.,* 78, 131–137.

Uenaka, K. & Kitoh, H. 2011. Mechanical behaviour of concrete filled double skin tubular circular deep beams. *Thin Wall Struct.,* 49, 256–263.

Underwood, J. M., Sobey, A. J., Blake, J. I. R. & Shenoi, R. A. 2012a. Determination of critical factors for the damaged strength assessment of steel grillages. *Proceedings of the International Offshore and Polar Engineering Conference.*

Underwood, J. M., Sobey, A. J., Blake, J. I. R. & Shenoi, R. A. 2012b. Ultimate collapse strength assessment of damaged steel-plated structures. *Eng Struct.,* 38, 1–10.

Van Es, S. H. J., Gresnigt, A. M., Kolstein, M. H. & Bijlaard, F. S. K. 2013. Local Buckling of Spirally Welded Tubes. *Twenty-Third Int. Offshore Polar Eng. Conf.*

Wang, J. & Zang, S. 2011. Ultimate Strength Experimental Research for Longitudinal Box Girders Module Model. *Shipbuilding of China* 2, 008.

Wang, R., Han, L. H. & C.C., H. 2013. Behaviour of concrete filled steel tubular (CFST) members under lateral impact: experiment and FEA model. *J. Constr. Steel Res.,* 80, 188–201.

Wang, X., Qian, X., Liew, J. Y. R. & Zhang, M. H. 2014. Experimental behaviour of cement filled pipe-in-pipe composite structures under transverse impact. *Int. J. Impact Eng.,* 72, 1–16.

Windenburg, D. F. & Trilling, C. 1934. Collapse by instability of thin cylindrical shells under external pressure. *Trans, ASME.,* 56, 819–825.

Wu, H., Wu, W., Gan, J. & Sun, H. 2013. Ultimate strength analysis of a river-sea ship under combined action of torsion and bending. *OMAE 2013.*

Xu, J. X., Zhao, J. C., Song, Z. S. & Liu, M. L. 2012. Prediction of ultimate bearing capacity of tubular T-joint under fire using artificial neural networks. *Safety Sci.,* 50, 1495–1501.

Xu, M. C., Garbatov, Y. & Soares, C. G. 2013a. Ultimate strength assessment of a tanker hull based on experimentally developed master curves. *Journal of Marine Science and Application,* 12, 127–139.

Xu, M. C. & Soares, C. G. 2013a. Experimental Study on the Collapse Strength of Narrow Stiffened Panels. *Journal of Offshore Mechanics and Arctic Engineering,* 135, 021402–10.

Xu, M. C. & Soares, C. G. 2013b. Experimental study on the collapse strength of wide stiffened panels. *Marine Structures,* 30, 33–62.

Xu, M. C., Yanagihara, D., Fujikubo, M. & Guedes Soares, C. 2013b. Influence of boundary conditions on the collapse behaviour of stiffened panels under combined loads. *Mar. Struct.,* 34, 205–225.

Yamada, Y. 2014. Numerical Study on the Residual Ultimate Strength of Hull Girder of a Bulk Carrier after Ship-Ship Ccollision. *Proceedings of the ASME 2014 33rd International Conference on Ocean, Offshore and Arctic Engineering, OMAE2014.* San Francisco, California: USA.

Yamamoto, Y. 1965. General instability of a reinforced cylindrical shell under external pressure. *Journal of the society of naval architecture of Japan* 113.

Yang, N., Das, P. K. & Yao, X. 2011. Ultimate strength and reliability assessment of laminated composite plates under axial compression. *Ships and Offshore Structures,* 6, 105–113.

Yang, Q. J., Hayman, B. & Osnes, H. 2013. Simplified buckling and ultimate strength analysis of composite plates in compression. *Composites Part B: Engineering,* 54, 343–352.

Yao, T. & Nikolov, P. I. 1992. Progressive collapse analysis of a ship's hull girder under longitudinal bending (2nd report). *J. of Soc. Naval Arch. of Japan,* 172, 437–446.

Yasuoka, A., Tanaka, S., Yanagihara, D., Okazawa, S. & Yao, T. 2012. Collapse Behaviour and Ultimate Strength of Stiffened Panels with Arbitrary Number of Stiffeners Subjected to Longitudinal Thrust. *Presented at the The Twenty-second International Offshore and Polar Engineering Conference.* International Society of Offshore and Polar Engineers.

Ye, Q., Jin, W. L., He, Y., Shi, Z. M. & Qu, Y. 2012. Assessment of ultimate strength of semi-submersible platform. *Journal of Ship Mechanics,* 16, 277–295.

Yoshikawa, T. & Yoshimura, K. 2006. General Buckling Strength of Ring-Stiffened Cylindrical Shells under External Pressure and Effective Breadth of Ring-Stiffeners. *Journal of The Japan Society of Naval Architects and Engineers,* 3, 253–260.

Yoshikawa, T. & Yoshimura, K. 2008. General Buckling Strength of Ring-Stiffened Cylindrical Shells under External Pressure and Effective Breadth of Ring-Stiffeners. *Proceedings of OMAE2008, 27th International Conference on Offshore Machanics and Arctic Engineering.*

Yu, C. & Lee, J. S. 2012. Ultimate Compressive Strength of Unstiffened Plate with Rectangular Opening. *Proceedings of the 26th Asian-Pacific Technical Exchange and Advisory Meeting on Marine Structure.* Kyushu University, Fukuoka: Japan.

Yu, W. J., Zhao, J. C., Luo, H. X., Shi, J. Y. & Zhang, D. X. 2011. Experimental study on mechanical behaviour of an impacted steel tubular T-joint in fire. *J. Constr. Steel Res.,* 67, 1376–1385.

Yudo, H. & Yoshikawa, T. 2012. Mechanical Behaviour of Pipe under Pure Bending Load. . *Proceedings of the 26th Asian-Pacific Technical Exchange and Advisory Meeting on Marine Structure.* Kyushu University, Fukuoka: Japan.

Yudo, H. & Yoshikawa, T. 2014. Buckling phenomenon for straight and curved pipe under pure bending. *J. Mar. Sci. Technol.*, 1–10.

Zahurul Islam, S. M. & Young, B. 2011. FRP strengthened alumnium tubular sections subjected to web cripplin. *Thin-Walled Structures,* 49, 1392–1403.

Zareei, M. R., Khedmati, M. R. & Rigo, P. 2012. Application of artificial neural networks to the evaluation of the ultimate strength of uniaxially compressed welded stiffened aluminium plates. *Proceeding of the Institution of Mechanical Engineering.* Journal of Engineering for the Maritime Environment.

Zayed, A., Garbatov, Y. & Soares, C. G. 2013. Reliability of ship hulls subjected to corrosion and maintenance. *Structural Safety,* 43, 1–11.

Zha, Y. & Moan, T. 2003. Experimental and numerical prediction of collapse of flatbar stiffeners in aluminum panels. *Journal of Structural Engineering,* 129, 160–168.

Zhang, J., Shen, Z., Ji, C. & Yin, Q. 2012. The influence research of ultimate strength to deepwater semi-submersible platforms structure under corrosion damage. *Proceedings of the International Conference on Offshore Mechanics and Arctic Engineering.*

Zhang, S. 2013. Buckling and ultimate strength assessments of ship structures. *International Conference on Offshore Mechanics and Arctic Engineering - 2013.* San Francisco.

Zhang, W., Luo, X. & Wu, W. 2013. Ultimate strength of river-sea container ship. *Marstruct.* Finland.

Zhao, X. L. & Tong, L. W. 2011. New development in steel tubular joints. *Adv.Struct. Eng.,* 14, 699–715.

Zhu, B. & Frangopol, D. M. 2013. Reliability assessment of ship structures using Bayesian updating. *Engineering Structure,* 56, 1836–1847.

Zubair, M., Alie, M., Fujikubo, M., Iijima, K., Oka, S. & Takemura, K. 2012. Residual longitudinal strength analysis of ship's hull girder with damages. *Proceedings of the International Offshore and Polar Engineering Conference.*